Investigating the effects of liver fat content and composition on autophagy, inflammation and insulin resistance



Felix Westcott

Green Templeton College

University of Oxford

A thesis submitted for the degree of

DPhil in Inflammatory and Musculoskeletal Disease

Michaelmas 2024

Memorandum

The work in this thesis is the original work of the author and was carried out at the Oxford Centre for Diabetes, Endocrinology and Metabolism; work done by anyone else or at different institutions is clearly stated. Supervision was carried out by Professor Leanne Hodson, Dr Shilpa Nagarajan, Professor Katja Simon and Professor Jeremy Tomlinson and funding was provided by the Kennedy Trust Oxford MB PhD Programme. No part of this thesis has been submitted for any degree at this or any other university however some of the work has formed the basis of publications and/or presentations:

Publications

Westcott et al. "*Hepatic fatty acid and glucose handling in metabolic disease: Potential impact on cardiovascular disease risk*", in *Atherosclerosis* (July 2024).

Westcott et al. "*Dissociation between liver fat content and fasting metabolic markers of selective hepatic insulin resistance in humans*", in the *European Journal of Endocrinology* (September 2024).

Srnic et al. "*Influence of dietary fat quantity and composition on hepatic lipid metabolism: evidence from human in vivo and in vitro studies*", in *Disease Models & Mechanisms* (January 2025).

Presentations and prizes

The Physiological Society's Michael J Rennie Oral Communication Prize 2024 for the presentation entitled "*Investigating the impact of fatty acids and insulin on hepatocellular autophagic flux and inflammatory activation in metabolic dysfunction-associated steatotic liver disease (MASLD)*"

Best oral communication in the Diabetes session of the Early Career Life Scientists' Symposium 2023 for the presentation entitled "*Metabolic signatures of selective hepatic insulin resistance do not associate with insulin status or liver fat content in humans*"

Poster presentation at British Endocrinology Society Conference 2023 entitled "*Metabolic signatures of selective hepatic insulin resistance are not evident in humans across a range of liver fat content*"

Acknowledgements

There has barely ever been a day when I haven't wanted to come into work and continue my research. I think this is relatively rare for a DPhil student and a huge testament to the excellent support, supervision and environment I have had at OCDEM and more specifically within the Hodson Group. I cannot thank Leanne enough for fostering that environment and for the excitement that she brings to our research every day. I am also thankful to Shilpa who has taught me everything I know in the lab and set me up the with skills to keep learning and trying new techniques. Thank you to Katja and the rest of the Simon group for their guidance and help setting me off on the right track initially and to Jeremy for always providing valuable feedback and positive support throughout. I feel immensely privileged to have had these supervisors and so grateful for all that they have taught me.

Thank you to Kaitlyn, Eleanor, Charlotte and Paige for their help with the experiments and sample processing which I simply would not have been able to do on my own and to Eloise for her long-term collaboration on hepatocyte work. I am also hugely grateful to Elspeth for her tireless running of the GC area and machines and her inspirational troubleshooting when things go wrong. Thank you to all other members of the Hodson group, past and present, who have given me their support and who's hard work I have built on and to the participants and research nurses involved who have made this work possible in the first place. Many thanks to Fredrik, Katherine, Amy and the wider metabolic research group at OCDEM for their academic feedback and help in the lab. I would also like to thank Adam for being my academic muse, Nikola, Emily and the rest of the fellows room for the chatting and laughter that have made the last few years so immensely enjoyable. I am also thankful to The Kennedy Trust For Rheumatology Research for funding this MB PhD Programme and to the valuable friends I've made on the course.

A huge thank you to all my friends outside of work; those who have been around since undergraduate times and the ones I've made through student drama on the various productions who have filled my life with such fun, chaos and creativity.

Finally, I could not have done this without the constant love and support from Alex, who has helped make these past few years fly by with such joy, and from my family, who have made it possible for to take opportunities like this and have always been there for me throughout my life.

Abstract

Metabolic dysfunction-associated steatotic liver disease (MASLD) is characterised by the pathological accumulation of intrahepatocellular triglyceride (IHCTG). Although suggested to be initially benign, IHCTG accumulation may lead to insulin resistance (IR), inflammatory activation and progression to steatohepatitis and more severe liver disease. Dietary fat quantity and composition have been associated with MASLD development and progression which may be mediated through an aberrant decrease in autophagy. Therefore, the overall aim of this thesis was to determine the effects of IHCTG quantity and composition on hepatocellular autophagy, inflammatory activation and IR.

The effect of liver fat content on markers of selective hepatic IR and inflammation was assessed in fasting plasma samples from 177 human participants using stable isotope tracer methodology to measure fractional gluconeogenesis and hepatic *de novo* lipogenesis following an overnight fast. Hepatocytes were cultured in media supplemented with different fatty acid (FA) concentrations and compositions (predominantly unsaturated or saturated) to determine the effects of IHCTG content and composition on autophagic flux, inflammatory activation and IR. Human-derived triglyceride-rich lipoproteins (TRLs) labelled with stable isotope tracer were incorporated into this *in vitro* model of IHCTG to explore the role of IHCTG content and composition on the autophagic processing of TRLs.

No signature of selective hepatic IR was found to be associated with liver fat content in the human cohort but cultured hepatocytes treated with saturated FA showed markers of IR whereas cells treated with unsaturated FAs did not. Conversely, autophagic flux tended to be lower in hepatocytes cultured in unsaturated FAs and was associated with greater cytokine secretion than those cultured in saturated FAs. IHCTG accumulation was associated with decreased TRL processing which could be attributed to lower autophagic lipolysis in hepatocytes treated with unsaturated fatty acids.

Taken together, these results suggest that liver fat composition may be equally as important as liver fat content. Unsaturated fat may decrease hepatic autophagy leading to increased inflammatory activation and decreased TRL processing whereas saturated fat may be more associated with IR.

Contents

List of Figures **x**

List of Tables **xii**

List of Abbreviations **xiii**

1 Background **1**

1.1 Overview of the liver . . . 1

1.1.1 Structure . . . 2

1.1.2 Hepatic glucose handling . . . 2

1.1.3 Hepatic fatty acid handling . . . 4

1.2 Metabolic dysfunction-associated steatotic liver disease (MASLD) . . . 5

1.2.1 Insulin resistance and metabolic dysfunction in MASLD . . . 5

1.2.2 Inflammation in MASLD . . . 6

1.3 Hepatic autophagy . . . 7

1.3.1 The role of autophagy in MASLD . . . 9

1.4 Influence of dietary fat quantity and composition on MASLD . . . 10

1.4.1 *In vitro* models of intrahepatocellular triglyceride accumulation . . . 11

1.5 Concluding remarks . . . 12

2 Methods **13**

2.1 Cell culture procedures . . . 14

2.1.1 Routine cell culture . . . 14

2.1.2 Passaging cells . . . 14

2.1.3 Seeding cells for experiments . . . 14

2.1.4 Freezing cells for storage in liquid nitrogen . . . 15

2.1.5 Thawing cells from storage in liquid nitrogen . . . 15

2.1.6 Experimental treatments . . . 15

2.2 Quantification of gene expression . . . 16

2.2.1 RNA extraction . . . 16

2.2.2 RNA sequencing and data processing . . . 16

2.3 Transcriptomics analysis . . . 16

2.4 Protein quantification . . . 17

2.4.1 Total protein . . . 17
2.4.2 Western blotting . . . 18
2.5 Quantification of autophagic flux . . . 19
2.6 Lipid extraction and quantification . . . 19
2.6.1 Lipid Extraction . . . 19
2.6.2 Separation of lipid fractions . . . 20
2.6.3 Lipid methylation . . . 20
2.6.4 Gas Chromatography . . . 21
2.7 Cell viability assay . . . 21
2.8 Enzyme-linked immunosorbent assays (ELISAs) . . . 21
2.9 Calculations and statistical analysis . . . 22

3 The effect of liver fat content on markers of selective hepatic insulin resistance and systemic inflammation in humans 23
3.1 Introduction . . . 24
3.2 Methods . . . 26
3.2.1 Participants . . . 26
3.2.2 Study protocol . . . 27
3.2.3 Analytical methods . . . 27
3.2.4 Measurement of DNL . . . 28
3.2.5 Measurement of GNG and GLY . . . 28
3.2.6 Calculations and Statistical Analysis . . . 29
3.3 Results . . . 29
3.3.1 Participant characteristics . . . 29
3.3.2 The effect of fasting plasma insulin and liver fat content on fasting GNG and GLY . . . 30
3.3.3 The effect of fasting plasma insulin and liver fat content on fasting DNL 31
3.3.4 Further Phenotypic Grouping . . . 34
3.3.5 The associations between GNG and DNL and multivariate analysis . . . 38
3.3.6 The effect of fasting plasma insulin and liver fat content on systemic inflammation . . . 38
3.4 Discussion . . . 39
3.4.1 The effect of fasting plasma insulin and liver fat content on markers of selective hepatic IR . . . 40
3.4.2 The effect of fasting plasma insulin and liver fat content on systemic inflammation . . . 42
3.4.3 Limitations . . . 43
3.4.4 Conclusions . . . 44

4 Developing a suitable *in vitro* model of intrahepatocellular triglyceride accumulation 46
4.1 Introduction . . . 47
4.2 Methods . . . 49
4.2.1 Experimental treatments . . . 49
4.2.2 Analytic techniques . . . 49
4.2.3 Culture of primary human hepatocytes . . . 49
4.2.4 Lipid droplet imaging and quantification . . . 50
4.3 Results . . . 51
4.3.1 The effect of media fatty acids on hepatocyte viability . . . 51
4.3.2 The effect of media fatty acids on intrahepatocellular triglyceride accumulation . . . 52
4.3.3 The effect of media fatty acids on autophagy . . . 55
4.3.4 The effect of media fatty acids on autophagic and inflammatory gene expression . . . 55
4.4 Discussion . . . 60
4.4.1 The effect of FAs on cell viability . . . 60
4.4.2 The effects of FAs on IHCTG accumulation . . . 61
4.4.3 The effects of FAs on autophagy . . . 62
4.4.4 The effect of FAs on inflammatory activation . . . 63
4.4.5 Conclusions . . . 64

5 The effect of fatty acid composition on hepatocellular autophagy, inflammatory activation and insulin resistance 65
5.1 Introduction . . . 66
5.2 Methods . . . 67
5.2.1 Experimental treatments . . . 67
5.2.2 Analytic techniques . . . 68
5.2.3 Quantification of cytokine secretion . . . 68
5.2.4 Co-culture with hepatic stellate cells . . . 68
5.2.5 Glucose production assay . . . 69
5.2.6 Analysis of proteomic data . . . 70
5.3 Results . . . 70
5.3.1 The effect of media fatty acid composition on Huh7 cell viability . . . 70
5.3.2 The effect of media fatty acid composition and insulin concentration on intrahepatocellular triglyceride accumulation . . . 70
5.3.3 The effect of media fatty acid composition and insulin concentration on autophagy . . . 71
5.3.4 The effect of media fatty acid composition and insulin concentration on inflammatory activation . . . 72

5.3.5 The effect of media fatty acid composition and insulin concentration on hepatocellular injury . . . 74
5.3.6 The effect of media fatty acid composition on insulin resistance . . . 75
5.3.7 The effect of media fatty acid composition and insulin concentration on gene expression . . . 76
5.4 Discussion . . . 80
5.4.1 Model assessment . . . 81
5.4.2 The effect of FA composition on autophagy . . . 82
5.4.3 The effect of FA composition on inflammatory activation . . . 83
5.4.4 The effect of FA composition on insulin resistance . . . 84
5.4.5 The effect of hyperinsulinemia on autophagy and inflammatory activation 84
5.4.6 Limitations . . . 85
5.4.7 Conclusions . . . 85

6 Investigating the role of autophagy in triglyceride-rich lipoprotein processing 86
6.1 Introduction . . . 87
6.2 Methods . . . 88
6.2.1 Overview of experimental design . . . 88
6.2.2 Participants . . . 90
6.2.3 Experimental diet . . . 90
6.2.4 Post-prandial study day . . . 90
6.2.5 Isolation and quantification of human-derived TRLs . . . 90
6.2.6 Hepatocyte pretreatment . . . 91
6.2.7 Incubation with TRLs . . . 91
6.2.8 Lipid extraction and quantification . . . 92
6.2.9 Imaging experiments . . . 92
6.3 Results . . . 93
6.3.1 TRLs are processed via the endolysosomal pathway . . . 93
6.3.2 The effect of autophagic inhibition on TRL processing . . . 93
6.3.3 The effect of intrahepatocellular triglyceride accumulation on TRL processing 95
6.3.4 The effect of TRLs on IHCTG accumulation . . . 97
6.4 Discussion . . . 97
6.4.1 The role of autophagy in TRL processing . . . 98
6.4.2 The effect of IHCTG on TRL processing . . . 99
6.4.3 The contribution of TRL to IHCTG accumulation . . . 100
6.4.4 Limitations and future work . . . 100
6.4.5 Conclusions . . . 100

7 Discussion **102**
7.1 The effect of liver fat content and composition on autophagy 103
7.2 The effect of liver fat content and composition on insulin resistance 103
7.3 The effect of liver fat content and composition on inflammation 104
7.4 Future directions 104

References **107**

List of Figures

1.1 Overview of hepatic glucose and lipid handling 3
1.2 Overview of autophagy 8

3.1 Insulin regulation of glucose and triglyceride production in health and in selective hepatic insulin resistance 26
3.2 The effect of fasting plasma insulin and liver fat content on GNG, GLY and DNL in female participants 32
3.3 The effect of fasting plasma insulin and liver fat content on GNG, GLY and DNL in male participants 33
3.4 Further phenotypic grouping in female participants 36
3.5 Further phenotypic grouping in male participants 37
3.6 The effect of fasting plasma insulin and liver fat content on systemic inflammation 39
3.7 The effect of further phenotypic grouping on systemic inflammation 40
3.8 Proposed mechanisms underlying hyperglycemia and hypertriglyceridemia 44

4.1 Proposed effects of fatty acids on hepatocellular autophagy, triglyceride accumulation and inflammatory activation 48
4.2 Effect of individual fatty acids and fatty acid mixtures on hepatocyte viability . 51
4.3 The effect of media fatty acids on intrahepatocellular triglyceride accumulation in Huh7 cells 52
4.4 The effect of media fatty acids on lipid droplet formation 53
4.5 Effect of media fatty acids on intrahepatocellular triglyceride accumulation in Primary human hepatocytes 54
4.6 The effect of media fatty acids on autophagy 56
4.7 The effect of media fatty acids on autophagic and inflammatory gene expression in Huh7 cells 57
4.8 The effect of media fatty acids on autophagic and inflammatory gene expression in primary human hepatocytes 58
4.9 The effect of media fatty acids on cytokine gene expression in primary human hepatocytes 59

5.1 Experimental set-up for the co-culture with hepatocytes and hepatic stellate cells 69

5.2 Huh7 cell viability when cultured with individual fatty acids and fatty acids mixtures . . . 71
5.3 The effect of media fatty acids and insulin on intrahepatocellular triglyceride accumulation . . . 72
5.4 The effect of media fatty acids and insulin on autophagic flux . . . 73
5.5 The effect of media fatty acids on cytokine secretion . . . 74
5.6 The effect of media fatty acids and insulin on hepatocyte-media activation of hepatic stellate cells . . . 75
5.7 The effect of media fatty acids and insulin on hepatocellular injury . . . 76
5.8 The effect of media fatty acid composition on insulin resistance . . . 77
5.9 The effect of media fatty acids and insulin on gene expression . . . 78
5.10 Volcano plots showing the effect of media fatty acids and insulin on gene expression 79
5.11 The effect of media fatty acids and insulin on pathway regulation . . . 80

6.1 The proposed processing of TRL 13C 16:0 in TG by hepatocytes . . . 88
6.2 Overview of methods . . . 89
6.3 Localisation of TRLs to the early endosome . . . 94
6.4 The effect of autophagy on TRL processing . . . 95
6.5 The effect of IHCTG accumulation on TRL processing . . . 96
6.6 The contribution of autophagy to the lipolysis of TG from TRL . . . 97
6.7 The effect of TRLs on IHCTG accumulation . . . 98

List of Tables

3.1 Participant characteristics defined by fasting plasma insulin 30
3.2 Participant characteristics defined by liver fat content 31
3.3 Participant characteristics defined by phenotype 35

4.1 Primary human hepatocyte donor phenotype 50

List of Abbreviations

16:0 . . . . . Palmitic acid / palmitate
BAF . . . . . Bafilomycin A1
CVD . . . . . Cardiovascular disease
DNL . . . . . *De novo* lipogenesis
EGP . . . . . Endogenous Glucose Production
FA . . . . . Fatty acid
GLY . . . . . Glycogenolysis
GNG . . . . . Gluconeogenesis
HSC . . . . . Hepatic stellate cells
IHTG . . . . . Intrahepatic triglyceride
IHCTG . . . . Intrahepatocellular triglyceride
IR . . . . . Insulin resistance
LA . . . . . Linoleic acid
LD . . . . . Lipid droplet
MASLD . . . . Metabolic dysfunction-associated steatotic liver disease
MUFA . . . . . Monounsautrated fatty acid
NEFA . . . . . Non-esterified fatty acid
OA . . . . . Oleic acid / oleate
OPLA . . . . . Fatty acid mixture predominantly enriched in unsaturated fatty acids
PA . . . . . Palmitic acid / palmitate
POLA . . . . . Fatty acid mixture predominantly enriched in saturated fatty acids
PUFA . . . . . Polyunsaturated fatty acid
SFA . . . . . Saturated fatty acid
T2D . . . . . Type II diabetes mellitus
TG . . . . . Triglyceride
TRL . . . . . Triglyceride-rich lipoprotein
Veh . . . . . Vehicle

'Iecur, iocor, amor'

1 Background

Contents

1.1 Overview of the liver 1
1.1.1 Structure 2
1.1.2 Hepatic glucose handling 2
1.1.3 Hepatic fatty acid handling 4
1.2 Metabolic dysfunction-associated steatotic liver disease (MASLD) 5
1.2.1 Insulin resistance and metabolic dysfunction in MASLD 5
1.2.2 Inflammation in MASLD 6
1.3 Hepatic autophagy 7
1.3.1 The role of autophagy in MASLD 9
1.4 Influence of dietary fat quantity and composition on MASLD . . 10
1.4.1 *In vitro* models of intrahepatocellular triglyceride accumulation 11
1.5 Concluding remarks 12

1.1 Overview of the liver

The liver is a major metabolic organ, in humans situated below the diaphragm in the right upper quadrant of the abdomen, largely shielded by the rib cage. The liver has many functions, including the production of bile, regulation of systemic iron levels, regulation of blood clotting and detoxification of the blood. From a metabolic perspective, its main function is the regulation of the systemic blood concentrations of key nutritional substrates including glucose, fatty acids and amino acids. The liver is anatomically suited to this function as it receives the first pass of

glucose and amino acids from their point of absorption in the gastrointestinal tract through the hepatic portal vein. The same vein also delivers the pancreatic hormones, such as glucagon and insulin, that primarily control these regulatory processes in the liver.

1.1.1 Structure

Structurally, the liver can be split into four main lobes consisting of small hexagonal lobules containing four cell types: 1) sinusoidal endothelial cells, 2) hepatic stellate cells (HSCs), 3) Kupffer cells, and 4) hepatocytes. Along the corner of each lobule is a portal triad made up of the hepatic artery, the hepatic portal vein, and the common bile duct. As well as the oxygen-rich blood from the hepatic artery, the liver is unique in that it also receives nutrient-rich deoxygenated blood directly from the pancreas, spleen and the entire gastrointestinal tract through the hepatic portal vein. The blood from both vessels combine in the liver sinusoid and travel down to a central vein in the middle of each lobule which will eventually drain into the hepatic vein and then the inferior vena cava. The liver sinusoid is lined with sinusoidal endothelial cells and liver-specific tissue-resident macrophages known as Kupffer cells. Both cell types remove debris and foreign particles through the expression of a wide variety of endocytosis receptors and play a major role in innate immunity within the liver and regulate local inflammation. The endothelial cells are highly fenestrated, which allows selective communication between the sinusoid and the HSCs and hepatocytes. In the healthy liver, HSCs are quiescent and store vitamin A in lipid droplets (LDs) and may act as antigen-presenting cells [1]. However, during liver injury or inflammation they are activated and transform into fibroblast-like cells that produce extracellular matrix, leading to liver fibrosis. Hepatocytes occupy approximately 80 % of the total liver tissue (compared to only 5 % for all the other cell types and 15 % for extracellular space) [2] and perform the majority of metabolic and detoxification functions of the liver.

1.1.2 Hepatic glucose handling

Glucose is an important source of energy for the majority of organs and the liver plays a key role in maintaining circulating plasma glucose concentrations to ensure that all tissues throughout the body are adequately provisioned with this as an energy source. To achieve this, hepatocytes are uniquely able to switch rapidly between metabolic tasks of energy supply and storage

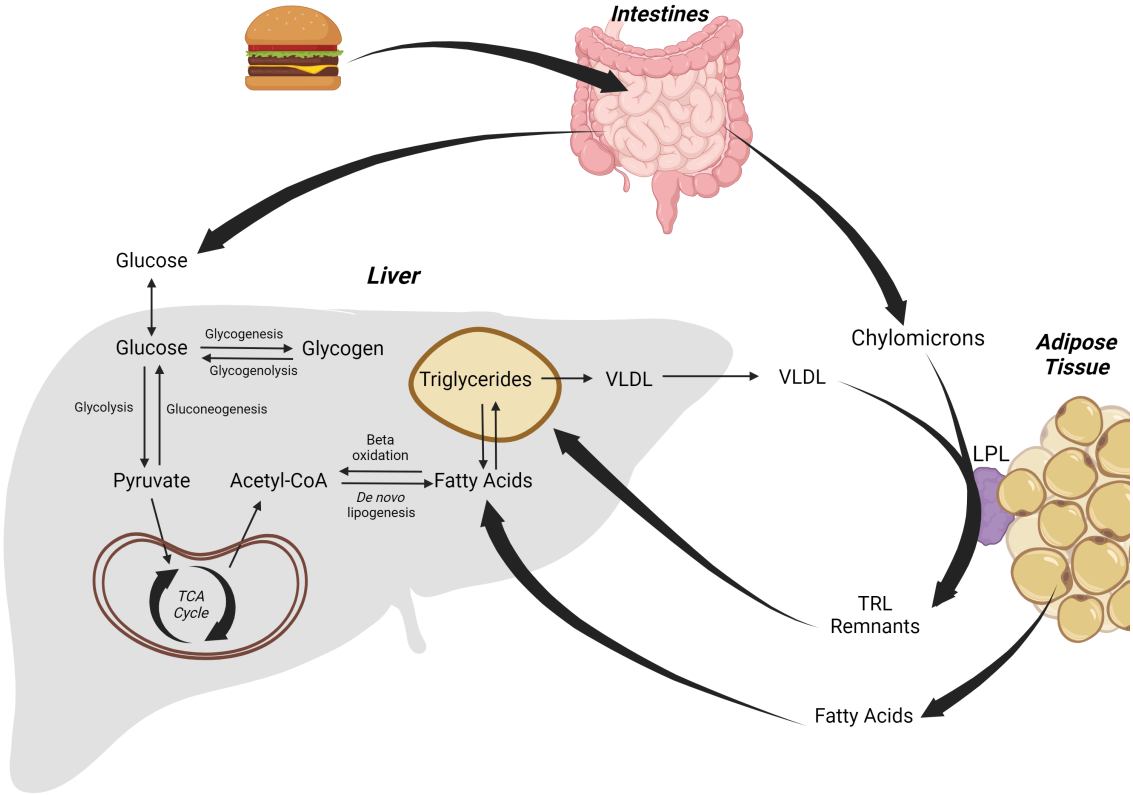


Figure 1.1: Overview of hepatic glucose and lipid handling. Glucose is taken up into the liver from the intestines where it can be stored as glycogen or broken down into pyruvate. Pyruvate can enter the TCA cycle in the mitochondria to be metabolised into acetyl-CoA which can re-enter the cytosol and be utilised in the *de novo* lipogenic pathway to form fatty acids. Fatty acids are then stored as triglycerides which can be packaged into VLDL and secreted into the blood. VLDL particles and chylomicrons from the intestine after a meal are hydrolysed by LPL in the adipose tissue to form TRL remnants which remain in circulation. Fatty acids are also released into circulation from adipose tissue TG lipolysis. TCA, Tricarboxylic Acid; VLDL, Very-Low Density Lipoprotein; LPL, Lipoprotein Lipase; TRL, Triglyceride-Rich Lipoprotein; TG, Triglyceride.

under the signalling of pancreatic hormones such as insulin and glucagon. In the fasting state, plasma glucose concentrations are maintained by the production of endogenous glucose which occurs predominantly in the liver [3]. Endogenous glucose production (EGP) is activated by the secretion of glucagon from the pancreas and consists of two processes: glycogenolysis (GLY), the breakdown of glycogen, and gluconeogenesis (GNG), the synthesis of glucose molecules from non-carbohydrate precursors (primarily lactate, alanine, glycerol and glutamine), as shown in Figure 1.1. Following the consumption of a meal, insulin is secreted from the pancreas to suppress EGP in the liver and increase glucose uptake in the adipose and skeletal muscle in order to maintain normoglycemia. The liver is also responsible for approximately one third of postprandial glucose uptake [4] which occurs through the insulin-independent conversion of

glucose to glucose-6-phosphate which can then be stored as glycogen or oxidised to acetyl-CoA.

1.1.3 Hepatic fatty acid handling

Although glucose is a primary energy source for most tissues, fatty acids (FAs) can yield substantially more energy per molecule and are therefore another vital source of energy, especially for organs with high energy requirements such as the heart. Additionally, FAs can also be esterified to triglyceride (TG) which can be stored in lipid droplets (LDs) within cells and transported in the blood in triglyceride-rich lipoprotein (TRL) particles. The liver plays a major role in the regulation of systemic FA and TG concentrations, to ensure adequate provision for all tissues which require these nutritional substrates. Following the consumption of a lipid-containing meal, dietary FAs are transported from intestinal epithelial cells as TG in chylomicron particles, which are hydrolysed by lipoprotein lipase (LPL) (Figure 1.1). LPL can be found on many tissues throughout the body and FAs are generally either utilised as an energy source (primarily in skeletal and cardiac muscle) or stored as TG in LDs (primarily in adipose tissue). The resulting chylomicron remnants can then be taken up into the liver through low-density lipoprotein (LDL) receptor-mediated endocytosis and the remaining TGs are lipolysed in the endolysosomal pathway and contribute to the hepatic FA pool [5]. Another source of FAs to the liver are those released from adipose tissue and transported in the blood bound to albumin. These non-esterified fatty acids (NEFAs) are taken up into hepatocytes through the FA transporters or through passive diffusion. Finally, FAs can also be synthesised in the liver from non-lipid precursors (primarily carbohydrates such as glucose) in a process known as *de novo* lipogenesis (DNL) which is transcriptionally upregulated by insulin [6, 7]. The hepatocellular FA pool is in constant turn-over, with FAs being mainly partitioned into oxidation or esterification pathways, or the synthesis of other lipid-derived species such as phospholipids [8, 9]. TG can also be secreted in VLDL particles which form from the endoplasmic reticulum (ER) and can provide a FA source to other tissues. All of these pathways are highly regulated and dysregulation of one or more of these processes may result in the accumulation of TG within the liver and the development cardiometabolic diseases such as MASLD [10].

1.2 Metabolic dysfunction-associated steatotic liver disease (MASLD)

In 2016, the World Health Organisation estimated 1.9 billion adults worldwide were overweight, with 650 million of these classified as obese [11], and the prevalence of obesity continues to increase rapidly [11, 12]. Obesity is a major risk factor for insulin resistance (IR), type-2 diabetes mellitus (T2D) and cardiovascular disease (CVD) [13–15] and is strongly associated with fat deposition in non-adipose tissue organs, including the liver, heart, and skeletal muscle. A pathological accumulation of TG within the liver (typically defined as steatosis) is when at least 5 % of liver volume is affected [16], and in those at risk of cardiometabolic disease, it is known as metabolic dysfunction-associated steatotic liver disease (MASLD) [17]. MASLD, formerly known as non-alcoholic fatty liver disease (NALFD), covers a spectrum of diseases from simple steatosis to metabolic dysfunction-associated steatohepatitis (MASH) and more severe liver disease, such as hepatocellular carcinoma and cirrhosis [17]. It has been estimated that globally 1 in 3 adults have MASLD and its prevalence is increasing [18–20]. Currently MASLD is also one of the leading causes of necessary liver transplants [21] and yet there are limited treatment options available for this condition [22] as the complete disease pathogenesis is still unclear. As hepatocytes are the predominant cell type in the liver and are primarily responsible for the metabolic functions of the liver, it is TG accumulation within these cells that is thought to drive MASLD [23]. Intrahepatocellular triglyceride (IHCTG) accumulation is determined by the balance of FA inputs (from adipose tissue, diet and DNL) and outputs (from oxidation and VLDL secretion) and although the disruption of this balance is not fully understood, it is thought that IR may play a role [7].

1.2.1 Insulin resistance and metabolic dysfunction in MASLD

IR is characterised by elevated plasma insulin, glucose and TG concentrations and is strongly associated with MASLD development and progression [7, 24, 25]. Insulin signalling usually occurs through activation of the insulin receptor, which in turn activates insulin receptor substrates (IRS), then Phosphatidylinositol-3-Kinase (PI-3K), and finally causes phosphorylation and activation of Akt. However in states of IR, this signalling pathway is thought to be disrupted, resulting in a reduction in insulin-mediated suppression of adipose tissue lipolysis that elevates

circulating NEFA concentrations [26, 27]. In addition, LPL activity is decreased leading to lower clearance of TRLs and greater circulating levels of TG [28, 29]. Together, systemic IR may lead to increased flux of lipids to the liver from extrahepatic tissues and contribute to IHCTG accumulation. However, within the liver, it is thought that hyperinsulinemia during IR may drive an increase in hepatic DNL, with hyperglycemia providing additional substrate. Therefore, increased hepatic DNL may also lead to IHCTG accumulation but although DNL has been shown to be higher in those with MASLD compared to those without [30, 31], there is still limited evidence to suggest a causal link [10]. As well as increased influx to the hepatocellular FA pool, it has also been suggested that FA disposal through oxidation may be decreased in those with MASLD. However, measurements comparing oxidation rates in those with and without MASLD have been inconclusive [32–34] which is possibly due to the effects of dietary and/or hepatic fat composition [35].

Euglycemic hyperinsulinemic clamp studies have demonstrated that hyperglycemia is driven by an increase in hepatic EGP and decrease in glucose uptake in adipose and skeletal muscle in those with IR [36, 37] and MASLD [38]. Use of stable isotope tracers or ^{13}C nuclear magnetic resonance (NMR) spectroscopy have shown that the increase in hepatic EGP is likely due to an increase in GNG and glycogen cycling in those with IR [36, 37]. Glycogen cycling is the simultaneous breakdown and synthesis of glycogen from plasma or newly synthesised glucose [39], which may cause excess intrahepatocellular glucose to be shunted towards other pathways such as DNL and also contribute to IHCTG accumulation. Taken together, the pathogenesis of MASLD is thought to be linked to IR however it is still unclear which comes first, the IHCTG accumulation or IR, and their relative contributions to hyperglycemia and hypertriglyceridemia are known.

1.2.2 Inflammation in MASLD

Although IHCTG accumulation can be benign, once it reaches a certain threshold the simple steatosis can develop into steatohepatitis, characterised by inflammation, hepatocellular injury and fibrosis. However, this threshold can vary between individuals, and what triggers this inflammatory activation in hepatocytes is currently unclear. It has been suggested that a mixture of extrahepatic factors, such as adipokines from adipose tissue inflammation or pathogen-associated molecular patterns (PAMPs) from gut barrier dysfunction, and intrahepatic

factors, such as lipotoxicity and mitochondrial dysfunction, may lead to increased hepatocellular production of reactive oxygen species (ROS) and ER stress [40] which activate pro-inflammatory and pro-apoptotic pathways such as c-jun N-terminal kinase (JNK) and nuclear factor kappa-B (NF-κB). JNK activation phosphorylates c-Jun which then can then upregulate pro-apoptotic Bcl-2 family members such as Bim and Bax [41–43]. NF-κB activation is thought to prime the activation of the NOD-, LRR- and pyrin domain-containing protein 3 (NLRP3) inflammasome which can cleave caspase 1 to induce interleukin-1β (IL-1β) production [44, 45]. As well as hepatocyte apoptosis, JNK and NLRP3 activation can lead to necroptosis and pyroptosis [46, 47] and the cytokines, damage-associated molecular patterns (DAMPs) and other hepatokines released by these cells activates Kupffer cells and macrophages. As the inflammation progresses, interleukin-6 (IL-6), IL-1β and tumour necrosis factor-α (TNF-α) secretion from the liver recruits neutrophils to infiltrate and HCSs are activated by transforming growth factor-β (TGF-β) which drives fibrosis, a hallmark of MASH [48].

Autophagy may play a role the progression of MASLD by regulating inflammation and apoptosis within hepatocytes. Kwanten et al. developed hepatocyte-specific autophagy knock-out mice and observed hepatocellular steatosis, injury and apoptosis as well as inflammatory infiltration and fibrosis of the liver [49]. Although this demonstrates the potential importance of autophagy within MASLD development and progression, the mechanisms underlying these associations are yet to be elucidated.

1.3 Hepatic autophagy

Autophagy occurs in the majority of cells in the body, to degrade intracellular cargo through lysosome-dependant mechanisms. Autophagy is a highly evolutionarily conserved process which allows cellular components to be recycled and reused by the cell. There are several recognised types of autophagy, including macroautophagy, microautophagy and chaperone-mediated autophagy, of which macroautophagy is the most well-understood. Macroautophagy (which for simplicity will hereon be referred to as autophagy) is thought to be the primary form of autophagy and will be the focus of this thesis as it has been shown to play a major role in hepatocellular lipid metabolism and inflammatory regulation [50, 51].

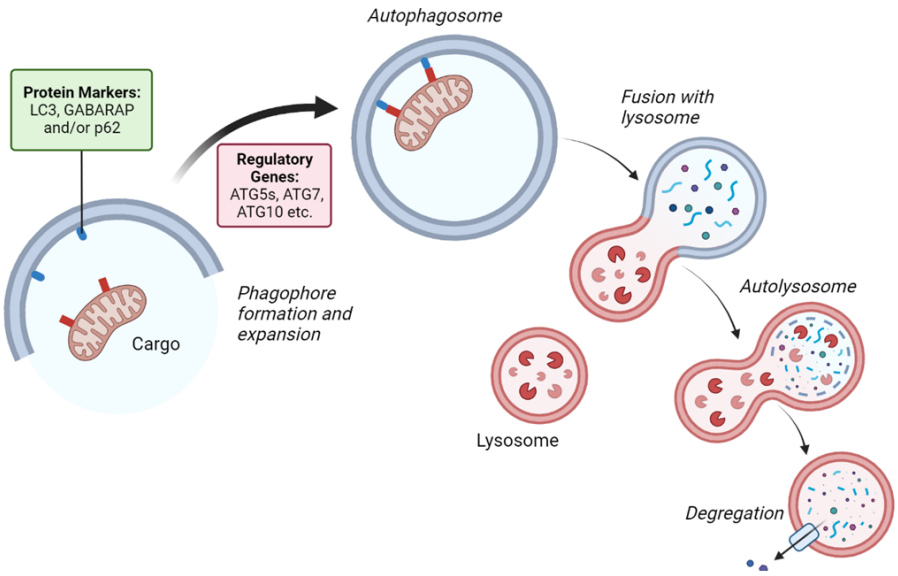


Figure 1.2: Overview of autophagy. Autophagic cargo is surrounded by a phagophore which expands to engulf the cargo and form an autophagosome. Autophagasomes will then fuse with a lysosome to form an autolysosome and the cargo will be degraded.

As shown in Figure 1.2, the process of macroautophagy begins when intracellular cargo tagged for degradation attaches to a phagophore which expands around the cargo to engulf it and form an autophagosome [52]. The autophagosome then fuses with a lysosome to form an autolysosome and the cellular cargo within is degraded by lysosomal enzymes in the acidic environment. The resulting cellular components can then be recycled to be reused by the cell. Autophagy is initiated by the UNC-like autophagy-activating kinase 1 (ULK1) initiation complex which is regulated by changes in nutrient status and intracellular stresses such as oxidative stress, inflammation, hypoxia and ER stress. During starvation, autophagy is induced by the activation of AMP-activated protein kinase (AMPK) and Sirtuin 1 (SIRT1) and suppression of the mammalian target of rapamycin complex 1 (mTORC1) whereas during conditions of nutrient excess, autophagy is inhibited by mTORC1 activation and AMPK and SIRT1 inactivation [53]. However, autophagy is also regulated by transcription factors such as Forkhead box O3 (FOXO3) and Transcription factor EB (TFEB) which control the expression of autophagy-related proteins that constitute the core machinery of the process [54].

Autophagy regulates cell stress through the degradation of dysfunctional mitochondria, misfolded proteins and PAMPs which could otherwise lead to ROS production, ER stress and

inflammatory activation, respectively. It has also been shown that autophagy is inhibited by insulin via mTORC1 activation following a meal and stimulated by glucagon during fasting to increase the breakdown of proteins which may act as substrates for GNG [55]. However, although there has been much research into the role of hepatic autophagy in MASLD, little is known about its role in IR [56].

1.3.1 The role of autophagy in MASLD

The suggestion that autophagy may play a role in MASLD development was initially driven by the association between autophagy and MASLD risk factors [50]. Conditions which increase MASLD risk, such as obesity and age, have been shown to decrease autophagy whereas protective factors, such as exercise and fasting, have been shown to increase autophagy [50]. The first mechanistic evidence for the role of autophagy in IHCTG accumulation came in 2009 from Singh et al. who showed an accumulation of IHCTG in both cultured hepatocytes treated with autophagic inhibitors and hepatocyte-specific autophagy knock-out mice [51]. The same study also demonstrated the autophagosomal delivery of IHCTG to lysosomes and proved that autophagy was a crucial component of hepatocellular lipid metabolism [51]. Thus, "lipophagy" was coined to define the degradation of lipids through autophagy.

Further studies using genetic and pharmacological modulation of autophagy in *in vitro* hepatocyte culture and *in vivo* animal work have confirmed that autophagy plays a causal role in regulating IHCTG accumulation through its degradation of TG from LDs [57–59]. However, these findings have yet to be replicated in humans as hepatocellular autophagic flux cannot be measured *in vivo* in humans. Instead, accumulation of marker proteins which are usually degraded through autophagy, can act as a marker of autophagy and give an indication of flux through the pathway [60]. Using this approach, Fukuo et al. found greater accumulation of the autophagic marker p62 in liver biopsies of those with MASLD compared to other chronic liver diseases suggesting a downregulation of autophagy in those with MASLD [61]. Further *in vivo* evidence for the role of autophagy in MASLD development was found in patients with lysosomal acid lipase deficiency (LAL-D), caused by an autosomal recessive mutation in lysosomal acid lipase (LAL) which is the sole enzyme responsible for lipolysis within the lysosome [62, 63]. The lack of lipophagy in patients with this inborn error of metabolism results in extreme hepatocellular

steatosis which causes rapid hepatomegaly and fibrosis [62, 63]. These symptoms are similar (albeit more extreme) to what is observed in MASLD and further confirm the importance of lipophagy in regulating human hepatic lipid metabolism *in vivo* and its possible implications in MASLD pathogenesis. Other studies exploring the role of lipophagy *in vivo* in MASLD patients have demonstrated a decrease in blood LAL activity in those with MASLD compared to dyslipidemia patients without MASLD and showed that blood LAL activity correlated strongly with LAL activity from liver biopsies [64]. Taken together, there is evidence that autophagy, and more specifically lipophagy, may be aberrantly decreased in patients with MASLD which could contribute to the IHCTG accumulation and disease pathogenesis. However, despite this association between decreased autophagy and IHCTG accumulation, the causal relationship is currently unclear but it is plausible that fat quantity and composition may play a role.

1.4 Influence of dietary fat quantity and composition on MASLD

In vivo human studies have shown that diet may play a major role in IHCTG accumulation and MASLD development. Interventional studies feeding hypercaloric diets have shown that increased caloric consumption leads to IHCTG accumulation, independent of the macronutrient composition of the diet [65, 66]. However, higher IHCTG accumulation and IR has been observed in hypercaloric diets enriched with saturated FA (SFA) compared to either polyunsaturated fats (PUFAs) or sugars [65–67]. Similarly, for isocaloric studies, diets enriched in saturated fats increased IHCTG accumulation and markers of IR whereas diets enriched in unsaturated fats did not [68]. Findings from cross-sectional studies that compared dietary FA composition in individuals with and without MASLD found that those with MASLD and MASH consumed more saturated fat, and less unsaturated fat than age- and BMI-matched healthy controls [69, 70]. Taken together, there is evidence to suggest that diets enriched in saturated fats may lead to greater IHCTG accumulation, IR and MASLD development than those enriched in unsaturated fats however the mechanisms underlying this are not currently known.

1.4.1 *In vitro* models of intrahepatocellular triglyceride accumulation

Whilst human studies have been vital in demonstrating the effects of dietary fat composition on IHCTG accumulation, it is difficult to directly investigate hepatocellular effects *in vivo* as the anatomical position of the liver makes biopsies more challenging and invasive than other tissues (such as adipose tissue or skeletal muscle). Stable isotope tracer methodologies can allow some insight into the pathways occurring in the liver at a whole-organ level however, it is also necessary to use *in vitro* models to better understand these mechanisms at a cellular level.

Current *in vitro* models of IHCTG accumulation culture primary human hepatocytes (PHHs) or human hepatocellular cancer cell lines (such as Huh7 and HepG2) in media containing high concentrations of glucose (typically 25 mM) and a single unsaturated FA (typically oleic acid, OA) or saturated FA (typically palmitic acid, PA) for a short period (typically between 6-48 hours) [71]. These studies have generally found a greater increase in IHCTG accumulation in hepatocytes treated with OA compared to PA [72–76] whereas hepatocytes treated with PA have increased markers of IR [75, 77, 78] and inflammatory activation [42, 78, 79]. However, a major limitation of these experiments is the use of a single FA which is not representative of the mixture of FA that the liver would be exposed to *in vivo*. Furthermore, several studies have demonstrated that treatment of hepatocytes with palmitate alone leads to rapid lipotoxicity [76, 80] which is rescued by the addition of OA to the PA-containing experimental media [74, 80]. Another limitation of these studies is the length of experimental treatment, which does not reflect the effect of chronically high levels of saturated or unsaturated FA in hepatocyte function and metabolism. Additionally, IR is often assessed *in vitro* by the expression levels or phosphorylation states of key proteins (such as Akt or FOXO1) which may not correlate with functional outputs (such as glucose clearance or production) [6, 81, 82].

Previous work in my lab has led to the development of an *in vitro* model of IHCTG accumulation which better reflects what the liver would be exposed to *in vivo*. This has been achieved by culturing hepatocytes in physiological mixtures of FAs; OPLA, a predominantly unsaturated FA mixture [83] and POLA, a predominantly saturated FA mixture [84]. The ratios of the four FAs contained in these mixtures reflect the physiological concentrations found in human serum [85] and are combined in media with a more representative concentration of glucose. Culturing hepatocytes under these conditions for prolonged periods of time may

provide novel insights into the effects of FA quantity and composition on IHCTG accumulation, IR and inflammatory activation.

1.5 Concluding remarks

MASLD is a leading cause of chronic liver disease worldwide and yet there are limited treatments as the underlying mechanisms are not fully understood. MASLD is associated with IR, inflammation and an aberrant decrease in autophagy, however the mechanisms underpinning these associations are unknown. Therefore, the aims of this thesis were the following:

1) To determine the effect of liver fat content on markers of selective hepatic insulin resistance and inflammation in humans;

2) To investigate the effects of fatty acid content and composition on autophagy, inflammatory activation and insulin resistance in an *in vitro* model of intrahepatocellular triglyceride accumulation; and

3) To explore the role of fatty acid content and composition on the autophagic processing of human-derived triglyceride-rich lipoproteins in an *in vitro* model of hepatocellular triglyceride accumulation.

'Nullae cogitationes,
vibes mondo'

2 Methods

Contents

2.1 Cell culture procedures 14
2.1.1 Routine cell culture 14
2.1.2 Passaging cells 14
2.1.3 Seeding cells for experiments 14
2.1.4 Freezing cells for storage in liquid nitrogen 15
2.1.5 Thawing cells from storage in liquid nitrogen 15
2.1.6 Experimental treatments 15
2.2 Quantification of gene expression 16
2.2.1 RNA extraction 16
2.2.2 RNA sequencing and data processing 16
2.3 Transcriptomics analysis 16
2.4 Protein quantification 17
2.4.1 Total protein 17
2.4.2 Western blotting 18
2.5 Quantification of autophagic flux 19
2.6 Lipid extraction and quantification 19
2.6.1 Lipid Extraction 19
2.6.2 Separation of lipid fractions 20
2.6.3 Lipid methylation 20
2.6.4 Gas Chromatography 21
2.7 Cell viability assay 21
2.8 Enzyme-linked immunosorbent assays (ELISAs) 21
2.9 Calculations and statistical analysis 22

2.1 Cell culture procedures

2.1.1 Routine cell culture

Human hepatocellular carcinoma cells (Huh7) were kindly provided by Dr Camilla Pramfalk (Karolinska Institutet, Sweden) and human hepatic stellate cells (LX2) by Hamish Miller (Blizard Institute, UK). Cells were cultured in maintenance media consisting of low glucose Dulbecco's modified Eagle's medium (DMEM) with GlutaMAX™ and pyruvate (ThermoFisher, 21885025) supplemented with 10 % foetal bovine serum (FBS, Seralab, EU-000-F), 1 % penicillin-streptomycin (P/S, Life Technologies, 15140122) and 1 % non-essential amino acids (NEAA, ThermoFisher, 11140035). Maintenance media was changed every 2-3 days and cells were kept in an incubator at 37 °C and 5 % carbon dioxide.

2.1.2 Passaging cells

Cells were grown to at least 80 % confluence in T175 (175 cm^2, Sarstdet, 83.3912.002) flasks before being washed with phosphate-buffered saline (PBS; Sigma, D1408-6X500ML) and then incubated for 5 mins in 4-5 mL of TrypLE™ (Life Technologies, 12604021). Flasks were then agitated to dislodge cells and 8 mL of maintenance media was added. Cells were centrifuged at 120 x g for 3 mins at room temperature. The supernatant was removed and the pellet was re-suspended in 5 mL of maintenance media before seeding 1:5 in new T175 flasks with maintenance media.

2.1.3 Seeding cells for experiments

Cells were isolated and re-suspended in maintenance media as described for passaging. 20 μL of cells were added to both sides of a Cellometer counting slide (VWR, NEXCCHT4-SD100-014) and cells were counted using a Cellometer Auto T4 Bright Field Cell Counter. An average of both sides was taken and cells were then diluted with maintenance media to a concentration of 1 x 10^5 cells per mL. Total cell number per well were as follows: 6-well plate - 2 x 10^5 (SLS, 3335), 12-well plate - 1 x 10^5 (SLS, 3336), 24-well plate - 0.5 x 10^5 (SLS, 3337), 96-well plate - 0.1 x 10^5 (SLS, 3300).

2.1.4 Freezing cells for storage in liquid nitrogen

During passaging, cells were isolated and resuspended in 10 mL freezing media made from 90 % maintenance media and 10 % dimethyl sulfoxide (DMSO, Sigma, D2650-5X5ML). 1 mL of the cell suspension was placed into each cryovial (Elkay, 127-T311-100) before being stored overnight in a -80 °C freezer in a Styrofoam holder to slow the rate of cooling. Cells were then transferred to liquid nitrogen for long-term storage.

2.1.5 Thawing cells from storage in liquid nitrogen

Frozen cells were placed in a 37 °C water bath to thaw rapidly. 500 μL of warm maintenance media was then added to the cryovial and mixed with a pipette. Cells were then seeded in a T75 (75 cm^2, Sarstdet, 83.3911.002) flask with maintenance media. Media was changed the next day and then every other day until cells reached at least 80 % and were passaged into a T175 flask.

2.1.6 Experimental treatments

Base experimental media was made from glucose-, phenol red- and glutamine-free DMEM (ThermoFisher, A1443001) supplemented with 2 % human serum (HS, Seralab, SM-412-HS, Lot BRH1108782), 1 % P/S, 1 % NEAA, 1 % GlutaMAX™ (Gibco™, 35050061) and 1 % sodium pyruvate (Gibco™, 11360070). Base media was supplemented with varying concentrations of human insulin (Life Technologies, 12585014), glucose (Life Technologies, A2494001), fructose or FA mixtures. The FA mixtures used in this thesis have been previously developed using a mixture of four FAs; oleic acid (OA; Sigma, O7501-1G), palmitic acid (PA; Sigma, P9767-5G), linoleic acid (LA; Sigma, L8134-100MG) and α-linolenic acid (Cayman Chemical, 90210-50 mg-CAY), in ratios that reflect the physiological concentrations found in human serum [85]: 45:30:24:1 (OPLA [83]) or 44:45:10:1 (POLA [84]). Cells were kept in an incubator at 37 °C and 5 % carbon dioxide for the duration of experimental treatments.

2.2 Quantification of gene expression

2.2.1 RNA extraction

Cells were cultured in 12- or 24-well plates and upon harvesting were washed twice with warm PBS before 250 μL of TRI Reagent® was added to each well. Cells were dislodged from the plate using a cell scraper and transferred into Eppendorf tubes to be frozen at -80 °C until required. Samples were then added to Phase Lock Gel tubes with 50 μL of chloroform and shaken vigorously and then left for 5 mins before being centrifuged for 15 mins at 1200 g and 4 °C. The clear supernatant was transferred to 2 mL tapered-bottom elution tubes containing 2 μL glycol blue and 200 μL isopropanol before being left overnight at -20 °C.

Samples were then centrifuged at 1200 g and 4 °C for 30 mins to allow an RNA pellet to form. The supernatant was removed and pellet resuspended in 80 % ethanol before being centrifuged again at 1200 g and 4 °C for 15 mins. The ethanol was then removed and the pellet allowed to dry before re-suspension in 15 μL RNase free water and incubation for 3 hours. RNA purity and concentration was then measured using a NanoDrop ND-1000 Spectrophotometer (ThermoFisher) and a 2200 TapeStation (Agilent, G2964AA).

2.2.2 RNA sequencing and data processing

Purified RNA samples were sent to Novogene for bulk RNA sequencing. Briefly, once RNA samples had passed their internal quality control, mRNA was isolated from total RNA using poly-T oligo-attached magnetic beads and a cDNA library was synthesised and then sequenced on an Illumina platform after further quality control checks.

Novogene also carried out the initial data processing which involved the following: Removal of low-quality reads or reads containing poly-N regions using in-house perl scripts, indexing and alignment of clean reads to a downloaded reference genome using Hisat2 (version 2.0.5) and finally counting reads mapped to each gene using featureCounts (version 1.5.0-p3).

2.3 Transcriptomics analysis

The following was carried out on all transcriptomic datasets in R (version 4.3.2) on RStudio (version 2024.04.2+764). Raw gene count data was filtered to remove genes with low expression,

and then normalised using the TMM method [86] with the EdgeR package (version 4.2.1) [87]. FactoMineR and factoextra packages were used to generate principle component analysis (PCA) plots to determine the main sources of variation in gene expression in each dataset.

The extreme differences in donor phenotype for the PHH dataset led to a large amount of variability in gene expression between replicates and so a mixed-effects model was used to analyse difference in gene expression for this dataset and all others. In this model, the experimental conditions are treated as fixed effects and the replicates are treated as a random effect rather than a fixed effect as well. This reduces the degrees of freedom and increases the statistical power of the model whilst still accounting for the random differences between replicates. Differential gene expression analysis using this model was performed using voomWithQualityWeights function from the limma package (version 3.60.4) to remove heteroscedascity from the data [88]. Genes were considered to be differentially expressed if the false discovery rate (FDR) < 0.05.

Venn diagrams were generated using the voomWithQualityWeights function from the limma package package (version 3.60.4), heatmaps using the gplots package (version 3.1.3.1) and Volcano plots using the EnhancedVolcano package (version 1.22.0) with cut-offs FDR < 0.05 and log fold change < 0.2. To determine which pathways were differentially regulated between conditions, gene set enrichment analysis (GSEA) was performed with the package clusterProfiler (version 3.0.4) using the Kyoto Encyclopedia of Genes and Genomes (KEGG) pathways database [89] and results were confirmed using the package fgsea (version 1.30.0) and the Molecular Signatures Database (MSigDB) hallmark gene set collection [90] as a comparison. Within each pathway, gene expression was visualised using KEGG pathways and the pathview package (version 1.44.0).

2.4 Protein quantification

2.4.1 Total protein

Cell samples were sonicated after harvesting and total protein content was measured using the Bio-Rad DC ™ kit (Bio-Rad, 5000111) according to the manufacturer's instructions. This assay is based on the Lowry method of protein quantification; the protein first reacts with copper in an alkaline solution, before Folin reagent is reduced by the protein-copper complex, which results in a blue colour change that can be read by spectrophotometer. Samples were diluted 1:5 in the same lysis buffer used to harvest and run in duplicate. Absorbance was read at 750

nm on a FLUOstar Omega plate reader (BMG Labtech) and a standard curve of bovine serum albumin (BSA) with concentrations 4-0.25 mg/mL run in duplicate and used for quantification.

2.4.2 Western blotting

Cells were harvested in radioimmunoprecipitation assay (RIPA) lysis buffer supplemented with protease (cOmplete™, 4693132001, Roche) and phosphatase (PhosSTOP™, 4906845001, Roche) inhibitors and total protein concentration was measured after sample sonication. Samples were diluted to 0.84 mg/mL protein in the lysis buffer and boiled for 10 mins at 80 °C in sodium dodecyl sulphate (SDS) sample loading buffer. The resulting denatured protein sample was then added to Criterion™ TGX Stain-Free™ Precast Gels at a volume of 30 µL, along with 5 µL BLUeye Prestained Protein Ladder (Sigma, 94964), and electrophoresis was carried out for 15 mins at 120 V and then 200 V for a further 30 mins in Tris Glycine SDS. The use of SDS as a buffer ensures the denatured proteins are negatively charged, meaning they move toward the positive charge generated at the bottom of the gel during electrophoresis. As smaller proteins move more quickly through the gel, proteins become distributed based on their molecular weight.

Proteins were then transferred onto methanol-activated Immobilon®-P PVDF membranes (Merck, IPVH00010) by electrophoresis using the Trans-Blot® Turbo™ Transfer System (Bio-Rad) at 25 V, 1 A for 30 mins in transfer buffer. Membranes were blocked with 5 % (w/v) powdered milk in tris-buffered saline with Tween 20 (TBST) for one hour to prevent non-specific antibody binding, before overnight incubation at 4 °C with primary antibodies diluted 1:1000 in 5 % milk in TBST. Membranes were then washed in TBST and incubated for one hour with the appropriate horseradish peroxidase-tagged secondary antibody diluted 1:5000 in 5 % milk in TBST. After washing again in TBST, protein bands were visualised by adding Immobilon® Crescendo Western HRP Substrate (Merck, WBLUR0100) and using a ChemiDoc™ MP Imaging System (Bio-Rad). Protein intensity was then quantified by densitometry and proteins of interest expressed relative to housekeeper proteins (β-actin or α-tubulin). The primary antibodies used in this thesis were as follows: anti-LC3 (Sigma, L8918), anti-p62 (Cell Signalling Technology, 5114), anti-α-tubulin (Abcam, ab52866), anti-β-actin (Abcam, ab8227).

2.5 Quantification of autophagic flux

Map1lc3b (LC3) is a small cytoplasmic protein which is lipidated to LC3-II and incorporated into the autophagosomal membrane during autophagy. When the autophagosome fuses with the lysosome, LC3-II is degraded along with the autophagosomal cargo [60]. Therefore, intracellular accumulation of LC3-II with and without an autophagic inhibitor can be used to quantify autophagic flux as follows: Autophagic flux (a.u.) = (LC3-II with inhibition - Basal LC3-II)/Basal LC3-II. LC3-II accumulation was measured by Western Blotting and bafilomycin A1 (BAF; Merck, B1793-2UG) was used as the autophagic inhibitor. BAF prevents both V-ATPase-dependent acidification of the lysosome and autophagosome-lysosome fusion and is a very commonly used in research as an autophagic inhibitor [91]. BAF concentration and length of incubation was optimised to maximised autophagic inhibition by quantifying the accumulation of LC3-II at different BAF concentrations and across different time points. Huh7 cells treated with 25 μM BAF for 3 hours showed the greatest LC3-II accumulation (and hence greatest autophagic inhibition) which is also in-line with the literature [92–94] and so this concentration and incubation time was used for all experiments.

2.6 Lipid extraction and quantification

Total lipids were extracted using the Folch method [95] and further lipid fractions (TG, FA and phospholipid) were then separated using solid phase extraction (SPE) and methylated [96]. Samples were then quantified by gas chromatography (GC). An internal standard containing known concentrations of glyceryl triheptadecanoate (15:0, Sigma-Aldrich, T2151-100MG), heptadecanoic acid (17:0, Sigma-Aldrich, H3500-1G) and 1,2-diheptanoyl-sn-glycero-3-phosphocholine (17:0, Sigma-Aldrich, P4148-100MG) was added to all samples before starting the extraction to calculate the concentration of the lipids in the sample.

2.6.1 Lipid Extraction

500 μL of cell (harvested in NP-40 lysis buffer and sonicated), media or plasma sample was used (or made up to this volume using 0.9 % saline). 5 mL of 2:1 chloroform:methanol (v:v) and 1 mL of 1 M sodium chloride solution was added and samples were mixed. Centrifugation

at 800 x g for 5 mins then separated the aqueous phase containing polar hydrophilic molecules from the lipid-containing solvent phase which was isolated and evaporated to dryness under nitrogen at 50 °C in a TurboVap LV (Biotage).

2.6.2 Separation of lipid fractions

ISOLUTE SPE columns (Biotage, 470-0010-A) contain aminopropyl silica, which forms hydrogen bonds with lipids and in combination with specific solvents, different lipid classes can be isolated using selective extraction and elution. Columns were firstly washed with acetone and chloroform before samples were reconstituted in 1 mL chloroform and applied to the columns. The TG and cholesterol ester fractions form weak bonds to the silica and were washed through and collected with further chloroform. FAs, which bond strongly to the columns, are then eluted and collected with the addition of 2 % acetic acid in diethyl ether (v/v) to disrupt this bond. The TG and cholesterol ester fraction was evaporated to dryness under nitrogen, reconstituted in 1 mL hexane and applied to new SPE columns prewashed with hexane. Hexane was further used to elute the cholesterol ester fraction and then hexane, chloroform and ethyl acetate (100:5:5 v/v/v) was used to elute the TG fraction which was collected.

2.6.3 Lipid methylation

TG and FA fractions were evaporated to dryness under nitrogen and methylated by reacting them with 400 μL toluene and 800 μL 1.5 % sulphuric acid in methanol (v/v) at 80 °C for 1 hour. Methylation is required to separate the FAs and reduce their polarity to allow accurate measurement via GC. Samples were then neutralised with 2 mL of neutralising solution (25 mM potassium hydrogen carbonate and 25 mM potassium carbonate in water) and 2 mL cyclohexane was added to extract the FA methyl esters (FAMEs). Samples were mixed and centrifuged at 800 x g for 5 mins before the solvent phase was collected and evaporated to dryness under nitrogen. Fractions were finally reconstituted in chloroform and had external standard (methyl tricosonate, 23:0, Sigma-Aldrich, T9900-1G) added.

2.6.4 Gas Chromatography

GC allows the separation of compounds within a sample based on the time it takes for them to travel through a column. Samples are initially vaporised and then the time taken for a compound to move through the column relies on its affinity to remain in the liquid, stationary phase or move with the mobile, gas phase. Samples were run on an Agilent 7890 GC using a J&W DB-WAX GC Column (Agilent, 125-7032) with helium as the reagent gas. Starting at 60 °C, the oven temperature was ramped to 200 °C at a rate of 20 °C per min, held for 12 mins, ramped to 220 °C at a rate of 2 °C per min, held for 2 mins, ramped to 230 °C at a rate of 1 °C per min and held for 25 mins. Sample FAMEs were identified by comparing their retention to a standard of 31 known FAMEs and quantified by comparing the peak area to that of the internal standard. The resulting micromolar quantities were summed and each FA was expressed as a percentage of this value (molar percentage; mol%).

2.7 Cell viability assay

Intracellular ATP concentration was measured as a reflection of the metabolic viability of the cell. Cells were cultured in black 96 well plates and the CellTiter-Glo 2.0 Assay (Promega, G9241) was performed to manufacturer's instructions. Luminescence was measured on a FLUOstar Omega plate reader (BMG Labtech) and compared to a standard curve of known ATP concentration.

2.8 Enzyme-linked immunosorbent assays (ELISAs)

Enzyme-linked immunosorbent assays (ELISAs) utilise antibodies and a detection signal to detect an antigen, usually a protein, peptide, hormone or antibody, from within a liquid sample in a 96-well plate format. For this thesis sandwich ELISAs were used, where capture antibodies are coated to the plate and will bind to the antigen in the sample during an incubation period. The plate is then washed to remove any unbound antigen before a detection antibody is added which also then binds to the antigen. The detection antibody may already be labelled or a labelled secondary antibody which binds to this detection antibody is added and the resulting signal can be quantified by absorbance measurement and compared to a standard curve of known concentration. ELISAs were performed according to the manufacturer's instructions and

read on a FLUOstar Omega plate reader (BMG Labtech). The ELISAs used in this thesis were as follows: IL-6 ELISA (Abcam, ab178013), Insulin ELISA (Mercodia, 10-1113-01), Glucagon ELISA (Mercodia, 10-1271-01) and Cytokeratin 18 Fragment ELISA (Abcam, ab254515).

2.9 Calculations and statistical analysis

All data was collected on Excel (Microsoft) and then analysed using R (version 4.3.2) on RStudio (version 2024.04.2+764). Unless stated otherwise, T-tests were used for comparisons between two groups of continuous data and for groups of more than two, one- or two-way ANOVAs were performed followed by *post-hoc* Tukey's testing for variables where ANOVA results indicated significance. All data is presented as mean ± standard deviation (sd) from at least three biological replicates unless otherwise stated and significance was set at $p < 0.05$.

'Nolle alere pretiosas machinas cum cannamella'

3

The effect of liver fat content on markers of selective hepatic insulin resistance and systemic inflammation in humans

Contents

3.1 Introduction 24
3.2 Methods 26
3.2.1 Participants 26
3.2.2 Study protocol 27
3.2.3 Analytical methods 27
3.2.4 Measurement of DNL 28
3.2.5 Measurement of GNG and GLY 28
3.2.6 Calculations and Statistical Analysis 29
3.3 Results 29
3.3.1 Participant characteristics 29
3.3.2 The effect of fasting plasma insulin and liver fat content on fasting GNG and GLY 30
3.3.3 The effect of fasting plasma insulin and liver fat content on fasting DNL 31
3.3.4 Further Phenotypic Grouping 34
3.3.5 The associations between GNG and DNL and multivariate analysis . . 38
3.3.6 The effect of fasting plasma insulin and liver fat content on systemic inflammation 38
3.4 Discussion 39
3.4.1 The effect of fasting plasma insulin and liver fat content on markers of selective hepatic IR 40
3.4.2 The effect of fasting plasma insulin and liver fat content on systemic inflammation 42
3.4.3 Limitations 43
3.4.4 Conclusions 44

3. The effect of liver fat content on markers of selective hepatic insulin resistance and systemic inflammation in humans

---

This chapter forms a large part of a manuscript by Felix A. Westcott, Shilpa R. Nagarajan, Sion A. Parry, Dragana Savic, Charlotte J. Green, Thomas Marjot, Elspeth Johnson, Thomas Cornfield, Kieran Smith, Ferenc E. Mózes, Paige O'Rourke, Jessica Mendall, David Dearlove, Barbara Fielding, Jeremy W. Tomlinson and Leanne Hodson, titled "Dissociation between liver fat content and fasting metabolic markers of selective hepatic insulin resistance in humans" *Published in the European Journal of Endocrinology. As the work presented in this chapter contains data from multiple published and unpublished studies, my contribution is as follows: Extraction of glucose from plasma samples and measurement of fractional gluconeogenesis, collation of data from studies and all data analysis. All other work was carried out by others using the methods described below.*

3.1 Introduction

In those free from metabolic disease, hormones such as insulin and glucagon orchestrate the switching of hepatic metabolism from energy release, in the fasting state to energy storage, in the postprandial state. These processes are thought to be dysregulated in IR, a condition strongly associated with obesity, MASLD, CVD and T2D [7, 14, 97]. IR is characterised by elevated plasma insulin, glucose and TG concentrations; however, it is unclear what drives these changes in humans.

Initially, it was thought that IR may be caused by impairments in the hepatic insulin receptor. Studies in rodents with a liver-specific insulin receptor knockout exhibited total hepatic IR with impaired suppression of GNG as well as impaired stimulation of DNL in response to insulin. The authors observed hyperglycaemia and hyperinsulinemia but normal plasma triglyceride concentrations and lack of hepatic steatosis in these animals, which was consistent with observations in humans with mutations in the insulin receptor but not those with IR [98, 99]. Based on these results, Brown et al. suggested that individuals with IR may instead exhibit a "selective resistance" to insulin whereby insulin loses its suppressive effect on GNG whilst paradoxically maintaining its stimulatory effect on DNL [100]. It was proposed that this so-called "selective hepatic insulin resistance" may drive the accumulation of liver

fat, along with the increased circulating levels of glucose, insulin and TG associated with IR; it implies that the impairment in insulin signalling must be downstream of the divergence of GNG and DNL pathways (Figure 3.1) [100–102]. While there are numerous studies in rodents and canines investigating the molecular mechanisms that drive this dichotomy [103–105], the existence of selective hepatic IR in humans has yet to be proven.

There are many ways of measuring insulin sensitivity in humans. Fasting plasma glucose and insulin are frequently used as markers of IR clinically however the current gold standard is the hyperinsulinemic-euglycemic clamp where the participant's plasma glucose pool is labelled by a primed infusion of a glucose stable isotope (most commonly ^{13}C glucose). Blood samples are taken and when isotopic enrichment is measured on the GC-MS, EGP and disposal can be calculated from the dilution of the labelled pool by newly synthesised unlabelled glucose molecules according to the Steele Equations [106]. The participants plasma glucose can then be clamped to a fixed concentration and, their EGP and glucose disposal in response to an insulin administration, can be measured. Although this method gives an indication of systemic insulin sensitivity, the concentration of insulin administered does not reflect the concentration the liver is exposed to from the hepatic portal vein following a meal. Similarly, hyperinsulinemic-euglycemic clamps cannot normally distinguish between GNG and glucose produced from glycogen breakdown (glycogenolysis, GLY), the only other major form of EGP [107] and rarely measure the effects of insulin on DNL or glycogen synthesis [6]. Therefore, for the work undertaken in this chapter, hyperinsulinemic-euglycemic clamps were not used and participants instead consumed deuterated water (^2H_2O) as a stable isotope tracer before an overnight fast to allow the relative contributions of both GNG to plasma glucose and DNL-derived FA to VLDL-TG to be measured [108, 109]. The aim of this work was to determine whether metabolic signatures of selective hepatic IR (increased GNG and DNL) are associated with hyperinsulinemia or liver fat content in fasting humans. Increased liver fat content and hyperinsulinemia are both thought to contribute to systemic inflammation which may drive disease progression in MASLD [110, 111]. However, their frequent co-existence in individuals can make it challenging to disentangle the relative effects of each but the sample size and spectrum of metabolic phenotypes of this cohort of participants made it possible to investigate these effects as well.

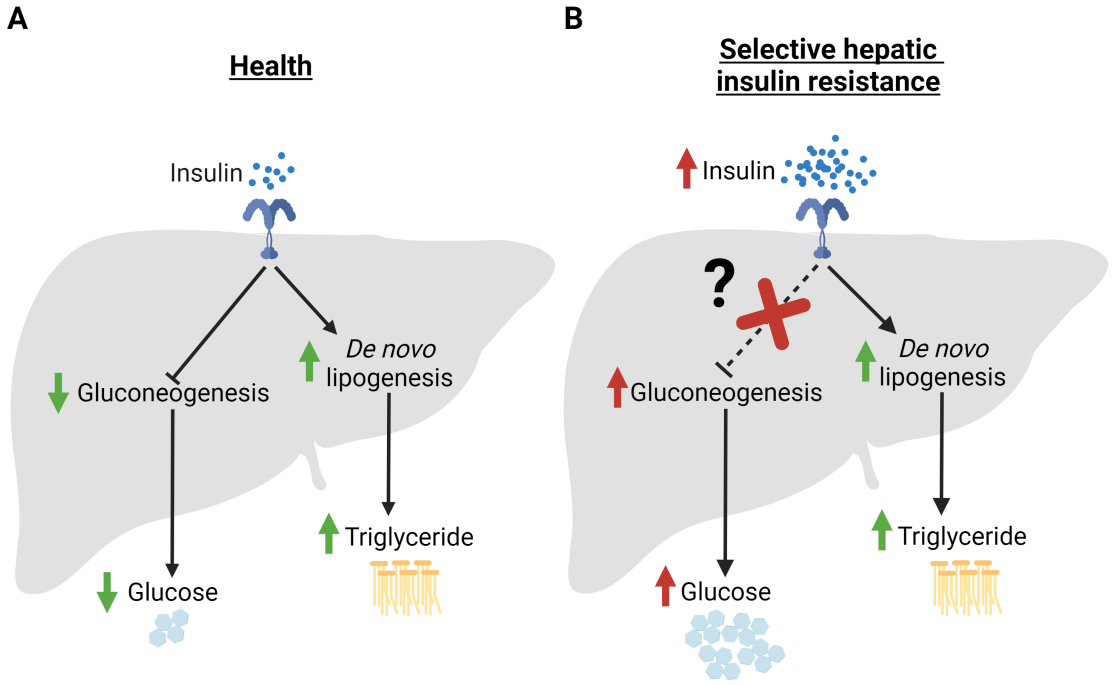


Figure 3.1: Insulin regulation of glucose and triglyceride production in health and in selective hepatic insulin resistance. A) In those free from metabolic disease insulin will up-regulate *de novo* lipogenesis and inhibit gluconeogenesis leading to an increase in plasma triglyceride concentrations and a decrease in plasma glucose concentrations. **B)** In those with insulin resistance it has been suggested that insulin loses its suppression on gluconeogenesis such that it is also upregulated in response to insulin leading to increased plasma concentrations of both glucose and triglyceride.

3.2 Methods

3.2.1 Participants

Participants (n=177, 101 female and 76 male) were recruited from the Oxford BioBank (www.oxfordbiobank.org.uk) [112], by advertisement and from hepatology clinics at the John Radcliffe Hospital. All volunteers were not taking medication known to affect lipid or glucose metabolism, did not smoke, and did not consume alcohol above recommended limits. 86 individuals (49 %) were considered hyperinsulinemic (HI) with fasting plasma insulin concentrations greater than the 75thcentile (11.2 U/mL) of the Oxford Biobank [113, 114] and 91 were considered normoinsulinemic (NI). When split by liver fat, 60 participants (34 %) were considered to have high liver fat (HF) with a liver fat content higher than the 95thcentile (5.56 % liver fat) of the Dallas Heart Study [115–117] and 117 participants were considered to have

low liver fat (LF). Participants were then further grouped as normoinsulinemic with low liver fat content (NILF), normoinsulinemic with high liver fat content (NIHF), hyperinsulinemic with low liver fat content (HILF) or hyperinsulinemic with high liver fat content (HIHF). The studies included were approved by the Oxfordshire, Portsmouth, North of Scotland, North West Lancaster, North East Tyne & Wear and South Clinical Research Ethics Committees. All subjects gave written informed consent. Some, but not all, of the data reported, constitute a reanalysis of previously published studies, and only data from the fasting time point of the pre-intervention/baseline study day has been included in this study [114, 118–122].

3.2.2 Study protocol

Participants were asked to avoid alcohol and strenuous exercise for 24 hours prior to their study day as this can affect basal metabolic state. The evening beforehand $^{2}H_2O$ (3 g/kg body water) was consumed in two doses (to minimise side-effects such as dizziness) for the measurement of fasting hepatic GNG and DNL. Participants then attended the clinical research unit the next morning after an overnight fast and a cannula was inserted into an antecubital vein on one arm from which a fasting blood sample was taken. Body composition and body fat percentage were measured using dual-energy X-ray absorptiometry (DEXA) which uses X-rays of two different energy levels to determine the density of tissue. Liver fat content was measured within one week of the study day using magnetic resonance spectroscopy (^{1}H-MRS), as previously described [123].

3.2.3 Analytical methods

Whole blood was collected into heparinized syringes (Sarstedt, Leicester, UK) and centrifuged at 4 °C to isolate plasma. Concentrations of plasma glucose, glycerol, NEFA, total and high-density lipoprotein (HDL) cholesterol, TG and 3-hydroxybutyrate (3-OHB) were analysed on a semi-automatic analyser (ILab 600/650 clinical chemistry; Werfen, Warrington, U.K.). For 125 participants (77 female and 48 male), fasting plasma concentrations of IL-6 were measured by ELISA (Abcam, ab178013) and fasting plasma concentrations of alanine and glycoprotein acetyls were measured using a nuclear magnetic resonance (NMR) metabolomics platform (Nightingale Health, Helsinki, Finland). Very low-density lipoprotein (VLDL) fractions (Svedberg flotation 20–400) were isolated using density gradient ultra-centrifugation [124].

3. The effect of liver fat content on markers of selective hepatic insulin resistance and systemic inflammation in humans

3.2.4 Measurement of DNL

TG was extracted from VLDL fractions and FA methyl esters were prepared as described in Chapter 2 section 2.6. FA compositions (µmol/100 µmol total FA) were determined using GC, which were subsequently used to calculate palmitate concentrations [113]. Tracer enrichments in extracted VLDL fractions were determined by gas chromatography-mass spectrometry (GC-MS) [113]. Deuterium incorporation from $^{2}H_2O$ in plasma water (Finnigan GasBench II; Thermo Fisher Scientific, Paisley, UK) into VLDL-TG palmitate was determined using GC-MS with monitoring ions with mass-to-charge ratios (m/z) of 270 (M+0) and 271 (M+1) [109]. DNL was calculated as the percentage contribution of newly synthesized palmitate to VLDL-TG (fractional DNL, frDNL) which could then be multiplied by the plasma concentration of VLDL to give an absolute concentration of newly synthesized palmitate to VLDL-TG.

3.2.5 Measurement of GNG and GLY

Glucose was extracted from participant plasma based on a previously described method [125]. Briefly, plasma was deproteinized with ethanol and 2 % methylhydroxylamine hydrochloride in pyridine (w/v) added to the dried supernatant. Samples were then heated, cooled and BSTFA + 1 % TCMS was added, before being reheated, cooled, and dried. Samples were reconstituted in decane, and tracer enrichment analysed by GC-MS with selected ion monitoring for ions with a mass-to-charge ratio (m/z) of 319 (M+0) and 320 (M+1). The contribution of GNG to plasma glucose concentration (fractional GNG, frGNG) was calculated using the "average" method [108] which was adapted and validated for my derivative [125]. Briefly, at low plasma water enrichments, it is assumed all of the hydrogen atoms have an equal chance of being labelled during the synthesis of a new glucose molecule. It is therefore possible to calculate the average deuterium enrichment of the glucose derivative by dividing the molar percent enrichment by the number of possible labelling sites on the glucose derivative which is then divided by the $^{2}H_2O$ enrichment in plasma water to give frGNG. Fractional GLY was determined as the inverse of frGNG [107]. As EGP was not measured, absolute rates of GNG and GLY could not be calculated. However, to include differences in pool sizes, the plasma glucose concentration derived from GNG and GLY was calculated by multiplying plasma glucose concentration by fractional GNG and GLY respectively.

3.2.6 Calculations and Statistical Analysis

The homeostatic model assessment for insulin resistance (HOMA-IR) was calculated based on fasting glucose and insulin measurements as previously described [126]. The glucagon-alanine index, a marker of hepatic glucagon signalling, was calculated by multiplying fasting plasma glucagon and alanine concentrations as previously described [127]. All statistical analysis was performed in R (version 4.2.2 for Windows, RStudio, US). For comparisons between groups, Chi-squared tests were used for categorical data and continuous data was tested for normality followed by independent t-tests or non-parametric equivalent using the Benjamini-Hochberg correction for multiple comparisons if required. Pearson's correlation coefficient is presented for normally distributed variables with a linear relationship, otherwise Spearman's rank correlation coefficient is used. For multivariate analysis, independent variables were entered only if they exhibited a significant univariate association and the model was then refined through backwards elimination. Homoscedasticity was checked using scatterplot of standardized residual over standardized predictors and the residuals were checked for approximately normal distribution using a normal Q-Q plot. Scatterplots are fitted with linear regression line and 95 % confidence interval.

3.3 Results

3.3.1 Participant characteristics

When participants were defined as either NI or HI, there was no difference in age or sex however those in the HI group had higher BMI, fat mass and liver fat content (Table 3.1). Analysis of participant fasting plasma biochemistry showed higher glucose, glucagon and TG concentrations in the HI group compared to the NI group (Table 3.1). When participants were defined by liver fat content, the HF group had a greater proportion of men compared to the LF group (60 vs 34 % respectively, $p<0.01$) but there was no difference in age between groups (Table 3.2). Participants in the HF group had a higher BMI and fat mass as well as higher fasting plasma glucose, insulin, glucagon, and TG concentrations compared to the LF group (Table 3.2). The HI and HF groups had higher HOMA-IR and glucagon-alanine indices than NI and LF groups, respectively.

3. The effect of liver fat content on markers of selective hepatic insulin resistance and systemic inflammation in humans

	NI (≤11.2 U/mL), *n = 91*	**HI** (>11.2 U/mL), *n = 86*
Female / Male	57 / 34	44 / 42
Age	48 ± 1	47 ± 1
BMI	25.6 (19.5 - 35.2)	29.5 (21.7 - 45.6)***
Fat mass (%)	33 ± 1	37 ± 1***
Lean mass (%)	67 ± 1	63 ± 1***
IHCTG (%)	2 (0 - 24)	6 (0 - 38)***
HOMA-IR	1.9 (0.2 - 2.8)	3.6 (2.3 - 23.5)***
Glucagon-alanine index[1]	1.3 (0.0 - 5.6)	3.4 (0.1 - 10.9)***
Fasting plasma biochemistry		
Glucose (mmol/L)	5.0 (3.4 - 6.2)	5.5 (4.5 - 11.2)***
Insulin (U/mL)	9 (1 - 11)	15 (11 - 72)***
Glucagon (pmol/L)	5 (0 - 29)	9 (0 - 46)***
NEFA (µmol/L)	513 (93 - 1,093)	536 (172 - 1,252)
TG (mmol/L)	0.9 (0.3 - 3.9)	1.4 (0.3 - 4.5)***
3OHB (µmol/L)	53 (15 - 580)	57 (14 - 560)
Total Chol (mmol/L)	5.1 ± 0.1	5.0 ± 0.1
HDL Chol (mmol/L)	1.4 (0.4 - 2.6)	1.1 (0.3 - 2.2)***
Non-HDL Chol (mmol/L)	3.6 (1.9 - 6.7)	3.8 (2.2 - 6.4)
Lactate (mmol/L)	0.9 (0.5 - 2.4)	1.0 (0.6 - 1.8)*
Glycerol (µmol/L)	47 (11 - 172)	46 (15 - 164)

Table 3.1: Participant characteristics defined by fasting plasma insulin. Normally distributed data are presented as mean ± sem. Non-normally distributed data are presented as median (min - max). *p<0.05, **p<0.01, ***p<0.001 normoinsulinemic (NI) vs hyperinsulinemic (HI) groups. [1]Measured in 117 participants. Abbreviations: BMI, Body Mass Index; IHCTG, Intrahepatic Triglyceride; HOMA-IR, Homeostatic Model Assessment for Insulin Resistance; NEFA, Non-Esterified Fatty Acid; TG, Triglyceride; 3OHB, 3-Hydroxybutyrate; HDL, High-Density Lipoprotein; Chol, Cholesterol.

3.3.2 The effect of fasting plasma insulin and liver fat content on fasting GNG and GLY

It was found that there was a sexual dimorphism in the contributions of GNG and GLY to fasting blood glucose concentration with male participants having significantly higher frGNG than female participants (27 vs 25 %, p=0.045). Due to this difference metabolic data was split by sex and analysed separately.

Despite differences in fasting plasma glucose concentration, when fasting frGNG was measured in this cohort I found no significant difference between NI and HI groups in either male or female participants (Figures 3.2a and 3.3a). However, there was a trend (p=0.068) for frGNG to be lower in the HF group compared to the LF group in male participants which was not seen

3. The effect of liver fat content on markers of selective hepatic insulin resistance and systemic inflammation in humans

	LF (≤5.56 %), *n = 117*	**HF** (>5.56 %), *n = 60*
Female / Male	77 / 40	24 / 36**
Age	47 ± 1	48 ± 1
BMI	25.6 (19.5 - 35.6)	30.5 (23.5 - 45.6)***
Fat mass (%)	34 ± 1	38 ± 1***
Lean mass (%)	66 ± 1	62 ± 1***
IHCTG (%)	1 (0 - 5)	12 (6 - 38)***
HOMA-IR	2.2 (0.2 - 4.9)	4.3 (1.0 - 23.5)***
Glucagon-alanine index[1]	1.4 (0.0 - 5.0)	4.1 (0.5 - 10.9)***
Fasting plasma biochemistry		
Glucose (mmol/L)	5.1 (3.4 - 6.6)	5.5 (3.9 - 11.2)***
Insulin (U/mL)	10 (1 - 21)	17 (4 - 72)***
Glucagon (pmol/L)	5 (0 - 35)	13 (1 - 46)***
NEFA (µmol/L)	497 (93 - 1,093)	562 (218 - 1,252)
TG (mmol/L)	0.9 (0.3 - 4.1)	1.7 (0.3 - 4.5)***
3OHB (µmol/L)	54 (15 - 580)	55 (14 - 301)
Total Chol (mmol/L)	5.0 ± 0.1	5.0 ± 0.1
HDL Chol (mmol/L)	1.4 (0.4 - 2.6)	1.1 (0.3 - 1.8)***
Non-HDL Chol (mmol/L)	3.6 (1.9 - 6.4)	3.9 (2.2 - 6.7)
Lactate (mmol/L)	0.9 (0.5 - 2.4)	1.0 (0.6 - 1.8)**
Glycerol (µmol/L)	45 (11 - 172)	48 (17 - 164)

Table 3.2: Participant characteristics defined by liver fat content. Normally distributed data are presented as mean ± sem. Non-normally distributed data are presented as median (min - max). *p<0.05, **p<0.01, ***p<0.001 low (LF) vs high (HF) liver fat groups. [1]Measured in 117 participants. Abbreviations: BMI, Body Mass Index; IHCTG, Intrahepatic Triglyceride; HOMA-IR, Homeostatic Model Assessment for Insulin Resistance; NEFA, Non-Esterified Fatty Acid; TG, Triglyceride; 3OHB, 3-Hydroxybutyrate; HDL, High-Density Lipoprotein; Chol, Cholesterol.

in female participants (Figures 3.2b and 3.3b). The absolute concentration of plasma glucose from GNG did not differ between the fasting plasma insulin or liver fat content groups but the absolute concentration of glucose from GLY was higher in the HI compared to NI group and the HF compared to LF group across all participants (Figures 3.2c-d and 3.3c-d).

3.3.3 The effect of fasting plasma insulin and liver fat content on fasting DNL

To examine the association of fasting DNL with hyperinsulinemia and liver fat content, fasting frDNL was measured and found to be higher in HI participants compared to NI participants (6.2 vs 5.2 %, p=0.034) but this significance was lost when split by sex (Figures 3.2e and 3.3e). There was also no difference in fasting frDNL between LF and HF groups (Figures 3.2f and

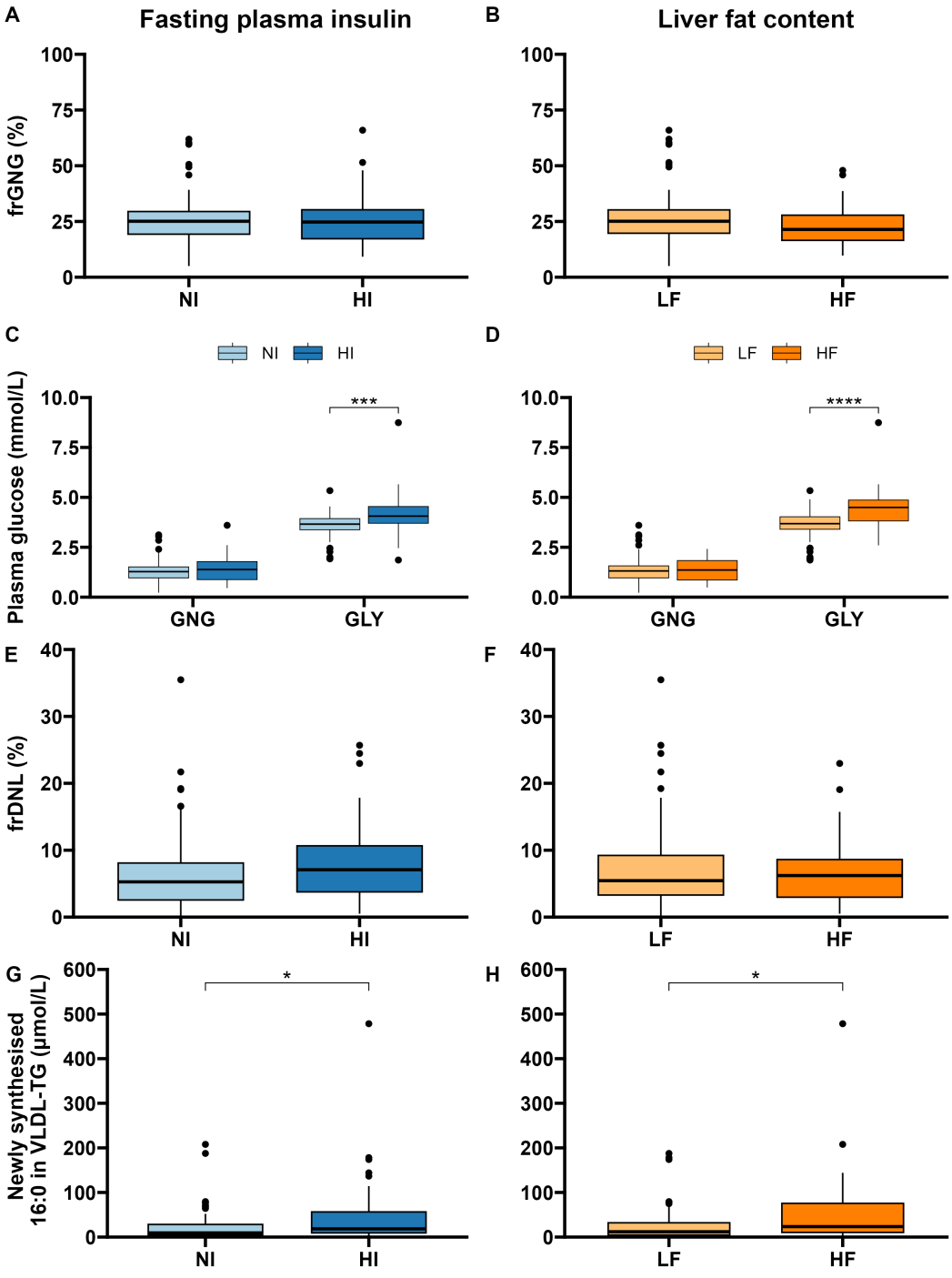


Figure 3.2: The effect of fasting plasma insulin and liver fat content on GNG, GLY and DNL in female participants. Female participants (n = 101) were classified as normoinsulinemic or hyperinsulinemic (NI or HI) and as having low or high liver fat content (LF or HF). **A-B)** Fractional gluconeogenesis (frGNG) was measured across the groups and **C-D)** the absolute contributions of gluconeogenesis (GNG) and glycogenolysis (GLY) to fasting plasma glucose concentration were calculated. **E-F)** Fractional *de novo* lipogenesis was measured across the groups (frDNL) and **G-H)** the absolute concentration of newly synthesized 16:0 to very-low-density lipoprotein-triglyceride (VLDL-TG) was calculated. Data presented as median and quartiles. $^{*}p<0.05$, $^{***}p<0.001$, $^{****}p<0.0001$ or p-value stated.

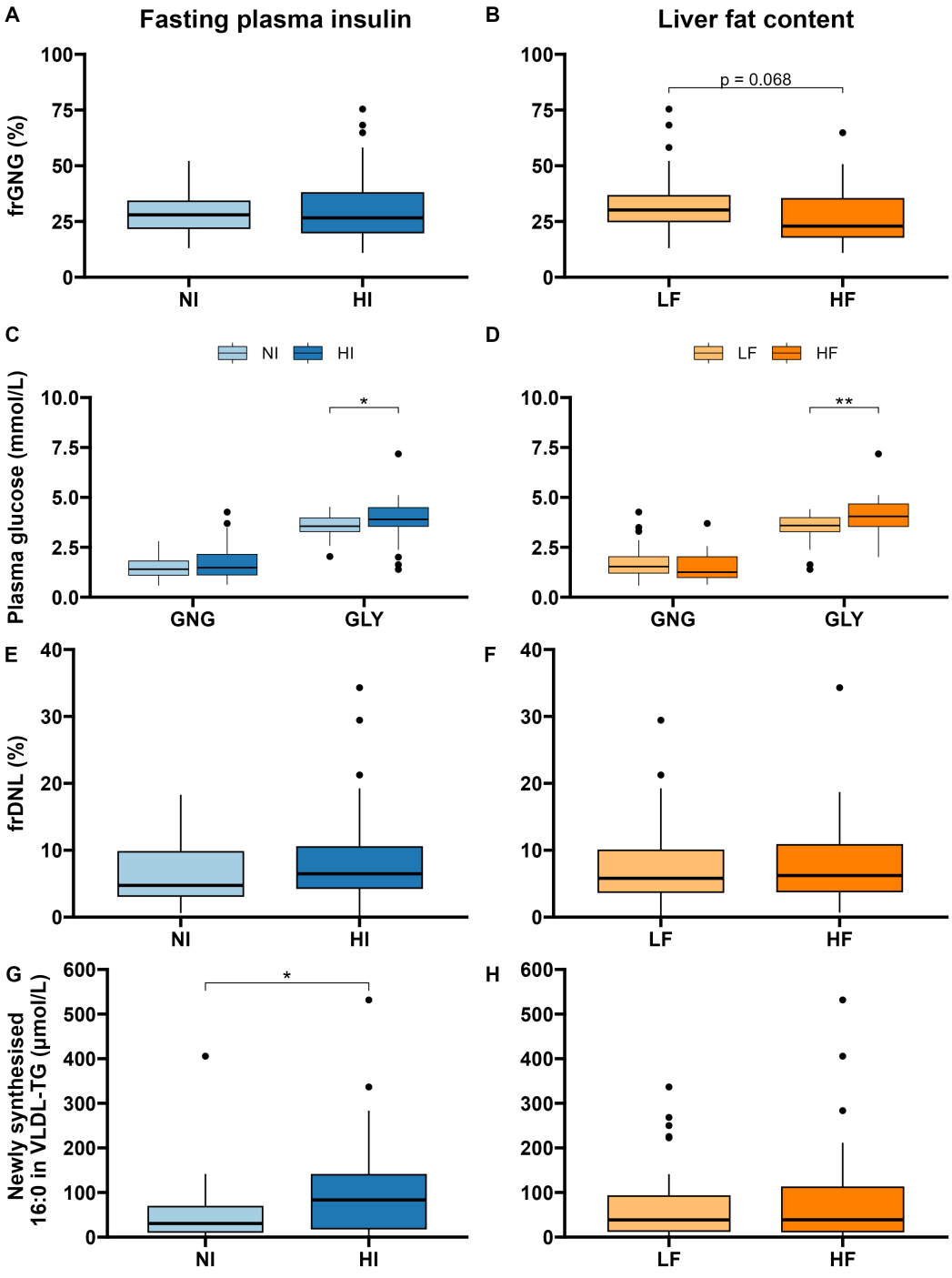


Figure 3.3: The effect of fasting plasma insulin and liver fat content on GNG, GLY and DNL in male participants. Male participants (n = 76) were classified as normoinsulinemic or hyperinsulinemic (NI or HI) and as having low or high liver fat content (LF or HF). **A-B)** Fractional gluconeogenesis (frGNG) was measured across the groups and **C-D)** the absolute contributions of gluconeogenesis (GNG) and glycogenolysis (GLY) to fasting plasma glucose concentration were calculated. **E-F)** Fractional *de novo* lipogenesis was measured across the groups (frDNL) and **G-H)** the absolute concentration of newly synthesized 16:0 to very-low-density lipoprotein-triglyceride (VLDL-TG) was calculated. Data presented as median and quartiles. $^{*}p<0.05$, $^{**}p<0.01$ or p-value stated.

3.3f). The absolute concentration of DNL-derived FA to VLDL-TG was higher in both the HI and HF groups compared to the HI and LF groups, respectively, in female participants (Figures 3.2g-h) but only the HI compared to NI group in male participants (Figures 3.3g-h).

3.3.4 Further Phenotypic Grouping

Although significantly different, there were large overlaps in liver fat content between the fasting plasma insulin groups and in fasting plasma insulin between the liver fat content groups (Tables 3.1-3.2) so to further explore the impact of both plasma and liver fat content together participants were characterised as NILF (n=75), NIHF (n=16), HILF (n=42) or HIHF (n=44). The NIHF and HIHF groups had significantly greater proportions of male participants compared to the NILF group (Table 3.3). There was no difference in age between the groups, but participants in the NILF group had significantly lower BMI compared to participants from each of the other groups. Participants in the NILF group also had significantly higher HDL cholesterol but lower plasma glucagon and TG compared each of the other groups, whilst those in the HIHF and HILF groups had significantly higher fasting plasma glucose compared to the NILF group (Table 3.3).

There were no significant differences in fasting frGNG between the four groups in female participants (Figure 3.4a) but there was a trend (p=0.085) for it to be higher in the HILF compared to HIHF group in male participants (Figure 3.5a). Correspondingly, the HIHF group had a higher absolute concentration of plasma glucose from GLY compared to each of the other groups in male participants (Figure 3.5b) and compared to all other groups except for NIHF in female participants (Figure 3.4b). However, there were no other differences in plasma glucose from either GLY or GNG between the groups in either sex (Figures 3.4b-c and 3.5b-c). When frDNL was measured across the four groups, no differences were found in either sex (Figures 3.4d and Figure 3.5d) however the HIHF group had a higher concentration of DNL-derived FA in VLDL-TG compared to the NILF group in female participants (Figure 3.4e). In contrast, the HIHF group had a higher concentration of DNL-derived FA in VLDL-TG compared to the NILF group in male participants (Figure 3.5e).

	NILF n = 75	**NIHF** n = 16	**HILF** n = 42	**HIHF** n = 44
Female / Male	54 / 21	3 / 13***	23 / 19	21 / 23**
Age	48 ± 1	47 ± 2	46 ± 1	48 ± 1
BMI	25.5 (19.5 - 31.3)	27.2 (24.2 - 35.2)*	27.3 (21.7 - 35.6)*	33.4 (23.5 - 45.6)***
Fat mass (%)	33 ± 1	33 ± 2	35 ± 1	40 ± 1***
Lean mass (%)	67 ± 1	67 ± 2	65 ± 1	60 ± 1***
IHCTG (%)	1 (0 - 5)	7 (6 - 24)***	2 (0 - 5)	14 (6 - 38)***
HOMA-IR	1.9 (0.2 - 2.8)	2.0 (1.0 - 2.6)	3.1 (2.3 - 4.9)***	5.2 (2.9 - 23.5)***
Glucagon-alanine index[1]	1.2 (0.0 - 3.8)	2.8 (0.7 - 5.6)**	1.9 (0.1 - 5.0)**	4.4 (0.5 - 10.9)***
Fasting plasma biochemistry				
Glucose (mmol/L)	5.0 (3.4 - 6.2)	5.1 (3.9 - 5.7)	5.2 (4.5 - 6.6)***	5.7 (4.5 - 11.2)***
Insulin (U/mL)	9 (1 - 11)	9 (4 - 11)	13 (11 - 21)***	20 (13 - 72)***
Glucagon (pmol/L)	5 (0 - 29)	9 (1 - 27)**	7 (0 - 35)**	16 (1 - 46)***
NEFA (µmol/L)	532 (93 - 1093)	508 (237 - 873)	455 (172 - 874)	578 (218 - 1252)
TG (mmol/L)	0.8 (0.3 - 2.0)	1.6 (0.5 - 3.9)***	1.1 (0.3 - 4.1)**	1.7 (0.3 - 4.5)***
3OHB (µmol/L)	56 (15 - 580)	40 (17 - 273)	50 (22 - 560)	60 (14 - 301)
Total Chol (mmol/L)	5.0 ± 0.1	5.3 ± 0.3	5.1 ± 0.1	4.9 ± 0.1
HDL Chol (mmol/L)	1.5 (0.4 - 2.6)	1.1 (0.5 - 1.3)***	1.2 (0.6 - 2.2)**	1.0 (0.3 - 1.8)***
Non-HDL Chol (mmol/L)	3.4 (1.9 - 6.0)	4.2 (2.2 - 6.7)**	3.7 (2.2 - 6.4)	3.8 (2.2 - 6.1)
Lactate (mmol/L)	0.8 (0.5 - 2.4)	1.0 (0.7 - 1.1)	0.9 (0.6 - 1.3)	1.1 (0.6 - 1.8)**
Glycerol (µmol/L)	51 (11 - 172)	38 (23 - 114)	37 (15 - 114)	49 (17 - 164)

Table 3.3: Participant characteristics defined by phenotype. Normally distributed data are presented as mean ± sem. Non-normally distributed data are presented as median (min - max). *p<0.05, **p<0.01, ***p<0.001 compared to the NILF group. [1]Measured in 117 participants. Abbreviations: BMI, Body Mass Index; IHCTG, Intrahepatic Triglyceride; HOMA-IR, Homeostatic Model Assessment for Phenotype Resistance; NEFA, Non-Esterified Fatty Acid; TG, Triglyceride; 3OHB, 3-Hydroxybutyrate; HDL, High-Density Lipoprotein; Chol, Cholesterol.

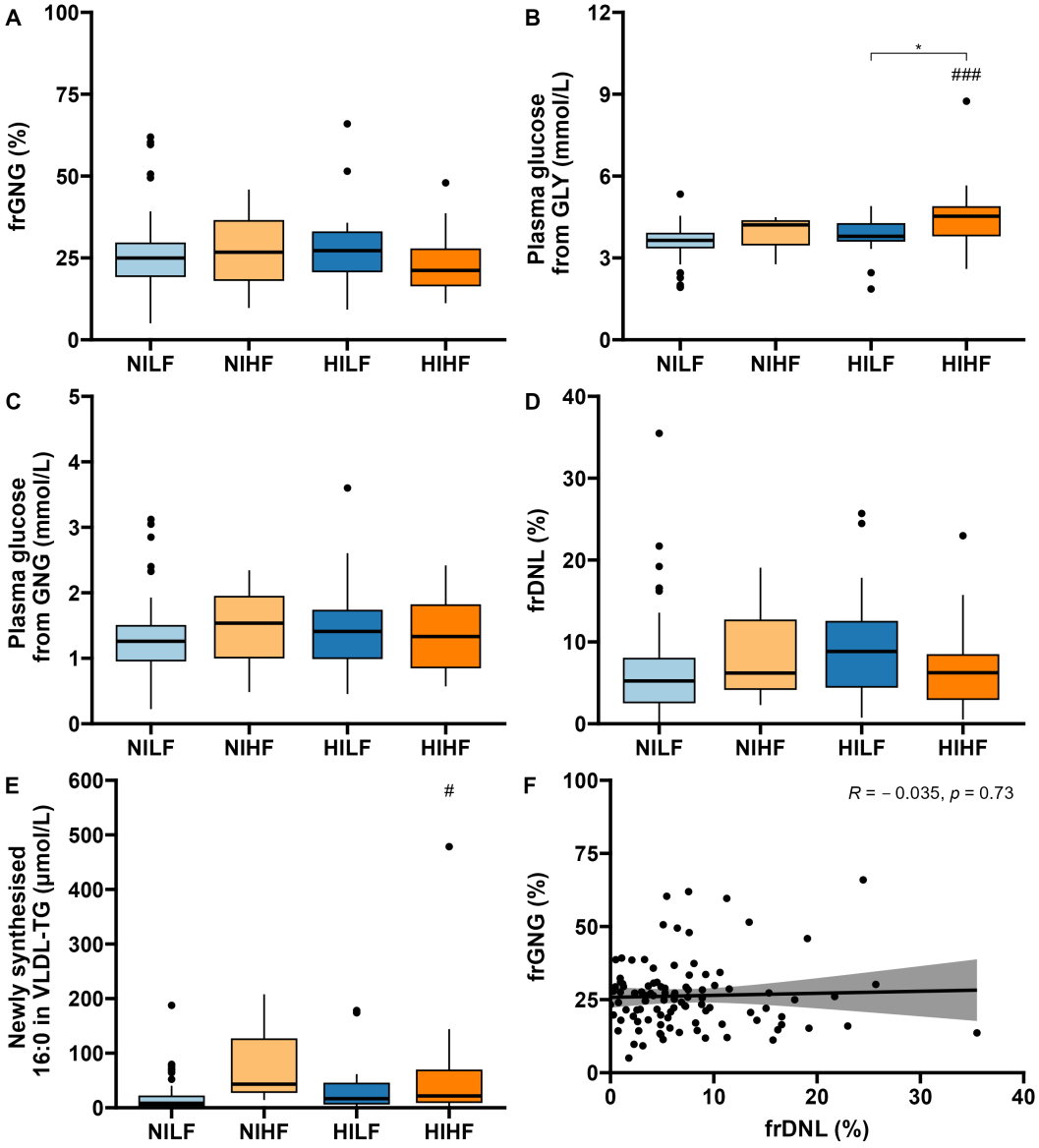


Figure 3.4: Further phenotypic grouping in female participants. Female participants were grouped as normoinsulinemic with low liver fat content (NILF), normoinsulinemic with high liver fat content (NIHF), hyperinsulinemic with low liver fat content (HILF) or hyperinsulinemic with high liver fat content (HIHF). **A)** Fractional gluconeogenesis (frGNG) was measured and the absolute contributions of **B)** glycogenolysis (GLY) and **C)** gluconeogenesis (GNG) to fasting plasma glucose concentration were calculated. **D)** Fractional *de novo* lipogenesis across groups (frDNL) and **E)** absolute contributions of newly synthesized 16:0 to very-low-density lipoprotein-triglyceride (VLDL-TG). **F)** A correlation was performed across female participants between fractional gluconeogenesis (frGNG) and fractional *de novo* lipogenesis (frDNL). Data presented as median and quartiles. $^{\#}p<0.05$, $^{\#\#\#}p<0.001$ compared to NILF group and $^{*}p<0.05$ for all other comparisons shown or p-value stated.

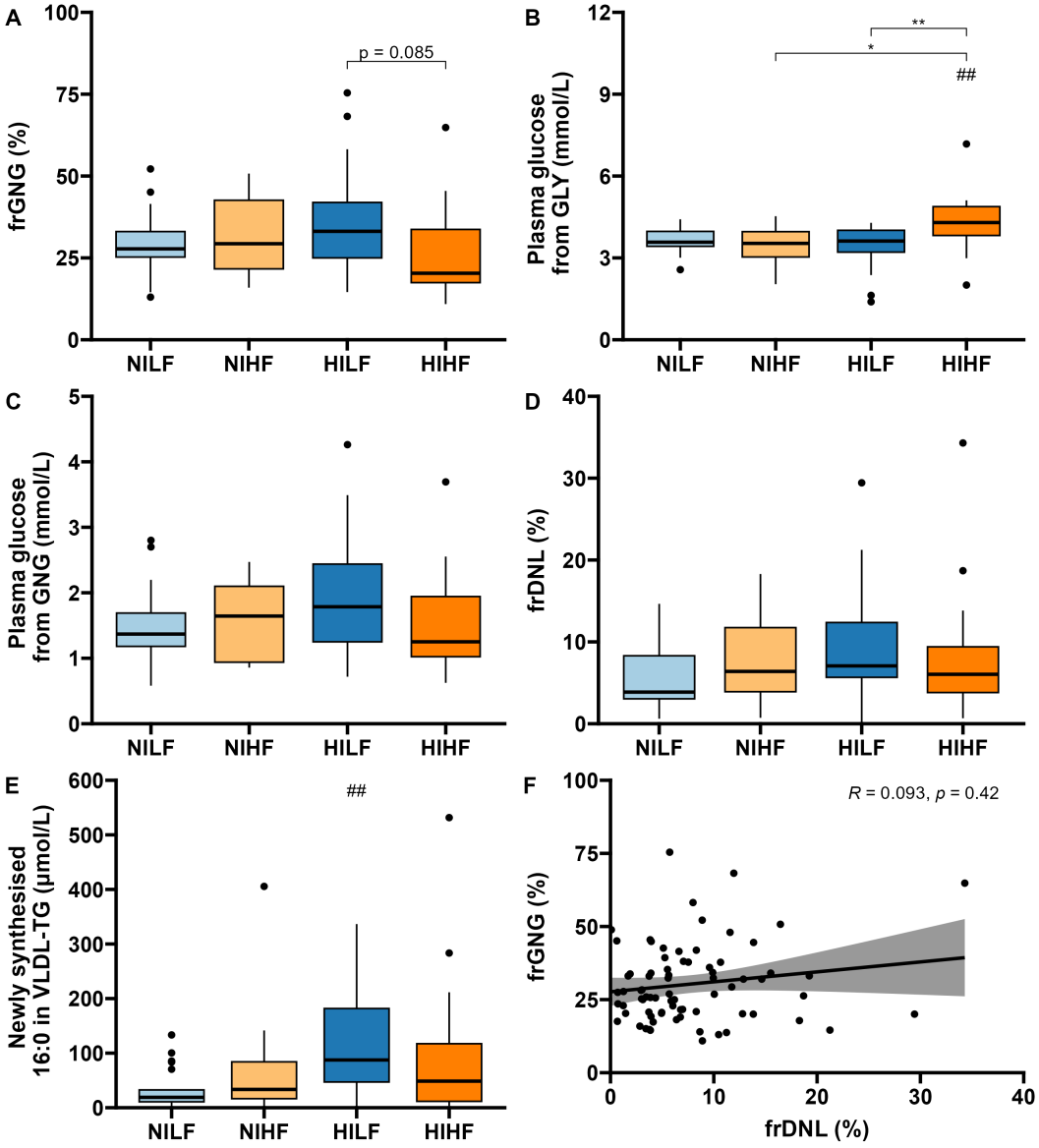


Figure 3.5: Further phenotypic grouping in male participants. Male participants were grouped as normoinsulinemic with low liver fat content (NILF), normoinsulinemic with high liver fat content (NIHF), hyperinsulinemic with low liver fat content (HILF) or hyperinsulinemic with high liver fat content (HIHF). **A)** Fractional gluconeogenesis (frGNG) was measured and the absolute contributions of **B)** glycogenolysis (GLY) and **C)** gluconeogenesis (GNG) to fasting plasma glucose concentration were calculated. **D)** Fractional *de novo* lipogenesis across groups (frDNL) and **E)** absolute contributions of newly synthesized 16:0 to very-low-density lipoprotein-triglyceride (VLDL-TG). **F)** A correlation was performed across male participants between fractional gluconeogenesis (frGNG) and fractional *de novo* lipogenesis (frDNL). Data presented as median and quartiles. $^{\#\#}p<0.01$ compared to NILF group and $^{*}p<0.05$, $^{**}p<0.01$ for all other comparisons shown or p-value stated.

3.3.5 The associations between GNG and DNL and multivariate analysis

As a key metabolic signature of selective hepatic insulin is the upregulation of both GNG and DNL, I assessed the association between fasting frGNG and frDNL and found no significant correlation in either sex (Figures 3.4f and 3.5f). To determine which variables best predicted participant insulin group (HI or NI) and liver fat content group (HF or LF), multiple logistic regression was carried out across all variables measured and on all participants. The main predictors for plasma insulin were BMI (β=0.179, p=0.002), fasting plasma glucose (β=1.71, p<0.001) and glucagon (β=0.0816, p=0.018) concentrations (pseudo-R^2=0.379). Whereas the main predictors for liver fat content were glucagon-alanine index (β=0.667, p=0.003), HOMA-IR (β=0.970, p=0.002), and fasting plasma HDL cholesterol (β=-4.03, p=0.003) and glycerol (β=0.0524, p<0.001) concentrations (pseudo-R^2=0.766). Neither frGNG nor frDNL were significant predictors in either model.

3.3.6 The effect of fasting plasma insulin and liver fat content on systemic inflammation

IL-6 and glycoprotein acetyls (GlycA) are two markers of systemic inflammation with the former being strongly associated with MASLD development and progression [128, 129] and the latter acting as a more stable and sensitive alternative to C-reactive protein (CRP) [130, 131]. Concentrations of these markers were measured to provide insight into the effect of fasting plasma insulin and liver fat content on systemic inflammation. IL-6 concentrations did not differ between participants split by either liver fat content or plasma insulin concentrations (Figure 3.6a-b) but GlycA was found to be higher in HI compared to NI and HF compared to LF participants (Figure 3.6c-d).

When participants were split by both fasting plasma insulin and liver fat content no differences in plasma IL-6 concentrations were seen across the four groups (Figure 3.7a). In contrast, GlycA was lower in participants in the NILF group compared to those in all other groups and HIHF participants had higher concentrations than HILF participants (Figure 3.7b).

3. The effect of liver fat content on markers of selective hepatic insulin resistance and systemic inflammation in humans

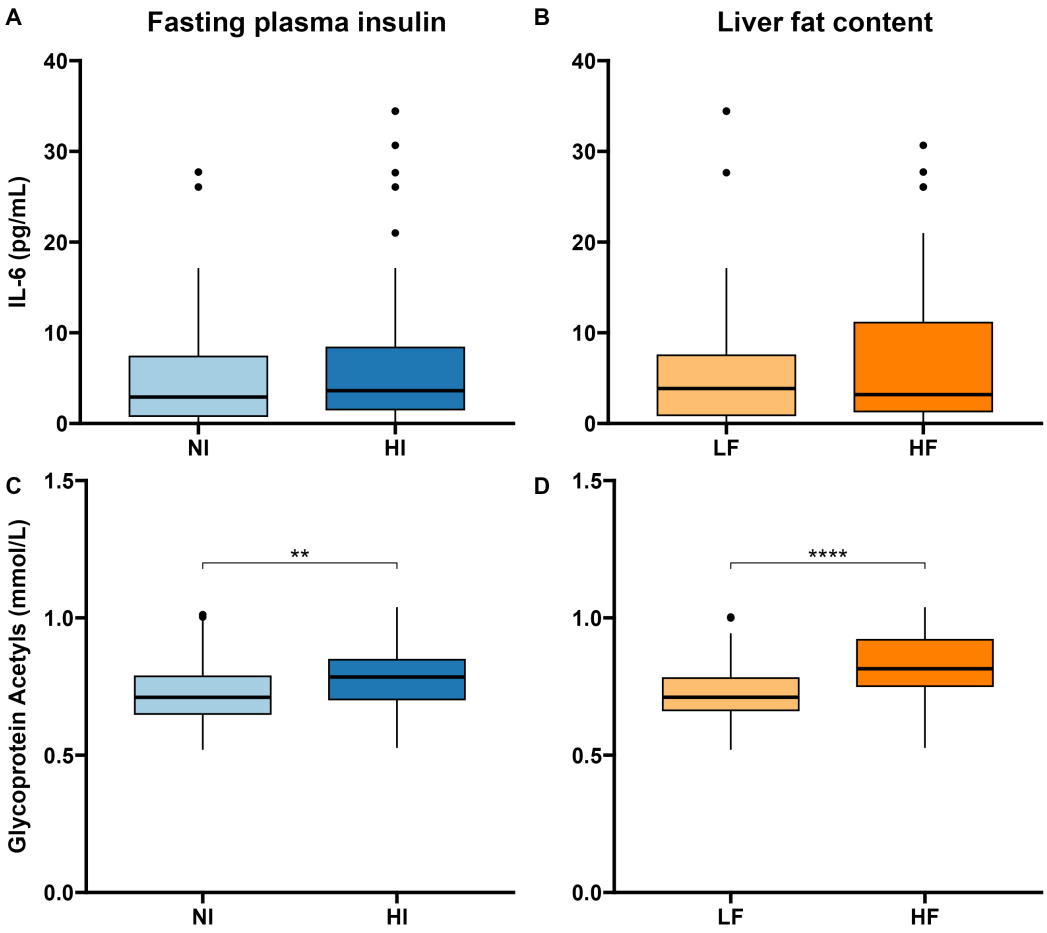


Figure 3.6: The effect of fasting plasma insulin and liver fat content on systemic inflammation. Participants (n = 125) were classified as normoinsulinemic or hyperinsulinemic (NI or HI) and as having low or high liver fat content (LF or HF). **A-B)** Concentrations of IL-6 and **C-D)** glcoprotein acetyls were measured across the groups. Data presented as median and quartiles. $^{**}p<0.01$, $^{****}p<0.0001$.

3.4 Discussion

Elevated fasting plasma glucose and TG concentrations are characteristic of IR, which is strongly associated with T2D and MASLD. The underlying mechanism in humans is unclear although rodent models have suggested this may be due to selective hepatic IR whereby insulin loses its inhibitory control over GNG but maintains its stimulatory effect on DNL [100]. As fasting hyperinsulinemia is a hallmark of IR, this would suggest a chronic upregulation of both GNG and DNL in those with IR which is suggested to drive the observed fasting hyperglycemia and hypertriglyceridemia. This study measured the relative and absolute contributions of both GNG to plasma glucose and DNL-derived FA to VLDL-TG in 177 fasted participants

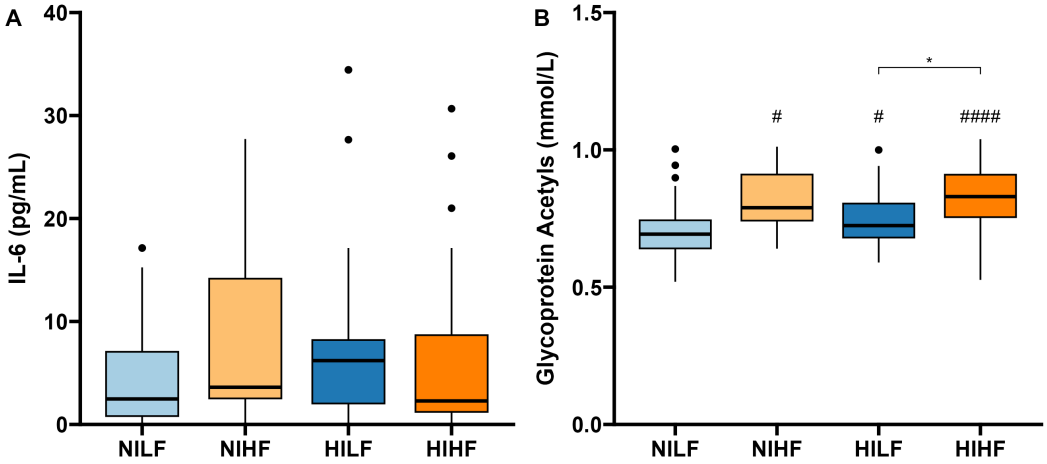


Figure 3.7: The effect of further phenotypic grouping on systemic inflammation. Participants (n=125) were grouped as normoinsulinemic with low liver fat content (NILF), normoinsulinemic with high liver fat content (NIHF), hyperinsulinemic with low liver fat content (HILF) or hyperinsulinemic with high liver fat content (HIHF).**A)** Concentrations of IL-6 and **B)** glcoprotein acetyls were measured across the groups. Data presented as median and quartiles. $^{\#}p<0.05$, $^{\#\#\#\#}p<0.0001$ compared to NILF group and $^{*}p<0.05$, $^{**}p<0.01$ for all other comparisons shown.

and found no clear metabolic signature of selective hepatic IR associated with fasting plasma insulin concentration or liver fat content. This suggests that such signatures may only be detected postprandially or in more extreme phenotypes.

3.4.1 The effect of fasting plasma insulin and liver fat content on markers of selective hepatic IR

In-line with others [14, 132], I found that individuals classified as HI or HF had significantly higher plasma glucose concentrations compared to those classified as NI and LF, respectively. Although increased fasting glucose concentrations are often suggested to be driven by increased hepatic GNG in those with metabolic disease [14, 133], I found no significant differences in fractional or absolute contributions of GNG between participants of either sex characterised by fasting plasma insulin or liver fat content.

Others who also utilised $^{2}H_2O$ to measure GNG and GLY, similarly reported no difference in fasting frGNG between individuals with and without T2D despite notable differences in plasma glucose concentration [37, 134, 135]. In conjunction with my results, this suggests that both GNG and GLY may be upregulated in those with IR and contribute equally to fasting hyperglycemia. However, glucose disposal was not measured so it is also plausible that

the elevation in fasting plasma glucose may also come from a decrease in glucose clearance as has also been observed in those with IR [136, 137]. Therefore, it would be of interest to measure the insulin sensitivities of other tissues (such as skeletal muscle and adipose) in a similar cohort of individuals. Glycogen cycling may also account for a proportion of the glucose produced from GLY when measured using this method [39]. Glycogen cycling is the simultaneous synthesis and breakdown of glycogen which is thought to be negligible in individuals free from metabolic disease but is higher in those with T2D [37].

There are fewer studies exploring the relationship between frGNG and liver fat content but those that have reported no association between these variables [38]. Similarly, I found no difference in frGNG between participants in the HF group compared to the LF group. There was, however, a tendency for frGNG to be higher in male HF participants than male LF participants suggesting a greater reliance on GLY, the only other form of EGP. Similarly, when participants were classified into groups based on both plasma insulin and liver fat content, male participants in the HIHF group tended to have lower frGNG than those in the HILF group and individuals defined as HIHF had a significantly higher contribution of GLY to plasma glucose concentrations compared to the other groups across both sexes. Previous studies have shown that excess hepatocellular glycogen is common in MASLD patients and associated with higher fasting plasma glucose concentrations [138]. Taken together this may suggest a positive association between liver fat content and glycogen storage in the liver and potentially other tissues (e.g. skeletal muscle) and that those with HF utilize this pool more for glucose production than LF individuals, contributing to a rise in plasma glucose concentration.

In conjunction with this hypothesis, previous studies have shown that MASLD is associated with disruption of the liver-α-cell axis [139] and similarly I found the glucagon-alanine index to be one of the strongest predictors of participant liver fat content group in multiple linear regression analysis. This is suggested to be due to an impairment in glucagon signalling at the level of hepatic amino acid metabolism [127] and elevated plasma glucagon concentrations, as also seen in HF compared to LF participants, are thought to be a compensatory mechanism to this impairment [127]. Glucagon is thought to preferentially drive an increase in EGP through GLY rather than GNG [140] and thus may further drive a GLY increase in HF participants. Taken together, this suggests that liver fat content is positively associated with an increase in

GLY, especially in those with HI. In this cohort, it appears that this effect is more prominent in men than women however, this is likely due to the significantly higher proportion of men in the HF group compared to the LF group.

Elevated fasting plasma TG concentration is associated with MASLD, T2D and IR [114, 132] and this is thought to be driven by an increase in hepatic DNL as several studies have shown an increase in fasting frDNL in these patients [30, 114, 141]. Whilst I also found that fasting plasma TG concentrations were significantly higher in HI and HF compared to NI and LF groups, respectively, frDNL was only higher in those with HI compared to NI but did not differ between the HF and LF groups. Similarly, when participants were classified by plasma insulin and liver fat, only those in the HILF group had significantly higher frDNL compared to NILF participants. However, these effects were lost when the participants were split by sex, possibly due to the lower statistical power. Despite similarities in frDNL, there were some sexual divergences in the absolute contributions of DNL-derived FA to VLDL-TG which suggested that HF female participants had a larger VLDL-TG pool than LF female participants but the VLDL-TG pool was relatively similar between liver fat content groups in male participants. Taken together, these observations suggest that DNL is predominantly driven by hyperinsulinemia, rather than liver fat content in both sexes. In support of this, previous studies have reported a higher frDNL in individuals with HI compared to NI despite a large overlap in liver fat between groups [114]. Previous studies which have shown higher frDNL in MASLD patients compared to lean and obese controls have had, on average, higher liver fat compared to those in my HF group [31]. Similarly, it is plausible that the duration of liver fat accumulation and the composition of the liver fat may have a greater effect on DNL than the quantity itself.

3.4.2 The effect of fasting plasma insulin and liver fat content on systemic inflammation

Both hyperinsulinemia and high liver fat content are associated with markers of systemic inflammation but few studies have examined the associations of both within the same cohort. In this study, higher GlycA concentrations were associated with both hyperinsulinemia and high liver fat content but the difference between HF and LF participants was higher than that between HI and NI participants. Similarly, within the HI group, those with HF had higher GlycA than

those with LF which together suggests a greater effect of HF on GlycA levels than HI. Despite having similar patterns to GlycA, no difference was observed in IL-6 concentration between groups. This may be due to GlycA being a more sensitive biomarker of low-grade systemic inflammation used to measure risk of metabolic disease [130, 131] whereas IL-6 is indicative of more severe systemic inflammation, as seen in those with T2D and MASLD [128, 129], which may not have been present in this cohort that was predominantly free from known metabolic disease.

3.4.3 Limitations

This study is not without limitations. Whilst clinical biomarkers of IR, such as plasma insulin and glucose, are commonly measured at fasting, this state is not reflective of a dynamic response to insulin. It has been suggested that insulin loses its suppression on glucose production in those with IR following a meal so it would be of interest to measure dynamic changes in GNG, GLY and DNL in the postprandial state or in response to insulin administration where more of a divergence may have been seen between my groups [6, 142, 143]. Similarly, I measured the contributions of GNG and GLY to fasting plasma glucose concentration but additional measurement of EGP to calculate the absolute rates of GNG and GLY may increase the sizes of the effects. Furthermore, the majority of the cohort studied were Caucasian middle-aged adults and it would be of interest to study a cohort across a broader spectrum of age and ethnicity. Similarly, it has been shown that fasting frGNG may only be increased in those with severe hyperglycemia whereas my HI and HF groups had only moderately raised plasma glucose concentrations [144, 145] so it may be beneficial to continue this study in participants with more extreme metabolic phenotypes. Participants were advised to consume a meal that was in accordance with the UK Eat Well Guidelines the evening prior to the study day, however I cannot exclude the possibility that differences in habitual macronutrient intake may have influenced my fasting measures of DNL and GNG.

While my values for frGNG tended to be lower than what has previously been reported [36, 146, 147], internal validation of this method with that of Chacko et al. [108] indicated that this was not due to the use of a different glucose derivative as a similar frGNG was observed using their derivative. Instead, the difference may be due to the length of the overnight fast being shorter at 10-12 hours, whereas most other studies have reported an overnight fast between 14-16 hours [36,

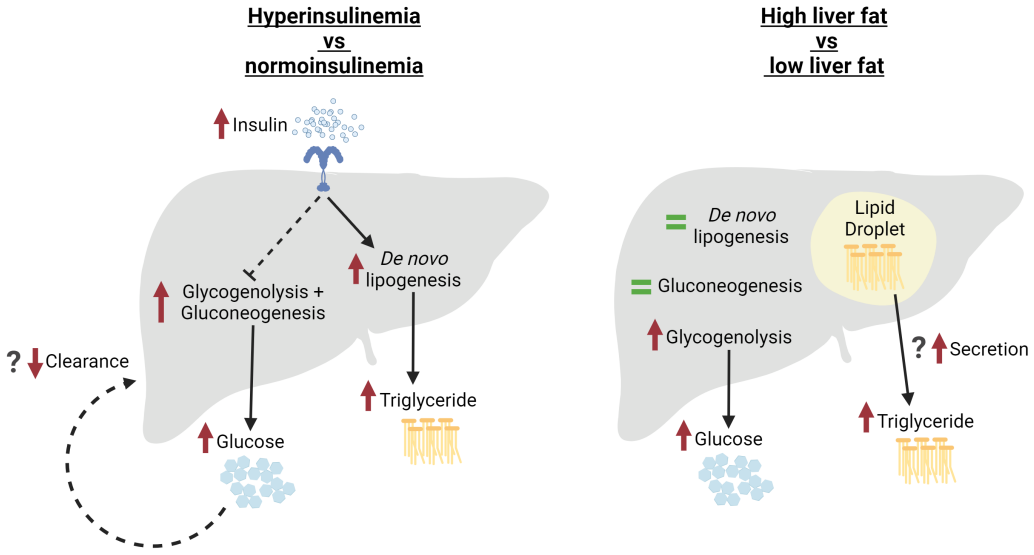


Figure 3.8: Proposed mechanisms underlying hyperglycemia and hypertriglyceridemia. Compared to participants with normoinsulinemia, those with hyperinsulinemia had higher de novo lipogenesis which may drive the elevated plasma triglyceride concentration. An increase in both gluconeogenesis and glycogenolysis (as well as a possible decrease in glucose clearance) may explain the higher plasma glucose levels in those with hyperinsulinemia compared to normoinsulinemia. Participants with high liver fat content had no change in either de novo lipogenesis or gluconeogenesis compared to those with low liver fat content and the elevated plasma glucose and triglyceride concentrations may be driven by increased glycogenolysis and triglyceride secretion from lipid droplets, respectively.

146]. In this study female participants had a significantly lower frGNG than the male participants, which may, in part, explain the lower levels of frGNG in this cohort, which was predominantly female compared to previous studies which have been predominantly male [36, 147].

3.4.4 Conclusions

It is often suggested that the fasting hyperglycemia and hypertriglyceridemia in humans with metabolic disease is driven by an upregulation of both GNG and DNL in the liver. Despite some initial evidence in rodents, this so-called selective hepatic IR has yet to be clearly demonstrated in humans. In a cohort of male and female UK adults I was unable to find the proposed metabolic signature of selective hepatic IR associated with hyperinsulinemia or high liver fat content.

Instead, I found that DNL appears to be driven by plasma insulin concentration rather than liver fat content and that GLY may play a larger role in contributing to fasting hyperglycemia than previously thought, especially in those with high liver fat content, which appears to be similar across both sexes (Figure 3.8). Additionally, low-grade systemic inflammation was associated with both hyperinsulinemia and high liver fat content with the latter having a greater effect.

'Habendum est oxygenium moleculis ut viverent'

4

Developing a suitable *in vitro* model of intrahepatocellular triglyceride accumulation

Contents

4.1 Introduction 47
4.2 Methods 49
4.2.1 Experimental treatments 49
4.2.2 Analytic techniques 49
4.2.3 Culture of primary human hepatocytes 49
4.2.4 Lipid droplet imaging and quantification 50
4.3 Results 51
4.3.1 The effect of media fatty acids on hepatocyte viability 51
4.3.2 The effect of media fatty acids on intrahepatocellular triglyceride accumulation 52
4.3.3 The effect of media fatty acids on autophagy 55
4.3.4 The effect of media fatty acids on autophagic and inflammatory gene expression 55
4.4 Discussion 60
4.4.1 The effect of FAs on cell viability 60
4.4.2 The effects of FAs on IHCTG accumulation 61
4.4.3 The effects of FAs on autophagy 62
4.4.4 The effect of FAs on inflammatory activation 63
4.4.5 Conclusions 64

4.1 Introduction

MASLD is a major disease burden worldwide, affecting almost one in three people [20]. It is characterised by the accumulation of ectopic fat in the liver (steatosis), identified by biopsy or scanning, in those at risk of cardiometabolic disease and covers a spectrum of diseases from simple steatosis to steatohepatitis and more severe liver disease, including hepatocellular carcinoma and cirrhosis [17]. The process underlying the intrahepatocellular triglyceride (IHCTG) accumulation is unclear, but biopsies from patients with MASLD have also shown a decrease in markers of autophagy [61]. Autophagy is a crucial cellular process for degrading intracellular cargo, such as LDs and mitochondria via the lysosome and can regulate other processes such as inflammatory activation and LD lipolysis [51, 148]. Previous *in vivo* human studies have suggested that an increase in dietary fat intake, specifically SFAs, can increase the risk of MASLD development and progression [149, 150] but the effects of FAs on autophagy remain unclear. Taking the available evidence together, it is plausible that a FA-mediated decrease in hepatocellular autophagy may contribute to the inflammatory activation and IHCTG accumulation seen in MASLD but this has yet to be demonstrated in human models (Figure 4.1).

Metabolic and autophagic processes occur in a constant flux which is especially challenging to measure *in vivo* in humans. One opportunity to gain insight is the use of stable isotopes as demonstrated in chapter 3, however quantification of *in vivo* autophagic flux is, as of yet, not possible so other models must be utilised. Liver biopsies can offer a unique opportunity to measure these processes *ex vivo* but these can only capture a single time point and do not provide insight into the aetiology and progression of MASLD. Similarly, difficulties in obtaining healthy tissue make it challenging to interpret data without a suitable control group. For *in vitro* models, although primary human hepatocytes (PHHs) are often considered the gold standard, they come with challenges that need to be considered such as variability in donor phenotype and genotype, short time frame of survival and cost [71]. Therefore, human hepatocellular cancer cells lines (such as Huh7 and HepG2) are frequently used.

The majority of *in vitro* models of IHCTG accumulation expose Huh7 or HepG2 cells to a single dose of a FA (typically either oleic acid (OA) or palmitic acid (PA)) for an acute period of time (between 8 and 48 hours) [71]. However, as hepatocytes are constantly exposed to a mix of FAs *in vivo*, culturing them in a single individual FA is not physiologically representative, nor

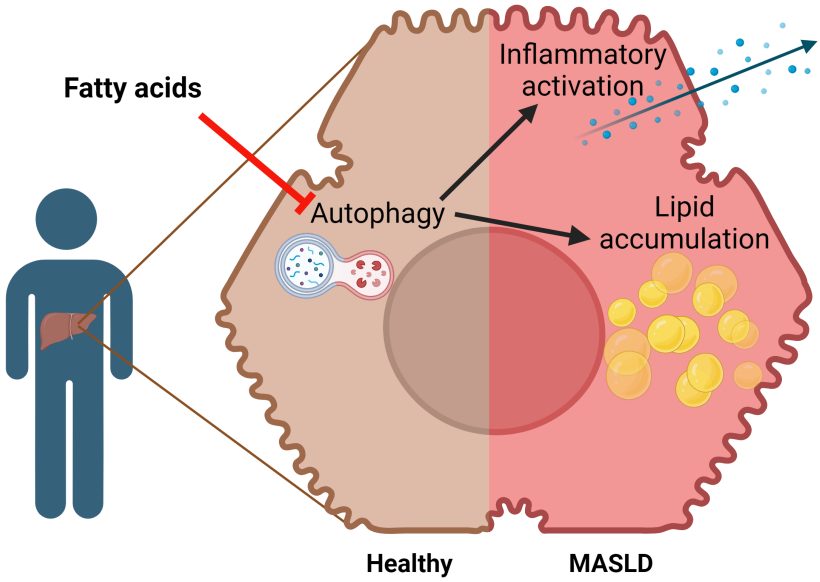


Figure 4.1: Proposed effects of fatty acids on hepatocellular autophagy, triglyceride accumulation and inflammatory activation. It has been suggested that fatty acids may inhibit hepatocellular autophagy which could lead to accumulation of lipids and inflammatory activation and hence MASLD development and progression. Abbreviations: MASLD, metabolic dysfunction-associated steatotic liver disease.

is the typically short treatment period, which may represent an acute insult to the hepatocyte rather than the chronic accumulation of intrahepatocellular TG seen in MASLD pathogenesis. Additionally, concentrations of FAs and sugars used are often supraphysiological with little rationale given, making it challenging to translate findings to humans *in vivo*.

Previous work in my lab has led to the development of an *in vitro* model of IHCTG accumulation which better reflects what the liver would be exposed to *in vivo* by culturing hepatocytes in physiological mixtures of FAs; OPLA, a predominantly unsaturated FA mixture [83] and POLA, a predominantly saturated FA mixture [84], along with a more representative concentration of glucose and use of HS instead of FBS. Hepatocytes are also cultured for at least four days with media changes every 2-3 days. This chapter aimed to determine if this more physiologically representative model of IHCTG accumulation could be used to investigate the effect of FA on autophagy and inflammation.

4.2 Methods

4.2.1 Experimental treatments

Base experimental media as described in Chapter 2 section 2.1.6 was then supplemented with 5.5 mM glucose, 0.1 nM insulin and 0 μM (Control) or 800 μM of FA mixture OPLA or POLA. Experimental media was changed every 2-3 days for either 4 or 7 days before harvesting.

4.2.2 Analytic techniques

Lipid extraction and quantification, autophagic flux and ATP assays, and RNA extraction and transcriptomic analysis were all carried out as described in Chapter 2 sections 2.2-2.6.

4.2.3 Culture of primary human hepatocytes

PHHs were purchased commercially (ThermoFisher, HMCPSQ) from human donors (three female and two male) and stored in liquid nitrogen. The donor phenotype was provided by the supplier and is shown in Table 4.1. When required for seeding an experiment, plating media was made consisting of 500 mL Williams E Medium (ThermoFisher, A1217601) supplemented with a Primary Hepatocyte Thawing and Plating Supplements (ThermoFisher, CM3000) which contained FBS, dexamethasone, and a cocktail of FBS, penicillin-streptomycin, insulin, GlutaMAX^{TM} and HEPES solution. The frozen cells were placed in a 37 °C water bath to thaw rapidly. 500 μL of warm plating media was then added to the cryovial and mixed with a pipette before the entire contents was transferred to a falcon tube containing 4.5 mL of warm plating media. Cell number and viability was then quantified using Trypan blue stain (ThermoFisher, 15250061) and a Cellometer Auto T4 Bright Field Cell Counter. Cells were then diluted with plating media and seeded into plates which had been pre-coated collagen type 1 (ThermoFisher, A1048301) at a density of 35,000 cells/well for 96-well plates, 150,000 cells/well for 24-well plates or 50,000 cells/well for 12 mm diameter glass cover slips for microscopy experiments. PHHs were cultured in plating media overnight following seeding before changing to experimental media which consisted of Williams E Medium (ThermoFisher, A1217601) and Primary Hepatocyte Maintenance Supplements (ThermoFisher, CM4000) containing dexamethasone and a cocktail of penicillin-streptomycin, insulin, transferrin, selenium complex, BSA, and LA, GlutaMAX^{TM}, and HEPES solution, supplemented with 2 % HS and either 0

Sex	Race	Age (years)	BMI	Tobacco history	Alcohol history	Drug history	Cause of death
Female	African american	31	18.9	Yes	Yes	Marijuana	Asphyxiation
Female	African american	65	39.6	Yes	Yes	Atorvastatin, cholecalciferol, bydureon	Unknown
Male	Caucasian	46	32.1	1 pack/day for 34 years	2-4 drinks per month	Cannabis for 30 years, cocaine for 1 year	Asphyxiation
Male	Asian	47	23.9	1 pack/day for 20 years	6 beers/day for 20 years	Cannabis daily for 20 years	Anoxia /stroke
Female	Caucasian	55	22.8	2-3 cigarettes /day for 2 months	4 drinks/day for 32 years	Cannabis daily for 5 years	Brain tumor

Table 4.1: Primary human hepatocyte donor phenotype. The phenotypic information on the donors of the primary human hepatocyte donors used in this thesis as provided by the supplier (ThermoFisher). Abbreviations: BMI, Body Mass Index.

μM (Control) or 800 μM OPLA or POLA. PHHs were cultured in experimental media for four days with media changes every other day.

4.2.4 Lipid droplet imaging and quantification

12,500 - 25,000 cells were seeded onto 12 mm diameter glass cover slips (VWR, 631-1577) in 24-well plates. After the treatment period, cells were washed with PBS and then fixed by incubation with 4 % paraformaldehyde in PBS for 15 mins. Cover slips were stored in PBS at 4 °C until staining. To allow penetration of the stains into cells, cover slips were kept in 0.01 % Triton-X in PBS for 25 mins. Coverslips were then washed twice with PBS and stained with HCS LipidTOX™ Red Neutral Lipid Stain (ThermoFisher, H34476) at 1:200 in PBS and RedDot™2 Far-Red Nuclear Stain (Biotium, 40061) at 1:125 in PBS for 1 hour followed by two more washes with PBS and staining with Oregon Green™ 488 Phalloidin (ThermoFisher, O7466) at 1:40

in PBS for 30 mins. Coverslips were then washed twice with PBS and mounted onto a slide with VECTASHIELD Vibrance® Antifade Mounting Medium (Vector Laboratories, H-1700) before imaging with a confocal microscope (Bio-Rad, Radiance 2100). For staining for LC3, coverslips were incubated in swine serum at 1:20 in PBS before the LipidTox staining and then left overnight in anti-LC3 antibodies (Sigma, L8918) at 1:50 in PBS. The next day the cover slips were washed twice with PBS and then incubated in Alexa Fluor™ 488 anti-rabbit secondary antibody (ThermoFisher, A-11008) at 1:200 in PBS before being washed twice again with PBS and mounted onto a slide with Fluoroshield mounting medium with DAPI (Abcam, ab104139).

4.3 Results

4.3.1 The effect of media fatty acids on hepatocyte viability

To investigate the effect of individual FA or FA mixtures on hepatocyte viability, Huh7 cells and PHH were cultured in media supplemented with 400 μM OA or PA as either a single FA or as part of a FA mixture (888 μM OPLA or POLA, respectively) for 4 days with media changed every other day. However, neither Huh7 cells nor PHHs showed any difference in cell viability between conditions (Figures 4.2A and 4.2B, respectively) but there was greater variability in the viability of Huh7 cells cultured in PA compared to other conditions. PHHs did have significantly lower ATP concentration than Huh7 cells suggesting a lower overall viability.

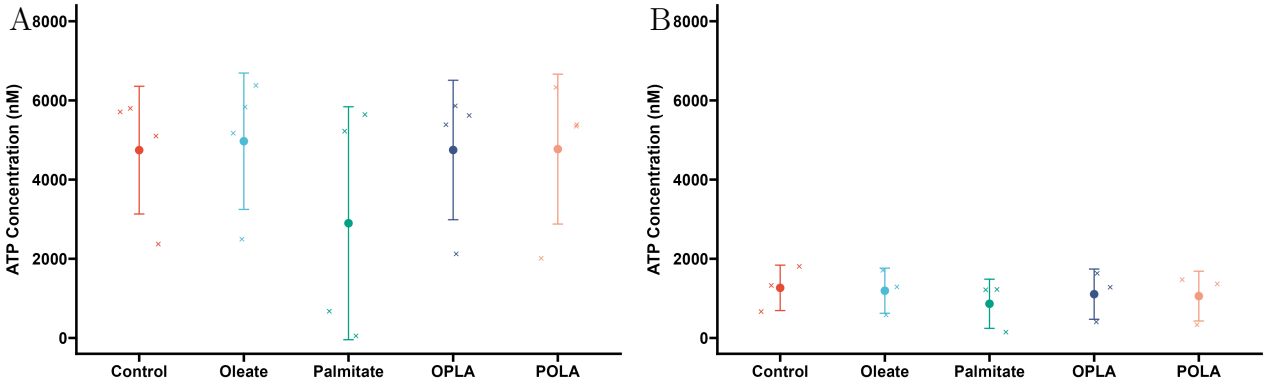


Figure 4.2: Effect of individual fatty acids and fatty acid mixtures on hepatocyte viability. **A)** Huh7 cells or **B)** primary human hepatocytes were cultured in media supplemented with no fatty acids (control) or 400 μM oleate and 400 μM palmitate as either single fatty acids or as a mixture of fatty acids (OPLA and POLA, respectively) for four days with media changed every other day. Data presented as mean ± sd from at least three biological repeats (**n=3**) carried out in technical duplicate.

4.3.2 The effect of media fatty acids on intrahepatocellular triglyceride accumulation

To characterise the IHCTG accumulation, Huh7 cells were cultured in media supplemented with 800 μM OPLA or POLA for 7 days with media changes every 2-3 days before harvesting and lipid extraction and quantification using GC. Huh7 cells cultured in OPLA and POLA had higher IHCTG than control cells cultured in FA-free media (Figure 4.3A). Although the total amount of IHCTG was the same between OPLA- and POLA-treated cells, the composition of the TG reflected that of the FA mixture in the media; there was no difference in oleate between the conditions but the proportion of palmitate was higher in POLA-treated cells and linoleate higher in OPLA-treated cells when compared to the other conditions (Figure 4.3B).

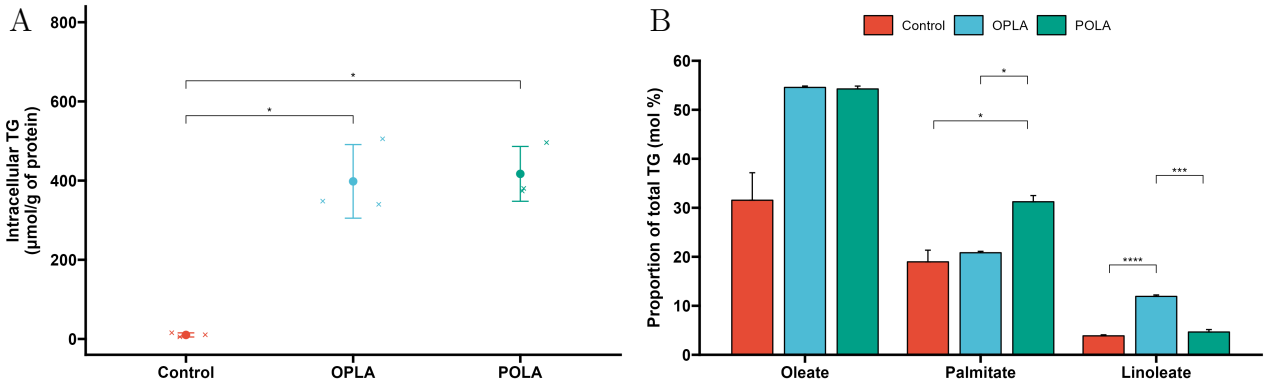


Figure 4.3: The effect of media fatty acids on intrahepatocellular triglyceride accumulation in Huh7 cells. Huh7 cells were cultured for four days in media without fatty acids (Control) or with 800 μM OPLA or POLA. **A)** Total intracellular triglycerides were extracted and **B)** their composition was analysed through gas chromatography. $^{*}p<0.05$, $^{***}p<0.001$, $^{****}p<0.0001$. Data presented as mean ± sd from three biological repeats (**n=3**). Abbreviations: TG, Triglyceride.

Formation of LDs was observed by fluorescent staining and confocal microscopy and in cells cultured in OPLA and POLA enriched media but not in control (FA-free) media (Figures 4.4A-4.4C). Further image quantification showed that cells cultured in media supplemented with FA had larger LDs than those cultured in FA-free media but there was no difference in LD size between OPLA- and POLA-treated cells (Figure 4.4D).

To confirm these findings, PHH were cultured in 800 μM OPLA or POLA enriched media for 4 days, with media being changed every other day, and accumulation of LDs was observed (Figures 4.5A-4.5C). In contrast to Huh7 cells, PHH did show a significant difference in LD size distribution between OPLA and POLA conditions with OPLA- but not POLA-treated

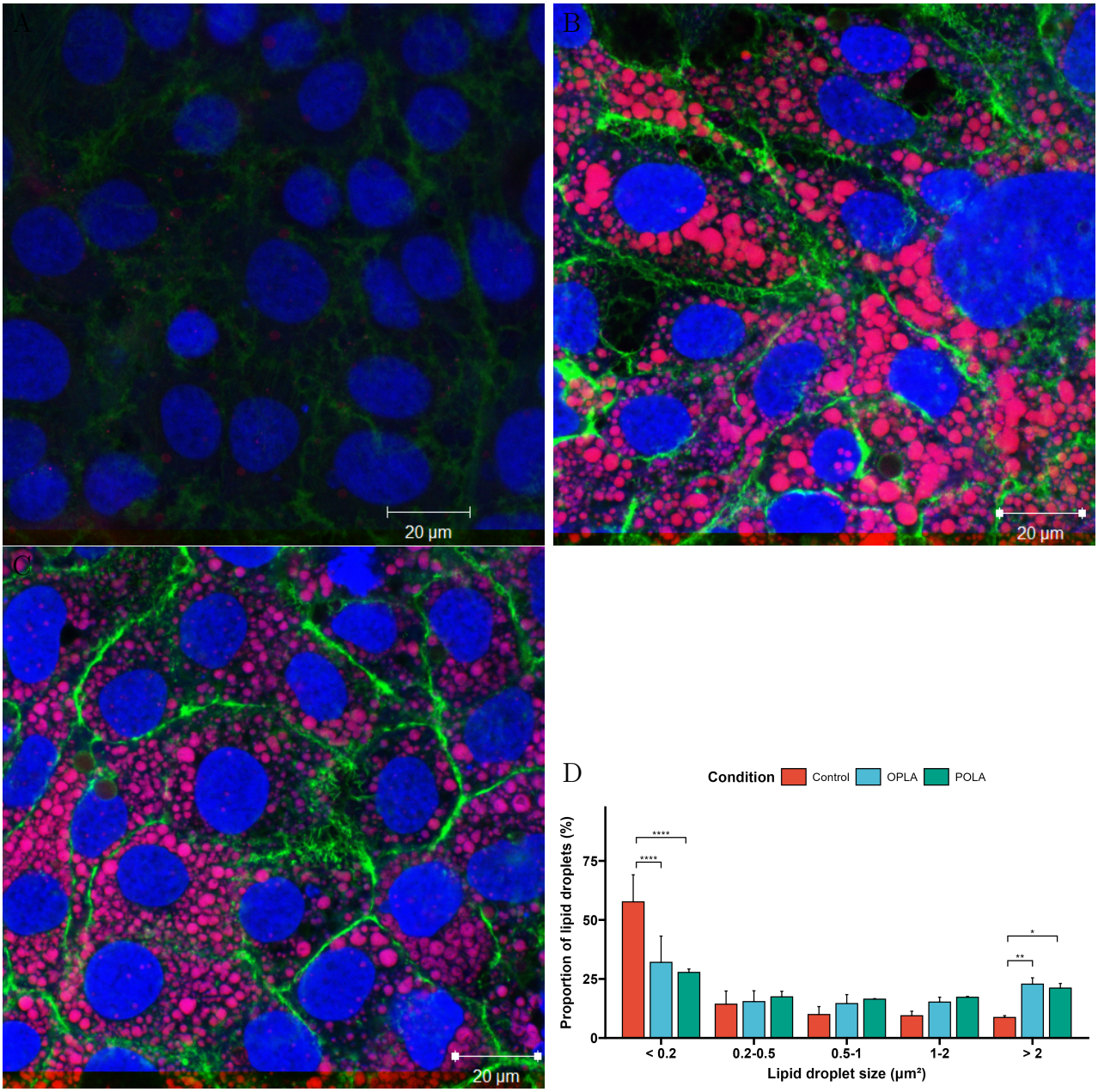


Figure 4.4: The effect of media fatty acids on lipid droplet formation. Representative images of Huh7 cells cultured for four days in media **A)** without fatty acids (Control) or **B)** with 800 μM OPLA or **C)** 800 μM POLA. Neutral lipids were stained in red, skeleton in green and nuclei in blue and confocal microscopy images were taken at 60 x magnification. **D)** Lipid droplet size was quantified from at least six images from each biological repeat. $^{*}p<0.05$, $^{**}p<0.01$, $^{****}p<0.0001$. Data presented as mean ± sd from three biological repeats (**n=3**) with at least six images from each.

cells having a smaller proportion of LDs below 0.2 μM and a larger proportion $>$ 2 μM than cells cultured in control media (Figure 4.5D).

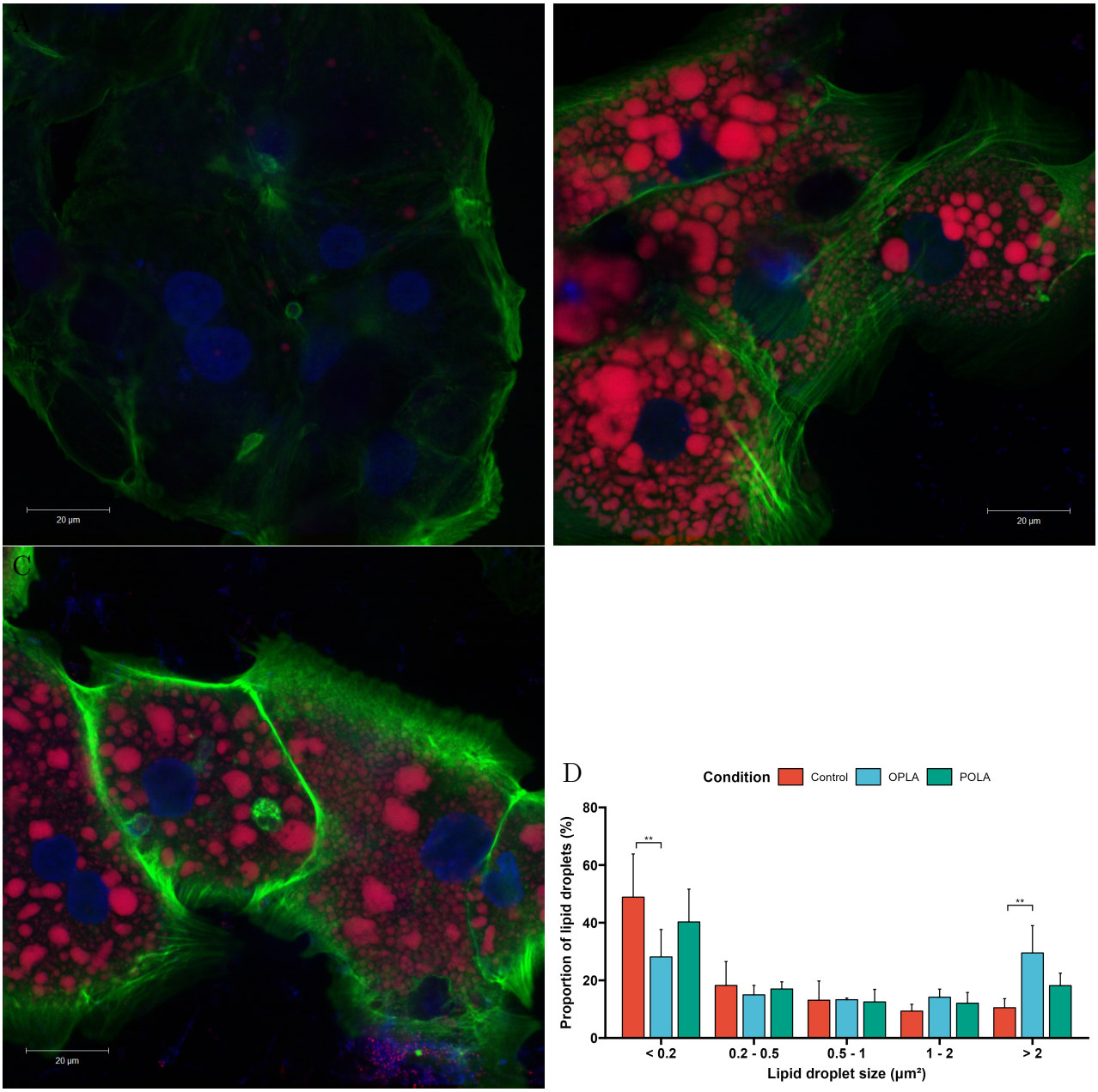


Figure 4.5: Effect of media fatty acids on intrahepatocellular triglyceride accumulation in Primary human hepatocytes. Neutral lipids were stained in red, skeleton in green and nuclei in blue. Representative images taken at 60x magnification of primary human hepatocytes cultured in media supplemented with **A)** no fat (Control), **B)** 800 μM OPLA or **C)** 800 μM POLA. **D)** Image analysis from at least six images per biological repeat allowed profiling of the lipid droplet size. $^{**}p<0.01$. Data presented as mean ± sd from three biological repeats (**n=3**) with at least six images from each. Abbreviations: TG, Triglyceride.

4.3.3 The effect of media fatty acids on autophagy

It has been suggested that an aberrant decrease in autophagy may contribute to IHCTG accumulation in MASLD [50]; however, the effect of FA composition is yet to be determined. Fluorescent staining of autophagosomal marker LC3 showed co-localisation of autophagosomes to LDs in both OPLA- and POLA-treated cells (Figures 4.6A and 4.6B, respectively) suggesting the occurrence of lipophagy in these cells. To further investigate this, autophagic flux was measured in Huh7 cells cultured in FA-free media or media supplemented with 800 μM OPLA or POLA for 7 days with media being changed every 2-3 days. Autophagic flux quantified by measuring LC3-II protein intensity (relative to housekeeper protein α-Tubulin) with and without the autophagic inhibitor BAF. As LC3-II is normally degraded during autophagy, its accumulation during autophagic inhibition is reflective of overall flux through autophagy [60]. There was no significant difference in autophagic flux between the conditions (Figures 4.6D - 4.6E).

4.3.4 The effect of media fatty acids on autophagic and inflammatory gene expression

Raw transcriptomic data, obtained from work that Eloise Cross had undertaken, was utilised to explore the effect of FA treatment on autophagic and inflammatory gene expression. Huh7 cells or PHHs had been cultured in FA-free media (Control) or media supplemented with 800 μM OPLA or POLA for 5 or 7 days (PHHs or Huh7s, respectively) with media changed every 2-3 days day.

For the data from Huh7 cells, the difference in gene expression between control and OPLA/POLA conditions accounted for the largest component of the total variance (dimension 1 - 77.1 %) in the data and the difference in gene expression between OPLA and POLA conditions accounted for the second largest component (dimension 2 - 9.3 %) as shown in Figure 4.7A. Gene set enrichment analysis (GSEA) showed that DNA replication and cell cycle associated genes were the most significantly activated pathways whereas autophagy, infection and endoplasmic reticulum protein processing pathways were the most significantly suppressed pathways in both OPLA- and POLA- treated cells compared to control cells (Figures 4.7B and 4.7C, respectively). The generation of a heatmap of genes involved in autophagic activation [151] further confirmed an overall suppression of autophagic processes in OPLA- and POLA-treated cells compared to controls cells (Figure 4.7D). Only 265 genes were differentially expressed between OPLA-

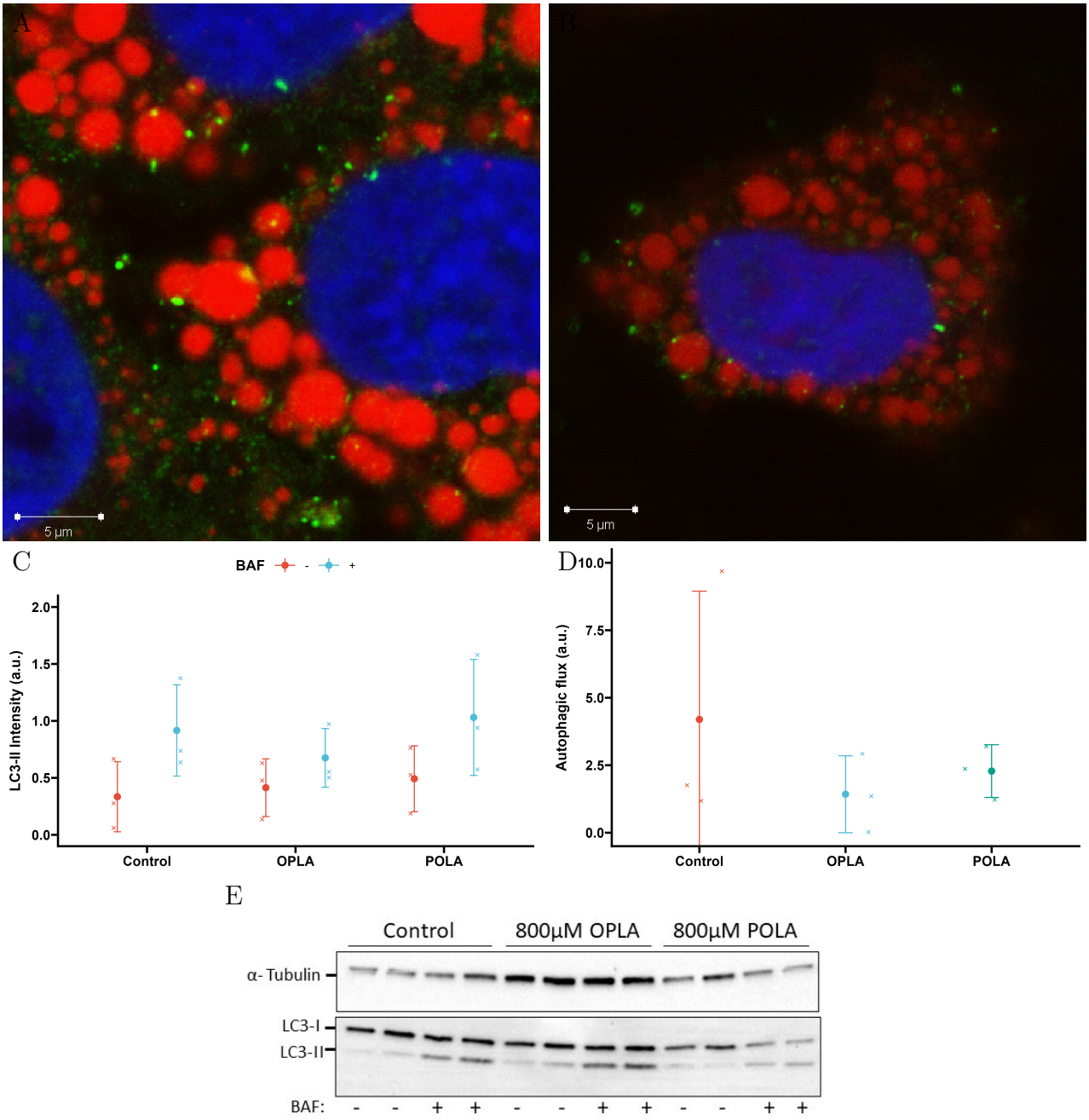


Figure 4.6: The effect of media fatty acids on autophagy. Representative images taken at 60 x magnification of Huh7 cells cultured in media supplemented with either **A)** 800 μM OPLA or **B)** 800 μM POLA with media changed every other day. LC3 stained in green, neutral lipids in red and nuclei in blue. **C-E)** Autophagic flux was calculated as LC3-II intensity (relative to housekeeper protein α-Tubulin): (BAF - Basal)/Basal. Data presented as mean $\pm$ sd from three biological repeats (**n=3**) carried out in technical duplicate. Abbreviations: BAF, Bafilomycin A1.

and POLA-treated cells which was not sufficient to carry out robust pathway enrichment analysis. However, two genes related to autophagy, SQSTM1 and ULK1, had significantly lower

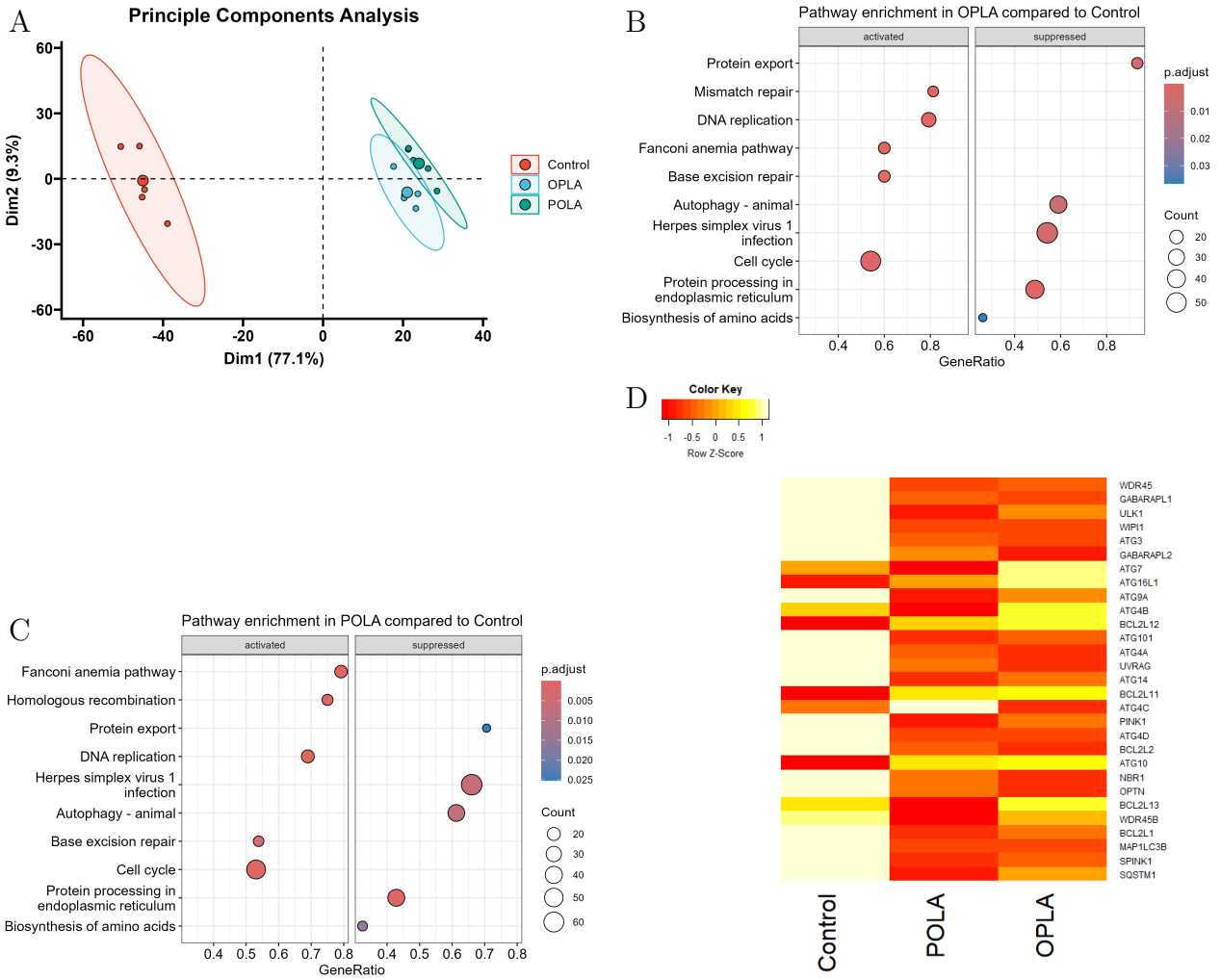


Figure 4.7: The effect of media fatty acids on autophagic and inflammatory gene expression in Huh7 cells. Transcriptomic data from Huh7 cells cultured in either media with no FAs (Control), 800 μM OPLA or 800 μM POLA for 7 days with media changed every 2-3 days. Data was analysed first by **A)** principal component analysis then **B)** gene set enrichment analysis comparing cells cultured in **B)** OPLA and **C)** POLA to Control. **D)** A heat map of genes associated with autophagy. Representative of five biological repeats (**n=5**) carried out in technical duplicate.

expression in POLA- compared to OPLA-treated cells but there were no other differences in expression of other autophagy or inflammation-associated genes.

In contrast to the Huh7 cells, as shown in Figure 4.8A, the largest component of total variance in the PHH transcriptomic dataset was driven by a difference in gene expression between donors (dimension 1 - 61.6 %). However, the second largest component of total variance appeared to be the difference in gene expression between the Control and OPLA/POLA conditions (dimension 2 - 17.3 %). GSEA highlighted the suppression of retinol and drug metabolism pathways and activation of cytokine and inflammatory pathways in both OPLA and POLA

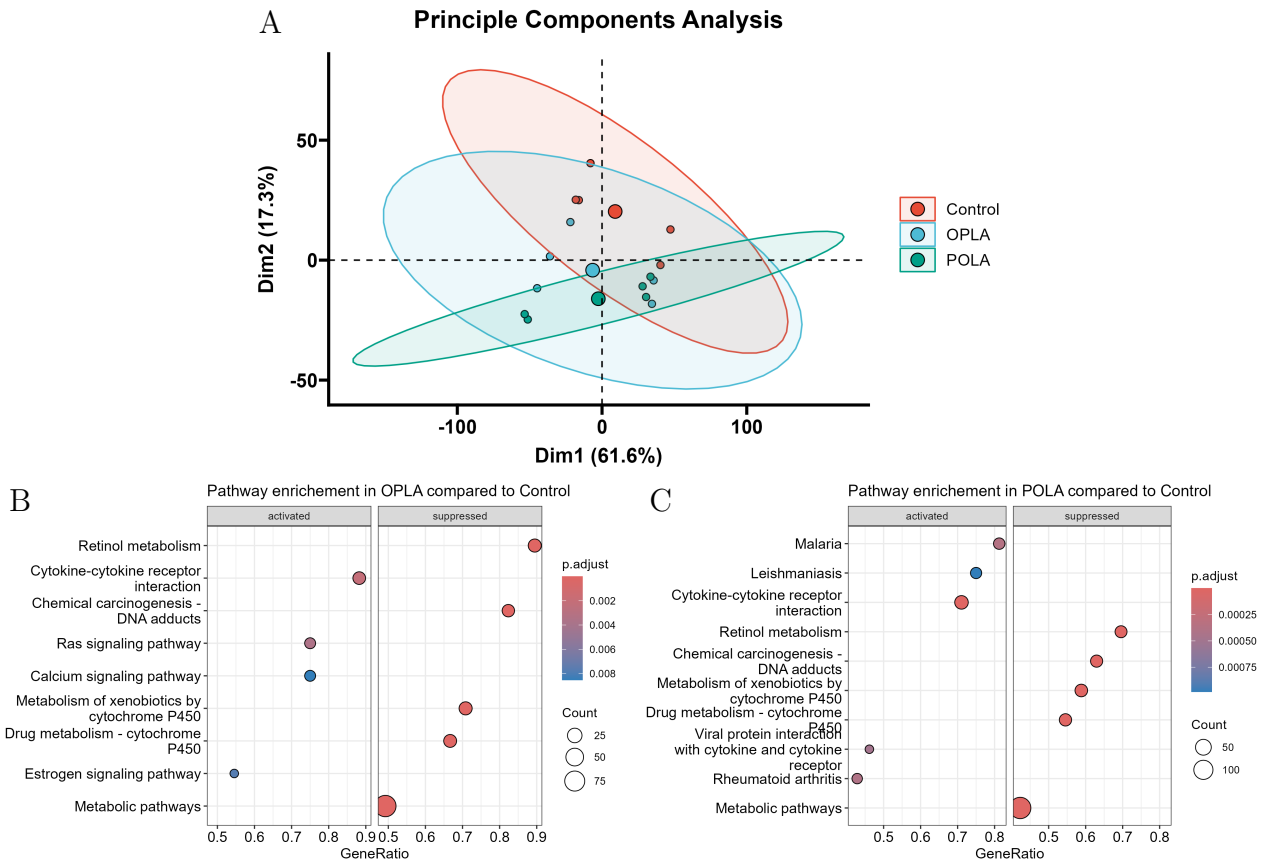


Figure 4.8: The effect of media fatty acids on autophagic and inflammatory gene expression in primary human hepatocytes. Transcriptomic data from primary human hepatocytes cultured in either media with no FAs (Control), 800 μM OPLA or 800 μM POLA for 7 days with media changed every 2-3 days. Data was analysed first by **A)** principal component analysis then **B)** gene set enrichment analysis comparing cells cultured in **B)** OPLA and **C)** POLA to Control. Representative of five biological repeats (**n=5**) carried out in technical duplicate.

conditions when compared to Control (Figures 4.8B and 4.8C, respectively). Further analysis using KEGG pathways showed an increase in expression of chemokine genes from the CXC subfamily (specifically CXCL1, CXCL2, CXCL6, CXCL8 and CXCL16), between Control- and both OPLA- and POLA- treated cells, although this was less marked in OPLA than in POLA conditions (Figures 4.9A and 4.9B, respectively). Other cytokines such as CSF1 and INHBE were also increased in OPLA and POLA conditions and TGFB1/2 had significantly higher expression in cells cultured with POLA but not OPLA compared to Control (Figures 4.9A and 4.9B). In contrast to transcriptomic data from Huh7 cells, the autophagy pathway was not significantly differentially expressed between Control and OPLA or POLA conditions in PHH. When comparing OPLA and POLA conditions, only 6 genes were significantly differentially

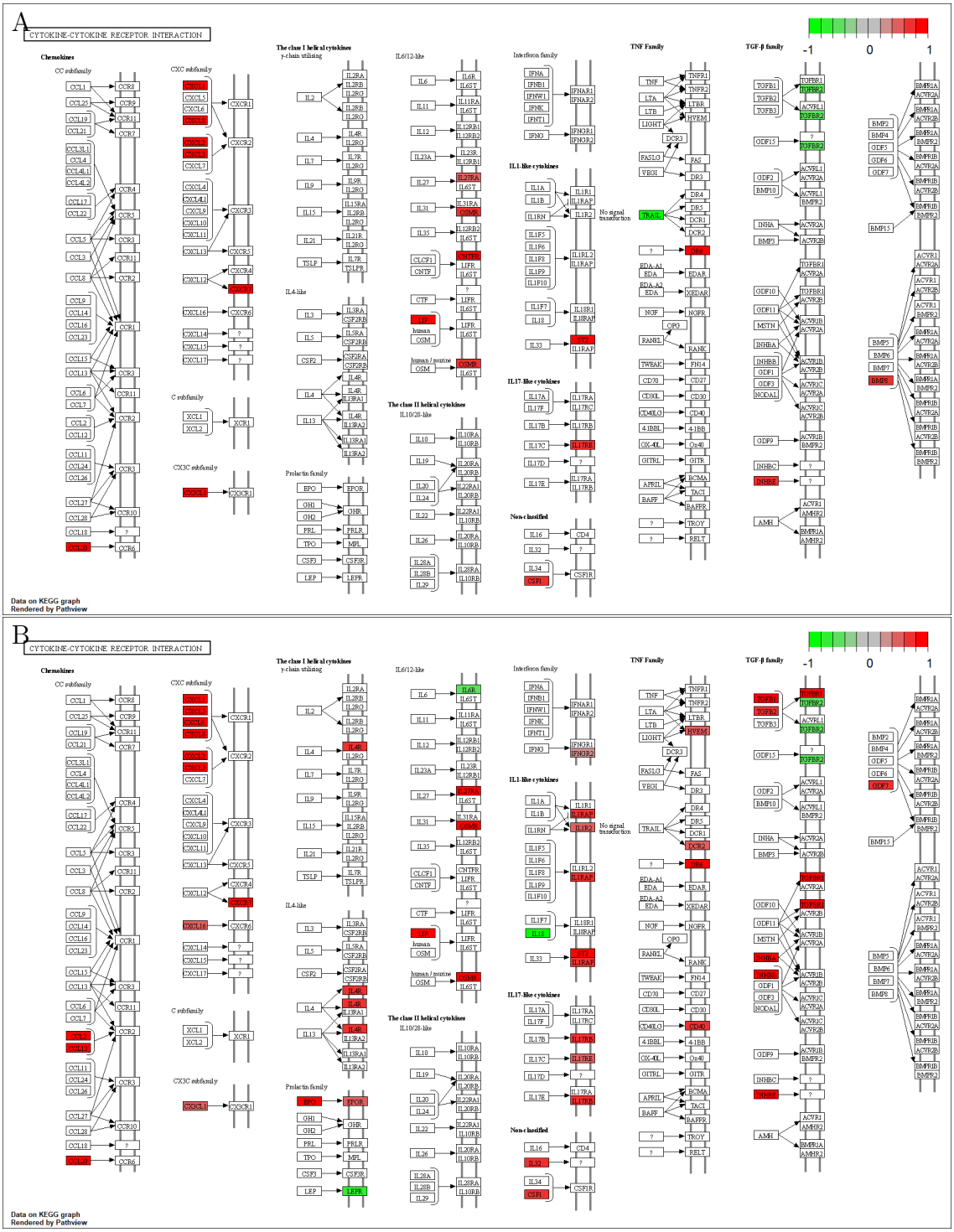


Figure 4.9: The effect of media fatty acids on cytokine gene expression in primary human hepatocytes. Transcriptomic data from primary human hepatocytes cultured in either media with no FAs (Control), 800 μM OPLA or 800 μM POLA for 7 days with media changed every 2-3 days. Generation of KEGG Pathways for cytokine-cytokine receptor interactions for **D)** OPLA- and **E)** POLA-treated cells compared to Control-treated cells. Representative of five biological repeats (**n=5**) carried out in technical duplicate.

expressed (MUM1L1, TMEM233, CBWD5, C1QL1, FGD5, and CAPN8) and all of which were downregulated in POLA compared to OPLA.

4.4 Discussion

It has been suggested that a FA-mediated decrease in hepatocellular autophagy may contribute to the inflammatory activation and IHCTG accumulation seen in MASLD [50], but the majority of *in vitro* models of IHCTG accumulation rely on culturing hepatocytes in a single FA for a short period (typically between 6-48 hours) which could be considered an acute response [71]. However, as my lab has developed a more physiologically representative model using chronic exposure to a mixture of FAs, I investigated if this more physiologically representative model of IHCTG accumulation could be used to investigate the effect of FAs on autophagy and inflammation.

4.4.1 The effect of FAs on cell viability

Previous studies have shown that PA can activate apoptotic pathways in hepatocytes which leads to cell death over 24 hours [42, 74, 75, 152]; therefore, it was important to measure the viability of hepatocytes cultured in the OPLA and POLA FA mixtures before using them further. Hepatocytes were cultured for four days in media containing a fixed concentration of PA or OA either as a single FA or as part of a mix of other FAs (OPLA and POLA, respectively) and viability was measured by ATP concentration to demonstrate cells are metabolically active. In contrast to others [42, 74, 75, 152], I did not observe any difference between hepatocytes cultured in PA compared to OA, which may be due to different measurements of viability. Previous studies have used caspase activation or nuclear staining to quantify apoptosis [42, 74, 75, 152], however ATP concentration was chosen as the measure of viability for the work presented here as it better represents the metabolic state of the cells. Taken together with the difference in length of culture between the present work and that of others, it is plausible that acute treatment with PA leads to activation of apoptotic pathways, but hepatocytes can adapt to the PA exposure over time. It would, therefore, be of interest to measure hepatocyte viability as a time course over these four days.

I found PHHs had significantly lower viability that Huh7 cells, which is in-line with previous work [71, 153] and has been suggested to be due to their limited lifespan after cryopreservation, as

well as other donor-associated factors such as steatosis, other liver diseases, and pharmacological or nutritional agent exposure [71]. Indeed, many of the donors used in these experiments had a history of alcohol and/or exposure to recreational and/or pharmacological drugs (Table 4.1) which is likely to have affected hepatocyte viability prior to the isolation of the PHHs.

4.4.2 The effects of FAs on IHCTG accumulation

It is well established that when hepatocytes are exposed to increasing concentrations of FA *in vivo* or *in vitro*, IHCTG accumulates and leads to the formation of LDs [65, 66, 71, 154]; this was observed in the present study in both cultured Huh7 cells and PHHs. However, the effect of FA composition on IHCTG is not as clear. *In vitro* studies which have directly compared the effects of single FA exposure on IHCTG accumulation in cultured hepatocyte cell lines have found PA to be more steatogenic than OA [72–76, 78], but less steatogenic than LA [155, 156]. However, when these hepatocytes are cultured in a mixture of FAs, there has generally not been any difference observed in IHCTG accumulation between unsaturated FA and SFA compositions [74, 80, 84]. In line with these observations, I did not see a difference in total IHCTG accumulation between the OPLA and POLA conditions. This is in contrast to *in vivo* human evidence which suggests that consuming excess SFA compared to excess unsaturated FAs leads to greater IHCTG accumulation [65, 67, 68, 157]. The discrepancies between whole-body *in vivo* findings and *in vitro* hepatocellular findings suggest that other organs may be responsible for SFA-induced IHCTG accumulation. For example, SFA-enriched diets have been shown to increase adipose tissue lipolysis in humans compared to unsaturated FA-enriched diets [150] which may expose hepatocytes to greater FA concentrations due to increased plasma NEFA levels. TRLs are also another route of dietary FA uptake for *in vivo* hepatocytes which are not present in *in vitro* models.

Although total IHCTG accumulation was the same between the OPLA and POLA conditions, the morphology of the LDs that these IHCTGs were stored in may differ. PHHs cultured in OPLA-enriched media had larger LDs than those cultured in POLA-enriched or FA-free media; however, this was not replicated in Huh7 cells. The increase in LD size when hepatocytes are treated with OA compared to PA has been previously reported by others [73, 79] and has been linked to LD-mitochondria interactions, whereby larger LDs associate closer to mitochondria than

smaller LDs. Measurement of cellular ATP concentration and mitochondrial transmembrane potential by Eynaudi *et al.* suggested that OA-treated cells may utilise mitochondrial ATP for TG production and storage whereas LDs from PA-treated cells provide TG for mitochondrial FA oxidation [73]. However, the differences between OPLA and POLA are primarily in the ratio of PA and LA, so it is unclear if similar effects may also explain the differences observed in the current study. Further work is currently being undertaken by others in the group to characterise the LD-mitochondria interaction in OPLA- and POLA-treated cells using the same live staining and confocal microscopy techniques as Eynaudi *et al.* [73]. It is unclear why Huh7 cells did not exhibit the same differences in LD size as the PHHs however, the lower viability of PHHs may lead to a more extreme phenotype in these cells and so may only be seen in Huh7 cells with a larger sample size, longer culture length or more frequent media changes. Differences in LD size have also been associated with expression of perilipin (PLIN) 2 and 5 [72, 73] however, there was no evidence from my transcriptomic data to suggest a difference in expression of these genes between OPLA and POLA conditions in either Huh7 cells of PHHs.

4.4.3 The effects of FAs on autophagy

It has been suggested that an aberrant decrease in autophagy may contribute to IHCTG accumulation in MASLD; however, the effect of dietary FA composition on autophagy is still unclear [50]. Whilst previous studies have demonstrated the effect of autophagy on ICHTG accumulation through the use of autophagic modulators, few have measured autophagic flux in *in vitro* models of IHCTG accumulation. Co-localisation between autophagosomes and LDs was observed on samples stained for autophagosomal marker LC3 and a neutral lipid dye (LipidTox) using confocal microscopy, confirming the occurrence of lipophagy in OPLA- and POLA-treated Huh7 cells. However, when autophagic flux was measured, there was no difference between the conditions. This is in contrast to the transcriptomic data from Huh7 cells undergoing the same experimental treatment which shows a significant down-regulation of autophagic pathways in OPLA- and POLA-treated cells compared to Control-treated cells. Although autophagy is regulated by the expression of autophagic genes (such as the ATGs), it has been shown that their expression does not necessarily reflect autophagic flux as the pathway is often regulated non-transcriptionally [60, 158]. The up-regulation of pathways associated with

DNA replication and the cell cycle and down-regulation of the ER protein processing pathway in Huh7 cells treated with FA mixtures compared to the control with no FAs, suggests a higher rate of proliferation in these cells. Taken together, it is plausible that Huh7 cells cultured in FA-free media (the Control condition) may be depleted of nutritional substrates and have activated starvation responses. One such starvation response is the inactivation of mTORC1, a major inhibitor of autophagy, which leads to an increase in autophagy under these conditions to provide additional substrates [53]. Whilst the Huh7 cells were cultured in a physiological concentration of glucose (5.5 mM), these hepatoma cells are highly glycolytic and the changing of media every 2-3 days may not be enough to prevent the activation of starvation responses. Furthermore, it also is not physiologically representative to culture hepatocytes in FA-free media as the liver has a near-constant supply of FAs *in vivo* [27]. To further support this, PHHs were cultured at a higher glucose concentration than Huh7 cells (11 mM vs 5.5 mM) and may be less glycolytic than Huh7 cells due to their lack of proliferation which further suggests an association of autophagy with nutrient availability rather than FA concentration *per se*.

4.4.4 The effect of FAs on inflammatory activation

Previous work has shown that culturing hepatocytes in PA can lead to the activation of inflammatory pathways [42, 78, 79] but the effect that FA mixtures have on hepatocytes during a prolonged culture is unknown. Transcriptomic data presented in this chapter showed that treatment with OPLA and POLA had no effect on hepatocellular expression of inflammation-associated genes in Huh7 cells but did activate cytokine gene expression in PHHs. Further pathway analysis showed that compared to PHHs treated with FA-free media, PHHs treated with OPLA and POLA showed an increase in chemokine gene expression which was more marked in POLA-treated cells and specifically chemokines of the CXC subfamily. CXC chemokines are characterised by the presence of a single variable amino acid in between the two cysteine amino acids closest to the N terminus. Expression of CXCL1 and CXCL8 genes are both highly upregulated in the liver of MASLD patients and murine MASLD models and are thought to be associated with neutrophil recruitment and infiltration into the liver [159–161]. CXCL6 and CXCL16 have been shown to activate and recruit HSCs and natural killer T cells respectively [162]. POLA-treated PHHs also had significantly higher gene expression of TGF-β and pathways

associated with TGF-β and TNF signalling compared to PHHs cultured in control media, but the same was not observed in OPLA-treated PHHs. TGF-β secretion is associated with fibrosis in MASLD due to its ability to activate HSC [48]; these results may suggest a greater inflammatory activation in livers exposed to SFAs compared to PUFAs. Increased expression of genes associated with inflammation in PHH but not Huh7 cells may be due to a greater basal level of hepatocellular injury which was worsened with FA-treatment as suggested by the general lower viability of PHHs compared to Huh7 cells.

4.4.5 Conclusions

Although PHHs are often deemed to be the "gold standard" of *in vitro* hepatocellular models, their cost, lower viability and variability in phenotype makes them challenging to use routinely. Instead, the data presented in this chapter shows that Huh7 cells cultured in FA mixtures for up to a week can serve as a good model of *in vitro* IHCTG accumulation. However, adaption of this Huh7 model to have daily media changes with media that is higher in other nutritional substrates may prevent activation of starvation responses observed in the Control condition and may also lead to greater inflammatory activation. Future work could explore the use of microfluidics systems to maintain constant nutrient flow over the hepatocytes with timed delivery of hormones to better recapitulate conditions *in vivo*. Similarly, co-culturing hepatocytes with other hepatic cell types such as Kupffer, endothelial and stellate cells could further enhance models aiming to investigate the propagation of inflammation *in vitro*.

'Praeterea num nemo evidentiam annumerationis requirit?'

5

The effect of fatty acid composition on hepatocellular autophagy, inflammatory activation and insulin resistance

Contents

5.1 Introduction 66
5.2 Methods 67
5.2.1 Experimental treatments 67
5.2.2 Analytic techniques 68
5.2.3 Quantification of cytokine secretion 68
5.2.4 Co-culture with hepatic stellate cells 68
5.2.5 Glucose production assay 69
5.2.6 Analysis of proteomic data 70
5.3 Results 70
5.3.1 The effect of media fatty acid composition on Huh7 cell viability . . . 70
5.3.2 The effect of media fatty acid composition and insulin concentration on intrahepatocellular triglyceride accumulation 70
5.3.3 The effect of media fatty acid composition and insulin concentration on autophagy 71
5.3.4 The effect of media fatty acid composition and insulin concentration on inflammatory activation 72
5.3.5 The effect of media fatty acid composition and insulin concentration on hepatocellular injury 74
5.3.6 The effect of media fatty acid composition on insulin resistance 75
5.3.7 The effect of media fatty acid composition and insulin concentration on gene expression 76
5.4 Discussion 80
5.4.1 Model assessment 81
5.4.2 The effect of FA composition on autophagy 82

5.4.3 The effect of FA composition on inflammatory activation 83
5.4.4 The effect of FA composition on insulin resistance 84
5.4.5 The effect of hyperinsulinemia on autophagy and inflammatory activation 84
5.4.6 Limitations 85
5.4.7 Conclusions 85

The cell viability and glucose production experiments included in this chapter were performed by Eleanor Caney under my supervision during the research placement component of her M.Biochem.

5.1 Introduction

Dietary fat composition has been demonstrated to influence IHCTG accumulation *in vivo* [149, 150] and evidence from MASLD patients suggests a decrease in autophagy may also play a role [61]. However, it remains unclear how dietary fat composition may influence autophagy in the liver. Previous *in vitro* studies investigating the effect of FA composition on autophagy have had conflicting results, with some suggesting that SFAs may inhibit autophagy and others showing induction of autophagy when compared to monounsaturated FA (MUFAs) [152, 163, 164]. Discrepancies may be due to different cell culture regimes and techniques for measuring autophagy but in all cases, hepatocytes were treated with either OA or PA for less than 18 hours and so it is plausible that these results may be due to an acute response to the treatment. Furthermore, *in vivo* human data suggests that a diet enriched in MUFAs has little effect on MASLD disease risk whereas a diet enriched in PUFAs may be protective [69, 70] but the comparison between PUFAs and SFAs is rarely made *in vitro* and the differences these FAs have on autophagic flux, inflammatory activation and IR is unknown.

Although hyperinsulinemia is associated with obesity and increased liver fat content (as demonstrated in Chapter 3), its effects on hepatocellular autophagy and inflammatory activation are poorly understood due to the lack of physiologically relevant models. Several murine studies have shown an inverse association between autophagy and plasma insulin concentrations in starvation or high fat diet-induced models of hyperinsulinemia but the casual effect of hyperinsulinemia on autophagic flux in human hepatocytes has yet to be shown [55, 165].

Similarly, as shown in Chapter 3, hyperinsulinemia is associated with systemic inflammation but its role in hepatocellular inflammatory activation is unclear.

In Chapter 4, I describe a model of *in vitro* IHCTG accumulation in Huh7 cells using the two distinct FA mixtures differing in PUFA and SFA composition that might be used to investigate autophagic flux and inflammatory activation. Although differences in autophagic flux were observed in that model, the analysis of RNA sequencing data suggested this may be due to activation of starvation responses in the control cells cultured in FA-free media. Similarly, unlike the PHH, media FA concentration and composition had no effect on expression of pathways associated with inflammation or stress in Huh7 cells. Therefore, in this chapter an adaption of the model from Chapter 4 is used whereby Huh7 cell media was changed every day instead of every 2-3 days with the aim of preventing activation of the starvation response and recapitulating a more extreme phenotype seen in the FA-treated PHHs. As well as daily media changes, the conditions in this chapter compare Huh7 cells cultured in a low-fat low-sugar media (LFLS) to those cultured in a high-fat high-sugar (HFHS) as it is not physiologically representative for hepatocytes to be cultured in FA-free media. Therefore, the aim of this chapter is to investigate the effect of FA composition and hyperinsulinemia on hepatocellular autophagy, inflammatory activation and IR in this more physiologically representative model of *in vitro* IHCTG accumulation.

5.2 Methods

5.2.1 Experimental treatments

For measurement of Huh7 cell viability, base experimental media as described in Chapter 2 section 2.1.6, was then supplemented with 5.5 mM glucose, 0.1 nM insulin and 400 μM of PA or OA FA either as a single FA or in a FA mixture (OPLA or POLA, respectively). Cells were cultured for four days with media changes every day. For all other experiments described in this chapter, base experimental media was supplemented with either 5.5 mM glucose and 200 μM OPLA (low-fat low-sugar media, LFLS), 11 mM glucose, 5.5 mM fructose and 800 μM OPLA (high-fat high-sugar OPLA media, HFHS-OPLA) or 11 mM glucose, 5.5 mM fructose and 800 μM POLA (high-fat high-sugar POLA media, HFHS-POLA) with either 0.1 nM or 100 nM insulin. 100 nM insulin is supraphysiological but is based on work from Dr Shilpa Nagarajan who showed greater metabolic differences in Huh7 cells cultured in media supplemented with 100 nM

insulin than 10 nM insulin when compared to insulin-free media suggesting these cells respond best at this supraphysiological concentration [84]. Huh7 cells were cultured in experimental media for seven days unless otherwise stated with media changed every day.

5.2.2 Analytic techniques

Lipid extraction and quantification, autophagic flux and ATP assays, the cytokeratin-18 fragment ELISA, RNA extraction and transcriptomic analysis were all carried out as described in Chapter 2 sections 2.2-2.6.

5.2.3 Quantification of cytokine secretion

Media from day seven of the cell culture was collected, samples were randomised to minimise batch effects and then sent to Olink® for proteomic analysis using the Olink® Target 48 Cytokine panel. Olink technology is based on proximity extension assay technology which uses pairs of DNA-tagged antibodies to bind to target proteins that can then hybridise to each other when they are bound to the same protein [166]. The resulting hybridised DNA is amplified through qPCR and can provide a readout which correlates to protein concentration.

All samples passed the Olink quality control checks however some samples were below the limits of detection for the assay. Where >50 % of the samples in an assay were below this limit the entire assay was removed, otherwise all other samples and assays were included. To account for proteins that maybe present in the HS that was added to the culture media, an average was taken from samples of stock media and subtracted from sample data for all proteins to calculate a concentration for protein secretion (pg/mL). Protein secretion concentrations were then corrected for cellular protein to give cellular cytokine secretion (ng/g of protein).

5.2.4 Co-culture with hepatic stellate cells

To explore the effects of hepatocellular inflammatory activation on hepatic stellate cell (HSC) activation, Huh7 hepatocytes and LX2 HSCs were co-cultured using Millicell® Cell Culture Inserts (Merck, PTSP12H48). LX2 cells were seeded into the wells of a 12-well plate and Huh7 cells were then seeded into hanging inserts placed into those wells. This allowed hepatokines produced by either cell type to diffuse through the 3.0 µm pores at the bottom of the inserts

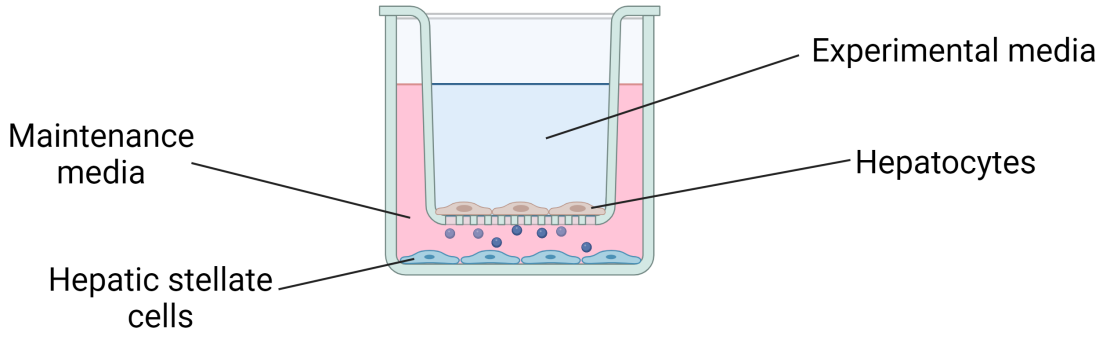


Figure 5.1: Experimental set-up for the co-culture with hepatocytes and hepatic stellate cells. LX2 hepatic stellate cells were seeded at the bottom of the well and cultured in maintenance media. Huh7 hepatocytes were seeded in hanging cell culture inserts which were placed into the wells. Huh7 hepatocytes were cultured in experimental media and any hepatokines produced by the cells can diffuse through the semi-permeable membrane to the other cell type.

to the other cell type (Figure 5.1). Both cell types were seeded at 100,000 cells/mL and then left overnight in maintenance media. Huh7 cells were then treated with the experimental conditions described above for seven days with daily media changes whereas LX2 cells continued to be cultured in maintenance media with media changes every other day. Therefore, any differences in LX2 activation would be due to hepatokines secreted by the hepatocytes in response to the experimental conditions.

5.2.5 Glucose production assay

After treatment with experimental media for seven days, hepatocytes were serum starved with overnight incubation in experimental media with 0.2 % BSA instead of 2 % HS. After serum starvation, cells were washed in PBS and then incubated for 30 mins in stimulation media which comprised of Krebs-HEPES buffer (KRH buffer) (10 mM HEPES, 120 mM NaCl, 4.8 mM KCl, 1.2 mM $MgSO_4$, 1.2 mM KH_2PO_4, 2.5 mM $CaCl_2$, 150 mM $NaHCO_3$) supplemented with 0.2 % bovine serum albumin (BSA; Sigma, A7030), 1 % P/S, 1 % NEAA, 1 % GlutaMAX™, 2 mM sodium pyruvate, 20 mM lactate, and either 0 nM or 100 nM insulin. After the 30 minutes, the media was collected and glucose concentration measured using the Glucose-Glo™ Assay (Promega, J6021). Glucose production was calculated by dividing the collected media glucose concentration by the incubation time (30 mins) and correcting for total protein concentration.

5.2.6 Analysis of proteomic data

Proteomic data was analysed using the Olink® Analyze package (version 3.9.0) on R (version 4.2.2 for Windows, RStudio). PCA plots were generated first followed by a two-way ANOVA to analyse the effects of LFLS, HFHS-OPLA and HFHS-POLA as well as media insulin concentration which used the Benjamini & Hochberg (1995) False Discovery Rate (FDR) method to adjust for multiple comparisons across all the proteins. Significant proteins then underwent post-hoc pairwise T-tests using the Tukey correction for multiple comparisons. Significance was set to $p<0.05$.

5.3 Results

5.3.1 The effect of media fatty acid composition on Huh7 cell viability

In Chapter 4, I observed no difference in viability of Huh7 cells treated daily with 400 μM OA or PA as either a single FA or in a FA mixture (OPLA or POLA, respectively). This result differed to previous studies which had shown a decrease in viability in hepatocytes cultured in PA compared to OA [76, 80]. For the work presented in this chapter, Huh7 cell media was changed daily instead of every 2-3 days and so the same experiment was carried out for this model. ATP concentration did not differ between hepatocytes cultured with OA, OPLA or POLA but, in contrast to the results of Chapter 4, hepatocytes treated with PA did show a decrease in viability over time (Figure 5.2A) with a lower viability compared to all other conditions at day four (Figure 5.2B).

5.3.2 The effect of media fatty acid composition and insulin concentration on intrahepatocellular triglyceride accumulation

FA composition and hyperinsulinemia have been associated with IHCTG accumulation *in vivo* [7, 24, 25, 65–67] and this was explored *in vitro* by culturing Huh7 cells in LFLS, HFHS-OPLA or HFHS-POLA media at either 0.1 nM or 100 nM concentrations of insulin with daily media changes. Hepatocytes cultured in HFHS media had higher IHCTG accumulation than those cultured in LFLS media but as observed in Chapter 4, FA composition had no effect on IHCTG accumulation as there was no significant difference between HFHS-OPLA and HFHS-POLA conditions in this model (Figure 5.3A). The IHCTG composition generally reflected the FA

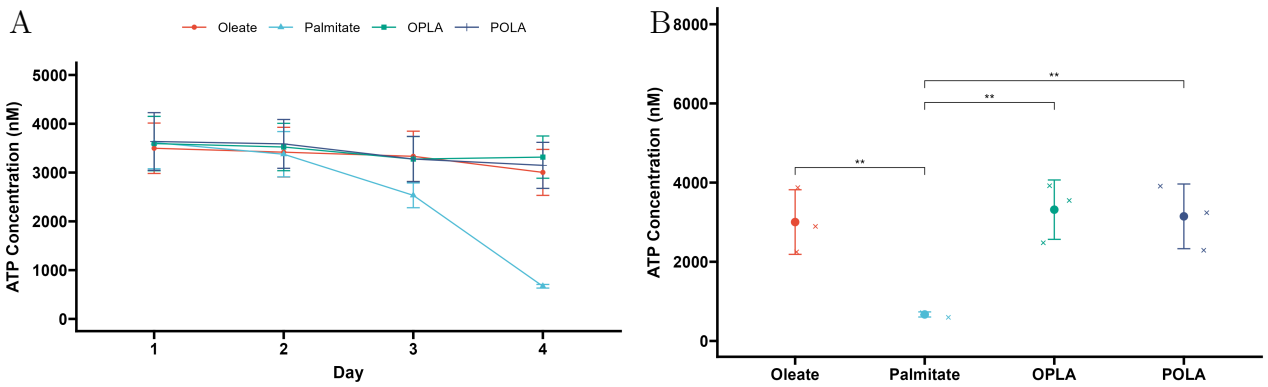


Figure 5.2: Huh7 cell viability when cultured with individual fatty acids and fatty acids mixtures. Huh7 cells were cultured in media supplemented with 400 µM oleate or 400 µM palmitate as either a single fatty acid or in a fatty acid mixture (OPLA or POLA, respectively) for 4 days with media changed every day. **A)** Time course of cell viability across the four days and **B)** cell viability on day 4. Data presented as mean ± sd from three biological repeats (**n=3**) carried out in technical duplicate. $^{**}p<0.01$. Abbreviations: ATP, Adenosine triphosphate.

composition that the cells were cultured in with no difference in the proportion of oleate observed between conditions (Figure 5.3B), and the HFHS-POLA condition having a higher proportion of palmitate and a lower proportion of linoleate (Figures 5.3C-5.3D). IHCTG quantity and composition was not different between cells cultured in high and low concentrations of insulin suggesting no effect of insulin on IHCTG accumulation or FA composition.

5.3.3 The effect of media fatty acid composition and insulin concentration on autophagy

Autophagy is often quantified by accumulation of marker proteins which are degraded through the pathway and one such marker protein which is frequently used is p62 [60, 61, 167]. Cells cultured in HFHS-OPLA but not HFHS-POLA media compared to LFLS media tended (p= 0.08) to have a higher relative intracellular concentration of p62 (Figure 5.4A) suggesting a lower level of autophagic flux. However, marker proteins alone do not always reflect flux through autophagy so autophagic flux was quantified by accumulation of LC3-II with and without incubation with autophagic inhibitor BAF. Similarly, this showed a tendency (p = 0.074) for hepatocytes cultured in HFHS-OPLA but not HFHS-POLA media, to have lower autophagic flux compared to those cultured in LFLS media.

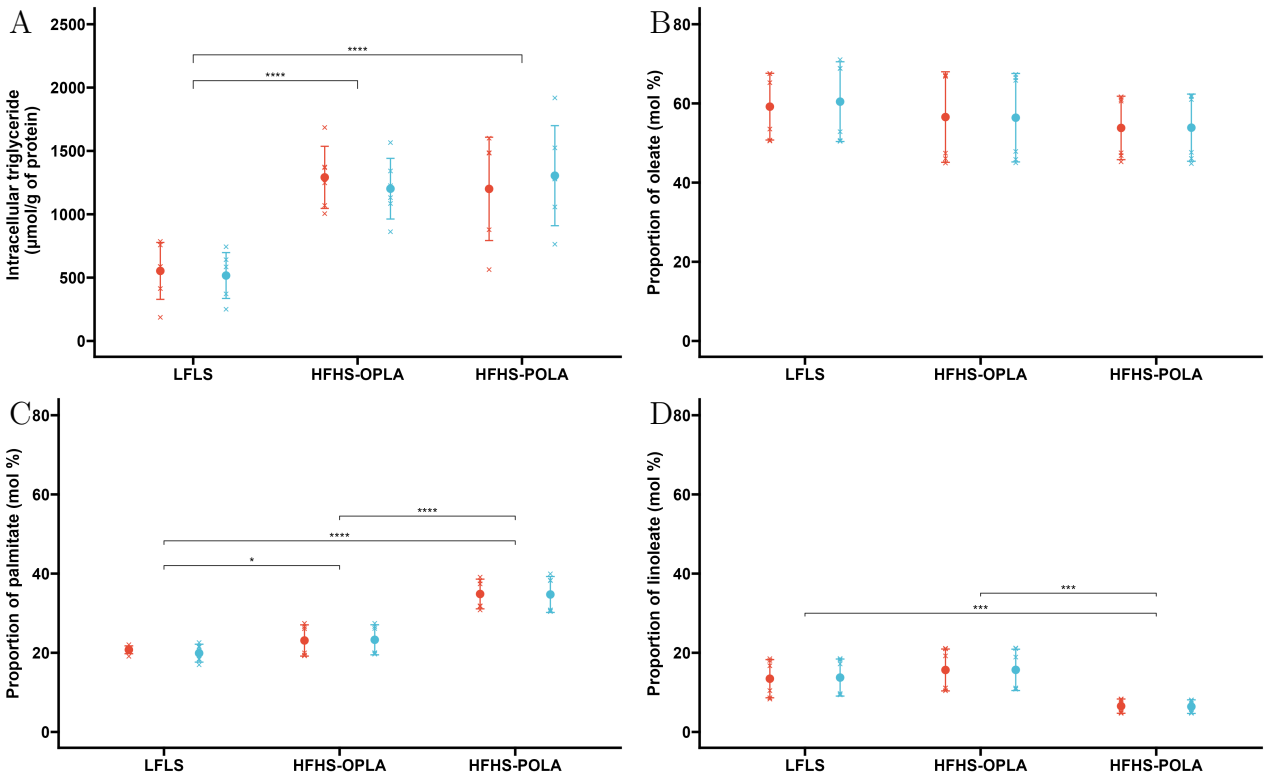


Figure 5.3: The effect of media fatty acids and insulin on intrahepatocellular triglyceride accumulation. Huh7 cells were cultured in low-fat low-sugar media (LFLS), high-fat high-sugar (HFHS-) OPLA or HFHS-POLA and 0.1 nM (red) or 100 nM (blue) of insulin for seven days with media changes every day. **A)** Total intracellular triglycerides were extracted and quantified. The intracellular proportion of **B)** oleate, **C)** palmitate and **D)** linoleate to intrahepatocellular triglyceride was analysed through gas chromatography. $^{*}p<0.05$, $^{***}p<0.001$, $^{****}p<0.0001$. Data presented as mean ± sd from six biological repeats (**n=6**).

5.3.4 The effect of media fatty acid composition and insulin concentration on inflammatory activation

Media was collected on day seven of the culture and cytokine secretion was quantified using the Olink® proteomics platform to investigate the effects of FA composition and hyperinsulinemia on inflammatory activation. Principal component analysis suggested that differences in cytokine secretion between LFLS- and HFHS-treated cells accounted for the first two components (dimension 1 - 42.68 % and dimension 2 - 26.53 %, Figure 5.5A). Hepatocytes cultured in HFHS-OPLA had significantly higher secretion of 7 cytokines (CCL3, CCL4, CSF1, CXCL9, CXCL10, IL6 and CXCL8) compared to hepatocytes cultured in LFLS (Figure 5.5B). In contrast, only 4 cytokines (CCL3, CCL4, CXCL9 and CSF1) had higher secretion in HFHS-POLA-treated cells compared to LFLS-treated cells and cells cultured in HFHS-OPLA had significantly higher

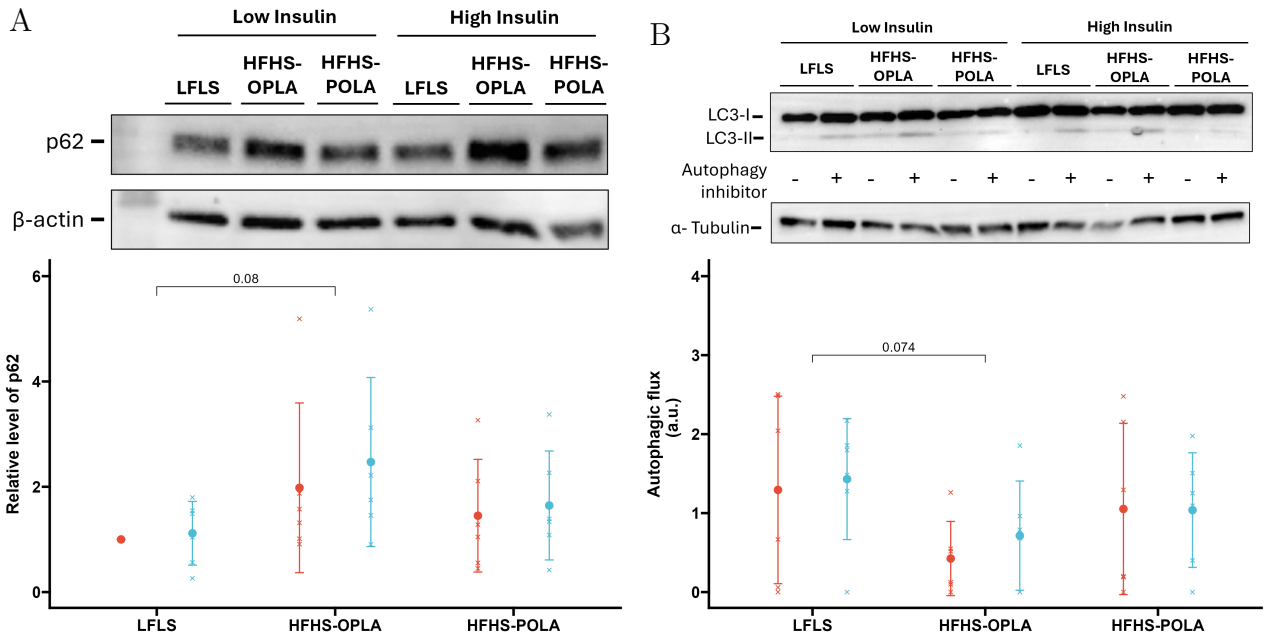


Figure 5.4: The effect of media fatty acids and insulin on autophagic flux. Huh7 cells were cultured in low-fat low-sugar media (LFLS), high-fat high-sugar (HFHS-) OPLA or HFHS-POLA and 0.1 nM (red) or 100 nM (blue) of insulin for seven days with media changes every day. **A)** Relative p62 protein accumulation was quantified and **B)** autophagic flux was calculated as LC3-II intensity (relative to housekeeper protein α-Tubulin): (Inhibition - Basal)/Basal. Data presented as mean ± sd from six biological repeats (**n=6**) carried out in technical duplicate.

secretion of CXCL10 than cells cultured in HFHS-POLA. Media insulin concentration had no effect on secretion of the cytokines measured.

To further investigate the effect of FA composition and insulin concentration on hepatocellular inflammatory activation, Huh7 hepatocytes were co-cultured with LX2 hepatic stellate cells (HSCs). HSCs are mesenchymal cells that reside in the liver in a quiescent state but are thought to be the main driver of fibrosis observed in MASLD once activated. Their activation can be measured by the expression of collagen type I alpha I (COL1A1) and α-smooth muscle actin (α-SMA) [168]. Hepatocytes were cultured in experimental media and HSCs were cultured in maintenance media so any differences in HSC activation would be from hepatokines secreted from the hepatocytes which diffused through the semi-permeable membrane the Huh7 hepatocytes were cultured on (Figure 5.1). There was no difference in HSC α-SMA or COL1A1 intensity regardless of the media FA composition or insulin concentration the hepatocytes were treated with (Figures 5.6A-5.6B). This suggests that the hepatokines secreted by hepatocytes in response to the treatment do not activate HSCs.

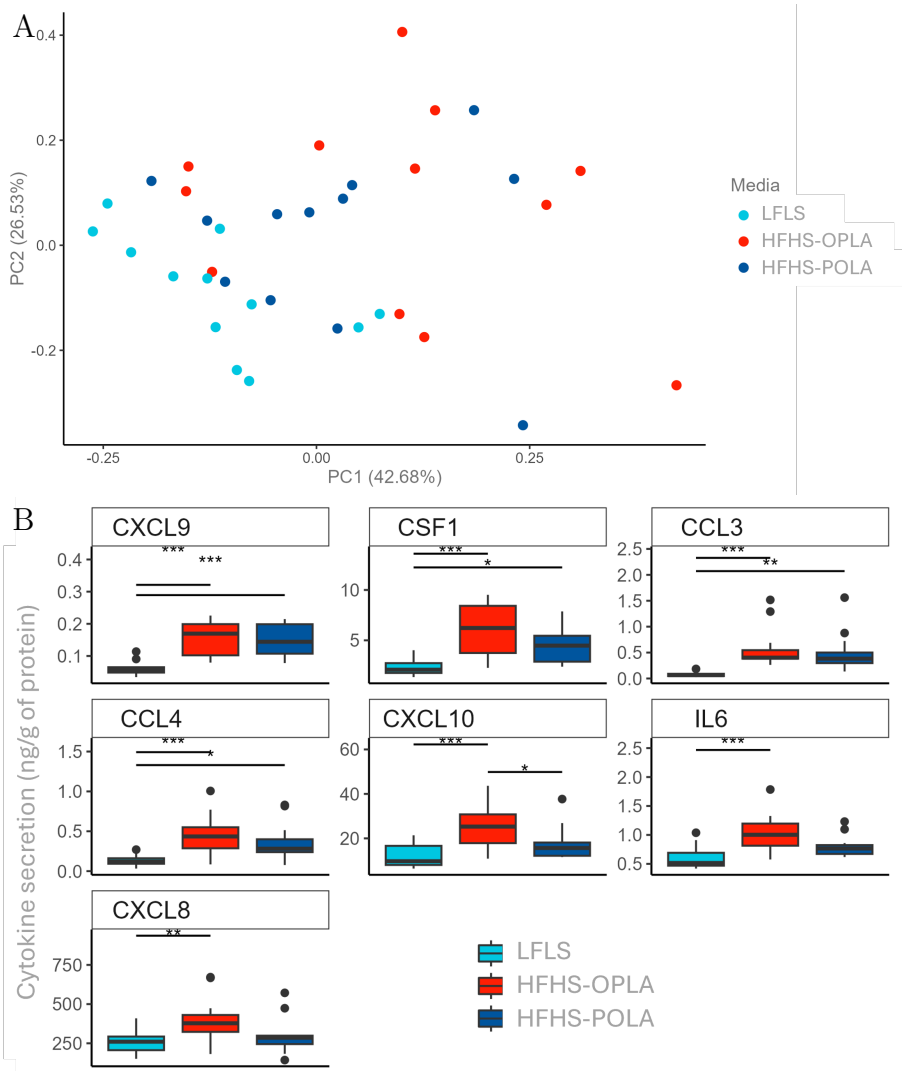


Figure 5.5: The effect of media fatty acids on cytokine secretion. Huh7 cells were cultured in low-fat low-sugar media (LFLS), high-fat high-sugar (HFHS-) OPLA or HFHS-POLA for seven days with media changes every day. Media was collected and cytokines quantified through Olink® proteomics platform. **A)** Principal component analysis was performed on the proteomics data and **B)** boxplots were generated for cytokines which showed significant differences in secretion. $^{*}p<0.05$, $^{**}p<0.01$, $^{***}p<0.001$ from six biological repeats carried out in technical duplicate (**n=6**). Abbreviations: PC, principal component.

5.3.5 The effect of media fatty acid composition and insulin concentration on hepatocellular injury

It has been suggested that saturated FAs may lead to a greater increase in hepatocellular injury [42, 78, 79] and similarly hyperinsulinemia is associated with MASLD progression to MASH [7, 24, 25]. Cytokeratin-18 (CK-18) fragment has been strongly associated with hepatocellular injury and can be used clinically as a biomarker for MASH [169]. Therefore, CK18 fragment

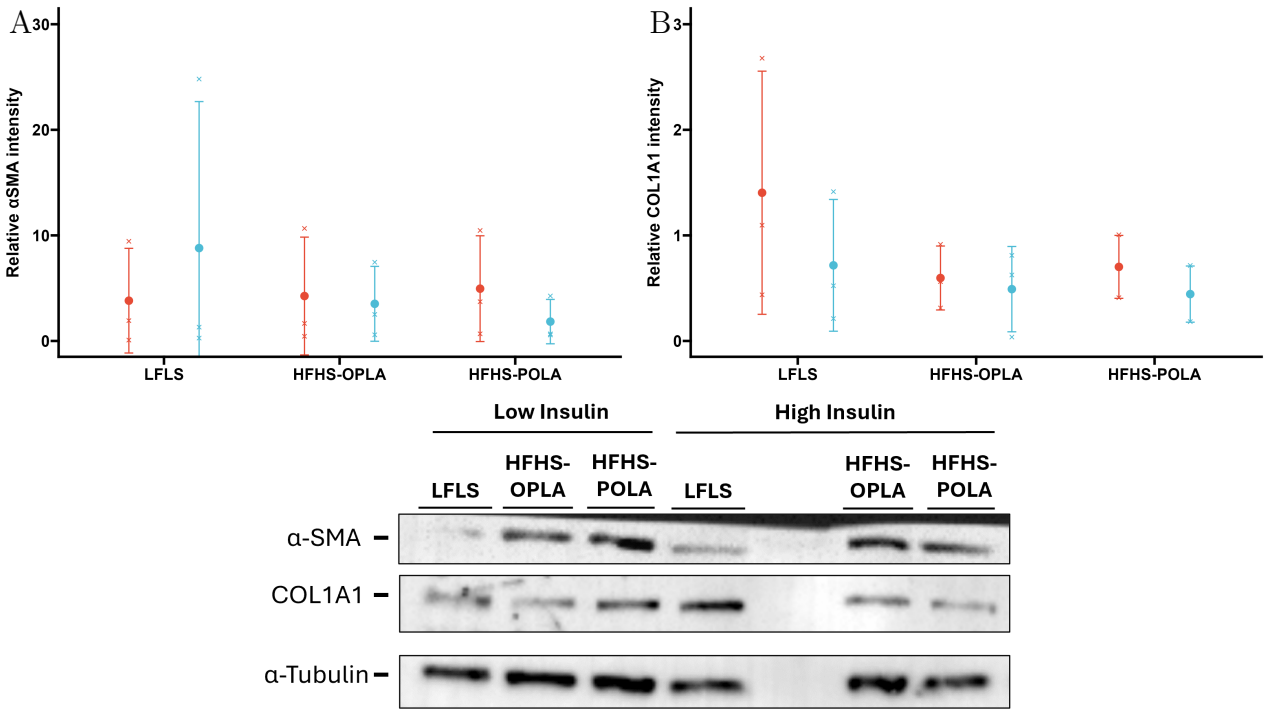


Figure 5.6: The effect of media fatty acids and insulin on hepatocyte-media activation of hepatic stellate cells. Huh7 hepatocytes treated with low-fat low-sugar media (LFLS), high-fat high-sugar (HFHS-) OPLA or HFHS-POLA for seven days with media changes every day were co-cultured with LX2 hepatic stellate cells. Hepatic stellate cell relative **A)** α-SMA and **B)** COL1A1 intensity as measured by Western Blot. Data presented as mean ± sd from three biological repeats carried out in technical duplicate (**n=3**). Abbreviations: α-SMA, α-Smooth muscle actin; COL1A1, Collagen type I alpha 1.

secretion was used as a marker to investigate the effect of media FA composition and insulin concentration on hepatocellular injury. After seven days of treatment, cells cultured in HFHS media had higher secretion of CK-18 fragments compared to cells cultured in LFLS media with no difference seen with insulin concentration (Figure 5.7A). CK-18 fragments were also measured in the media of cells cultured for 1, 3, 7 or 10 days at 0 nM insulin and a two-way ANOVA showed a significant main effect of media (p=0.014), with HFHS-treated cells having greater secretion than LFLS-treated cells, but no significant main effect for time (p=0.148) or interaction effect (p=0.930) (Figure 5.7A).

5.3.6 The effect of media fatty acid composition on insulin resistance

Although no signatures of selective hepatic IR were found to be associated with liver fat content in humans at fasting in Chapter 3, it has been suggested that liver fat composition may play

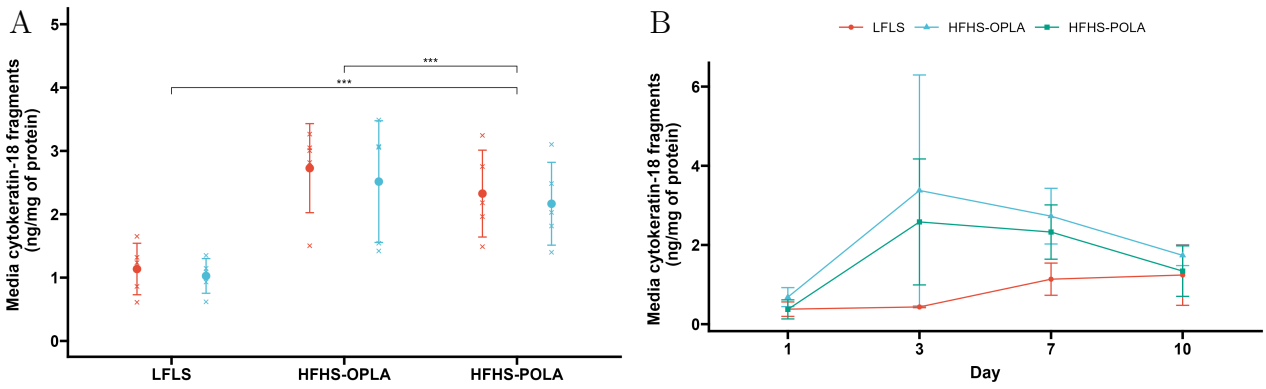


Figure 5.7: The effect of media fatty acids and insulin on hepatocellular injury. Huh7 cells were cultured in low-fat low-sugar media (LFLS), high-fat high-sugar (HFHS-) OPLA or HFHS-POLA and 0.1 nM (red) or 100 nM (blue) of insulin with media changes every day. Media was collected and cytokeratin-18 fragment concentration was measured as a marker of hepatocellular injury at **A)** day 7 and **B)** days 1, 3, 7 and 10. $^{***}p<0.001$. Data presented as mean ± sd from at least three biological repeats carried out in technical duplicate.

a role in the development of IR [68]. To investigate this, Huh7 cells were cultured in LFLS, HFHS-OPLA or HFHS-POLA media for seven days with media changes every day and glucose production was measured during 30 mins of stimulation with 0 or 100 nM insulin. Compared to LFLS-treated cells, HFHS-POLA treated cells had higher basal glucose production and following insulin stimulation glucose production in these cells was higher than both LFLS- and HFHS-OPLA-treated hepatocytes (Figure 5.8).

5.3.7 The effect of media fatty acid composition and insulin concentration on gene expression

RNA was extracted from Huh7 cells cultured in LFLS, HFHS-OPLA and HFHS-POLA at 0.1 nM and 100 nM concentrations of insulin with daily media changes and bulk RNA sequencing was undertaken by Novogene. Principal component analysis of this transcriptomics dataset showed that a batch effect was the primary source of variation in gene expression (dimension 1 - 70 %; Figure 5.9A) but the second dimension was due to differences in gene expression between LFLS- and HFHS-treated cells (dimension 2 - 8.1 %). Use of a mixed effects model accounted for the batch effect between rounds and resulted in a large number of deferentially expressed genes observed between conditions (Figure 5.9B). The majority of genes deferentially expressed between 0.1 nM and 100 nM insulin conditions overlapped with those deferentially

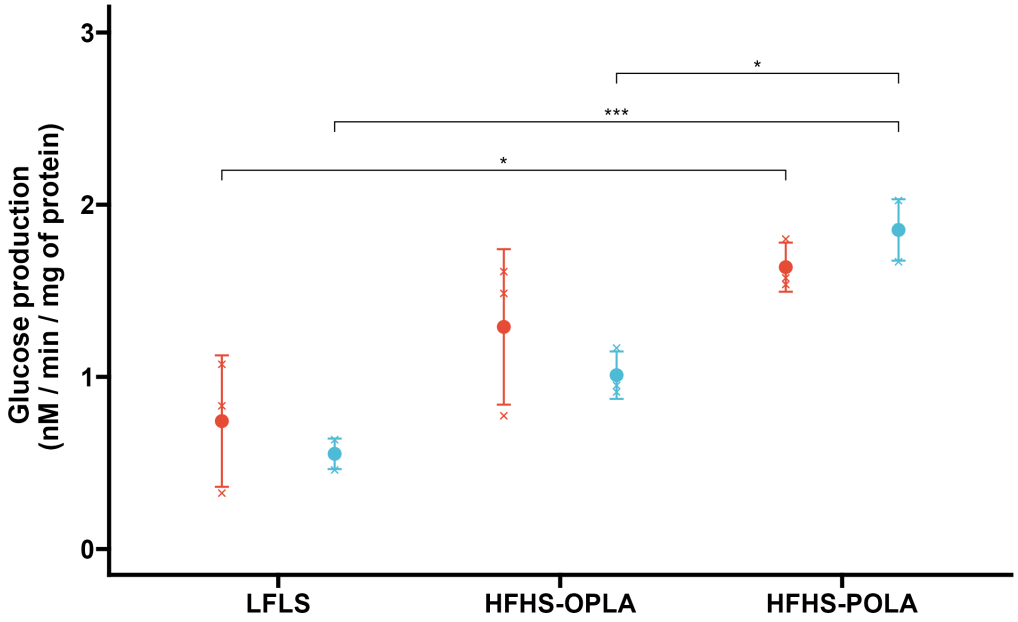


Figure 5.8: The effect of media fatty acid composition on insulin resistance. Huh7 cells were cultured in low-fat low-sugar media (LFLS), high-fat high-sugar (HFHS-) OPLA or HFHS-POLA for seven days with media changes every day. Glucose production was measured after stimulation with 0 nM (red) or 100 nM insulin (blue) for 30 mins. $^{*}p<0.05$, $^{***}p<0.001$. Data presented as mean ± sd from three biological repeats (**n=3**) carried out in technical duplicate.

expressed between HFHS-OPLA and LFLS or HFHS-POLA and LFLS (Figure 5.9B) suggesting that insulin may have a similar effect on gene expression as HFHS exposure.

There was a large overlap in differential gene expression when comparing the HFHS-OPLA and HFHS-POLA conditions to the LFLS condition (Figure 5.9B and Figures 5.10A-5.10B) indicating that differences in media sugar and FA concentrations have a far bigger effect on hepatocellular gene transcription than FA composition.

One of the top genes upregulated in both HFHS-OPLA- and HFHS-POLA-treated cells compared to LFLS-treated cells was LIPA which encodes LAL (Figures 5.10A-5.10B) which is the enzyme responsible for lipolysing TGs into FAs during lipophagy [62, 63]. Other top genes upregulated in cells cultured in HFHS compared to LFLS media were PDK4 and HMGCS2 which suggest a shift towards lipid metabolism with the former decreasing the conversion of pyruvate to acetyl-CoA by inhibiting pyruvate dehydrogenase with the latter being the first major enzyme in ketogenesis. There were 305 genes were deferentially expressed between HFHS-OPLA and HFHS-POLA conditions (Figure 5.10C) with the most significant being FADS2 that was upregulated in HFHS-POLA cells and codes for the FA Desaturase 2 enzyme which

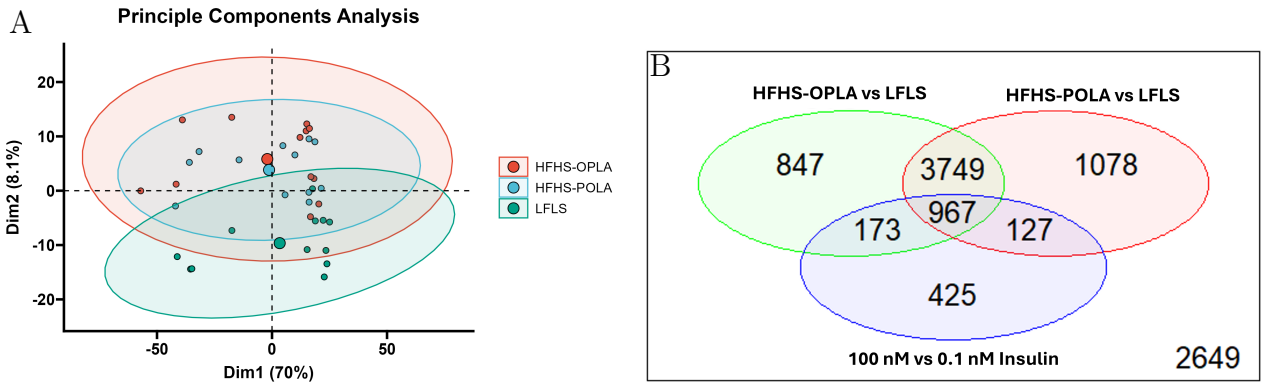


Figure 5.9: The effect of media fatty acids and insulin on gene expression. Huh7 cells were cultured in low-fat low-sugar media (LFLS), high-fat high-sugar (HFHS-) OPLA or HFHS-POLA at 0.1 nM or 100 nM of insulin for 7 days with media changes every day. Bulk RNA sequencing data was first analysed by **A)** principal component analysis. **B)** a Venn diagram showing the number of significantly deferentially expressed gene for each contrast. Data from six biological repeats (**n=6**) carried out in technical duplicate.

catalyses the introduction of a double bond into fatty acid chains. In contrast, CDK6 was the most significant gene to be upregulated in the HFHS-OPLA condition which might suggest a higher level of proliferation in these cells. 1,692 genes were also significantly deferentially expressed between 0.1 nM and 100 nM insulin concentrations with a generally larger fold change for genes which were significantly upregulated rather than down regulated (Figure 5.10D).

Gene set enrichment analysis (GSEA) using KEGG pathways showed a significant upregulation in pathways associated with FA metabolism, PPAR signalling and terpenoid backbone biosynthesis and a downregulation in pathways associated with complement and coagulation, bile secretion, HIF-1 signalling and starch and sucrose metabolism when comparing cells cultured in HFHS-OPLA or HFHS-POLA media to those cultured in LFLS media (Figures 5.11A-5.11B). HFHS-OPLA-treated cells also upregulated pathways associated with proliferation compared to LFLS-treated cells whereas HFHS-POLA-treated cells upregulated pathways associated with the ribosome and downregulated circadian rhythm pathways compared to LFLS-treated cells. Compared to cells cultured in 0.1 nM insulin, those cultured in 100 nM insulin upregulated pathways associated with glycolysis, oxidative phosphorylation, complement and coagulation, bile secretion and HIF-1 but down regulated Polycomb repressive complex and ribosome biogenesis pathways (Figure 5.11C). GSEA comparison between HFHS-OPLA and HFHS-POLA using GSEA was not possible due to an insufficient number of deferentially

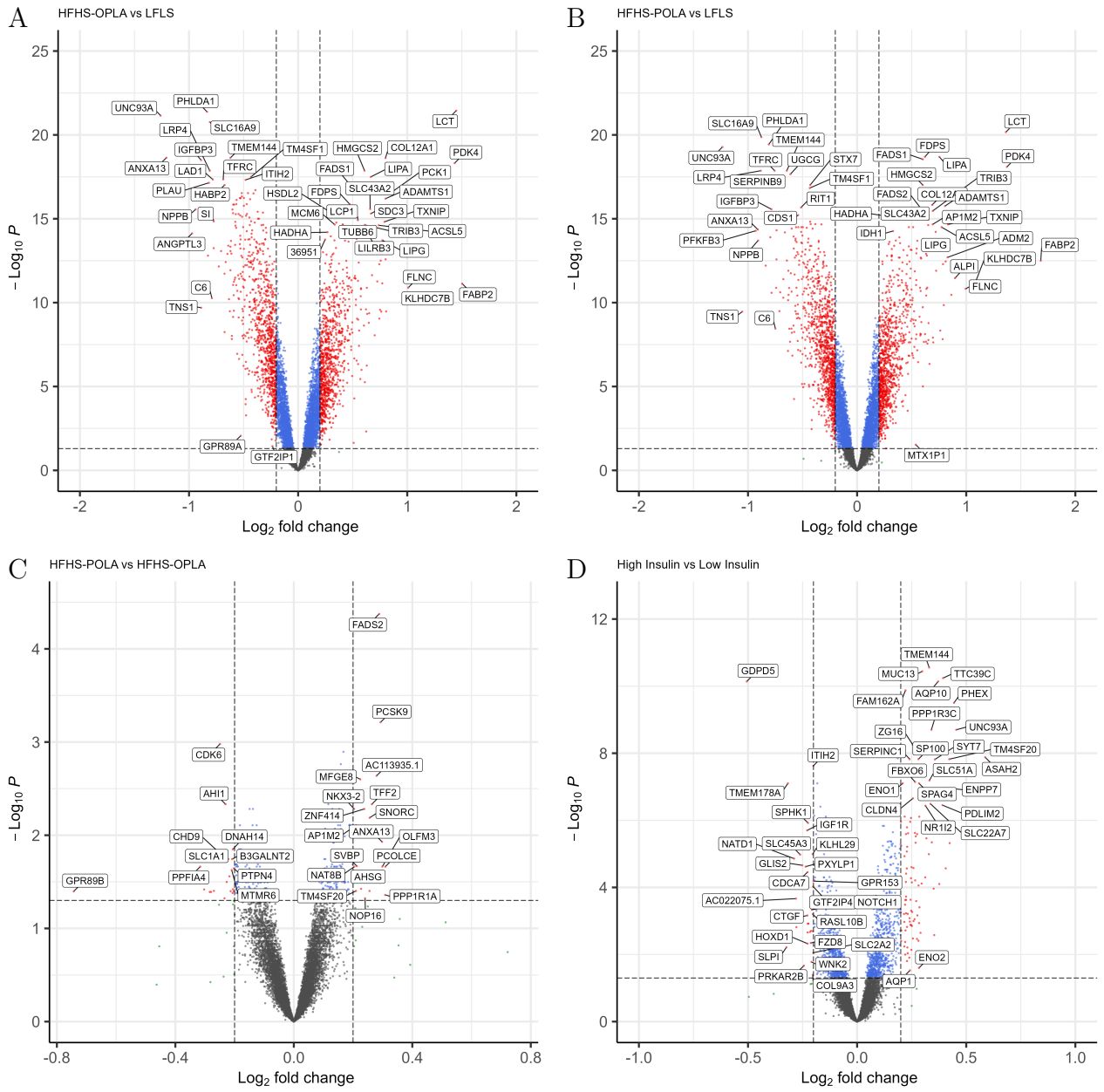


Figure 5.10: Volcano plots showing the effect of media fatty acids and insulin on gene expression. Huh7 cells were cultured in low-fat low-sugar media (LFLS), high-fat high-sugar (HFHS-) OPLA or HFHS-POLA at 0.1 nM or 100 nM of insulin for 7 days with media changes every day. Volcano plots were generated from bulk RNA sequencing data for **A)** HFHS-OPLA compared to LFLS, **B)** HFHS-POLA compared to LFLS, **C)** HFHS-POLA compared to HFHS-OPLA and **D)** high insulin compared to low insulin media. Points coloured in red represent deferentially expressed genes (p<0.05). Data from six biological repeats (**n=6**) carried out in technical duplicate.

expressed genes. Pathways associated with autophagy or inflammation were not significantly deferentially expressed between any of the comparisons made.

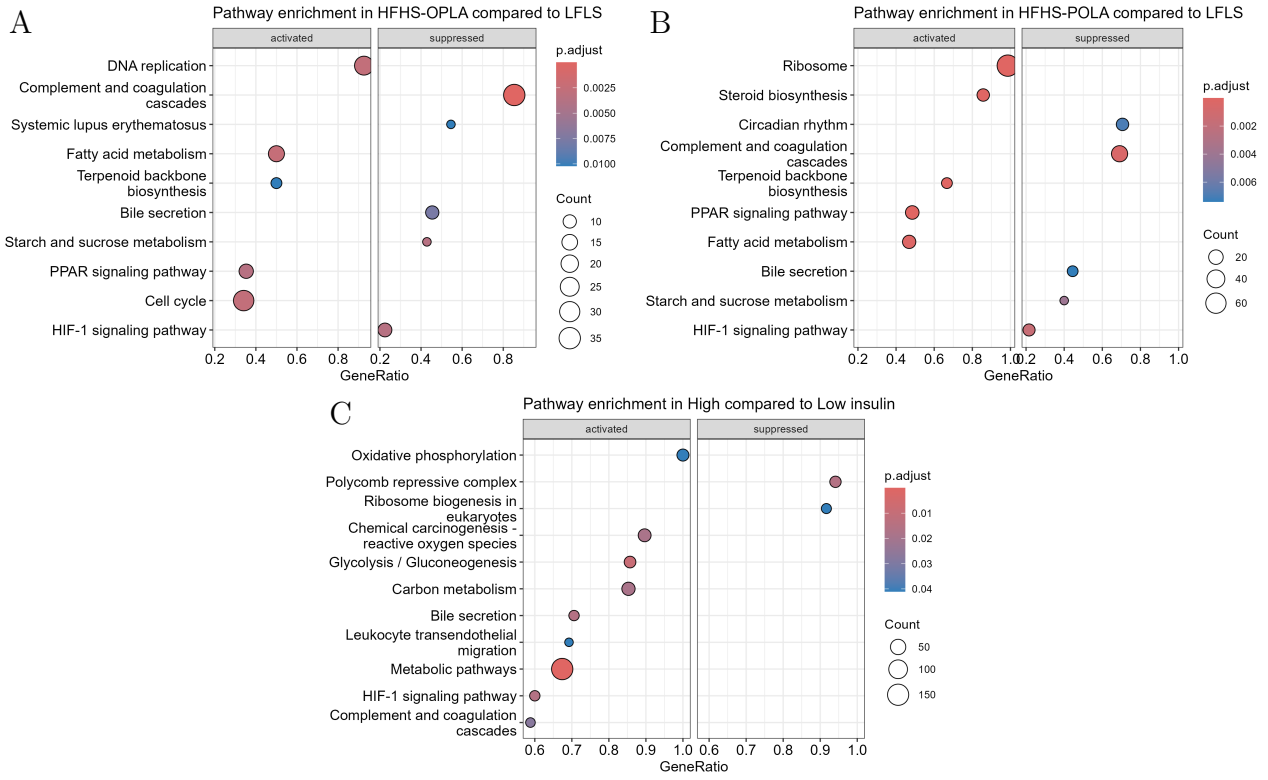


Figure 5.11: The effect of media fatty acids and insulin on pathway regulation. Huh7 cells were cultured in low-fat low-sugar media (LFLS), high-fat high-sugar (HFHS-) OPLA or HFHS-POLA at 0.1 nM or 100 nM of insulin for 7 days with media changes every day. Gene set enrichment analysis was for **A)** HFHS-OPLA compared to LFLS, **B)** HFHS-POLA compared to LFLS and **C)** high insulin compared to low insulin media. Data from six biological repeats (**n=6**) carried out in technical duplicate.

5.4 Discussion

Dietary FA composition and hyperinsulinemia have both been associated with MASLD development *in vivo* and it has been suggested that an aberrant decrease in hepatocellular autophagy may also play a role. However, the effects of FA composition and hyperinsulinemia on hepatocellular autophagic flux and the inflammatory activation which may trigger MASLD progression, have been largely overlooked. Based off the work from Chapter 4, which showed modest changes in inflammatory activation and autophagic flux in Huh7 cells, an optimised *in vitro* model of IHCTG accumulation was developed with use of the same FA mixtures but a daily media changing regime. In this chapter, I utilised this model to investigate the effects of FA composition and hyperinsulinemia on autophagy and inflammatory activation.

5.4.1 Model assessment

The difference in media changing regime did not affect cellular viability for Huh7 cells cultured in media supplemented with OA, OPLA or POLA, with ATP concentrations being comparable with the previous Huh7 cell culture model, where media was changed every other day. However, in contrast to the previous model, when Huh7 cell media was changed daily, there was a significant decrease in cell viability observed in hepatocytes cultured in PA compared to all other conditions. Indeed, PA-induced lipotoxicity is well reported [42, 74, 75, 152] and it has been suggested that it may be caused by increased oxidation leading to mitochondrial dysfunction and increased production of reactive oxygen species, diacylglycerols (DAG) or ceramides [78, 170]. Alternatively, it has been demonstrated that PA leads to the accumulation of the TG tripalmitin, which is solid at room temperature and may trigger endoplasmic reticulum stress and apoptosis [171]. Taking the current results and that of Chapter 4 together, my work suggests that PA does decrease hepatocellular viability but only after repeated daily exposure suggesting that there may be a threshold of accumulation above which hepatocytes are unable to appropriately process the FA. My observation that the same concentration of PA in combination with other FAs (the POLA condition) rescues this lipotoxicity further highlights the suitability of these FA mixtures for studying the effects of FA composition without significantly compromising hepatocellular viability.

Work presented in Chapter 3, as well as other *in vivo* human studies [114] have reported a strong positive association between hepatic DNL and hyperinsulinemia and on the basis of these observations, it has been suggested that hyperinsulinemia may drive an increase in IHCTG [7]. Similarly, it has been suggested that hyperinsulinemia suppresses autophagy which may decrease TG turnover for disposal through lipophagy, and lead to an increase in IHCTG [55, 165]. Despite an association between hyperinsulinemia and IHCTG, the causal relationship of this has yet to be properly established. In the work presented in this chapter, Huh7 cells were cultured for seven days at either 0.1 nM or 100 nM concentrations of insulin and was found to have no effect on IHCTG accumulation or composition. In contrast, cells cultured in HFHS media had higher IHCTG compared to those cultured in LFLS media and IHCTG composition reflected the composition of the FA the cells were exposed to as was also observed in the previous model described in Chapter 4. This is in-line with previously published data from our lab

which has shown no significant effect of media insulin concentration on IHCTG in Huh7 cells treated daily for either two or four days [84]. Although hyperinsulinemia has been associated with increased DNL in humans *in vivo*, the work presented in Chapter 3 shows no association between DNL and IHCTG and therefore, it is plausible that hyperinsulinemia did increase DNL in this *in vitro* model but that similarly did not lead to an increase in IHCTG. This dissociation between increasing DNL and IHCTG accumulation may be due to compensation by the liver in the form of increased TG secretion through VLDL or decreased FA uptake.

5.4.2 The effect of FA composition on autophagy

Despite an increase in IHCTG accumulation in cells treated with HFHS compared to LFLS media, there was no significant difference in autophagic flux or markers of autophagy. However, cells treated with HFHS-OPLA, but not those treated with HFHS-POLA, tended to have lower autophagic flux than those treated with LFLS. This might suggest that increasing media concentrations of PUFAs may lead to a decrease in autophagic flux which is not observed with SFAs. However, unlike the model used in Chapter 4, this was not accompanied by a significant decrease in general autophagic gene expression, suggesting this effect is not transcription mediated. Others have demonstrated autophagic suppression mediated by Beclin 1 cleavage in HepG2 hepatocytes cultured for 6-12 hours in PA compared to OA [152, 163]; it would be of interest to quantify Beclin 1 cleavage in my cell model. However, it is challenging to compare my results with other studies due to the use of different cell lines, the substantially longer length of culture and comparison of predominantly SFA and PUFA enriched FA mixtures instead of OA and PA.

Although there was no difference in general autophagic gene expression, the gene coding for LAL was one of the most significantly upregulated genes when comparing cells cultured in HFHS-OPLA and HFHS-POLA media to those cultured in LFLS media. This may suggest an increase in lipophagy with increased fat and sugar in the media, and it is possible that lipophagy actually increases despite a trend towards a decrease in general autophagy in HFHS-OPLA-treated cells compared to LFLS-treated cells. Future work could quantify LAL protein concentration and enzyme activity in these conditions, as these measurements could provide further insight into the level of hepatocellular lipophagy in cells treated with different FA compositions.

5.4.3 The effect of FA composition on inflammatory activation

To investigate the effect of FA composition on inflammatory activation, cytokines from the media of Huh7 cells cultured in HFHS-POLA or HFHS-OPLA were measured through targeted proteomics. HFHS-treated cells showed an increased in chemokine secretion compared to LFLS-treated cells which was generally more prominent in HFHS-OPLA compared to HFHS-POLA. These observations are in-line with results from Chapter 4 where PHH cultured in media supplemented with FAs compared to FA-free media had a higher gene expression of chemokines. Many of the same chemokines also had higher expression in HFHS-cells compared to LFLS-treated cells in this model and analysis of transcriptomic data also showed this was associated with greater chemokine gene expression. However, despite higher chemokine gene and protein expression in HFHS cells compared to LFLS cells, there was no difference in the expression of pathways associated with inflammation. This might suggest the effect is mediated by phosphorylation of transcription factors rather than an increase in transcription factor expression. For example, NF-κB is known to regulate chemokine expression and secretion however its activation and translocation to the nucleus would not be observed as an increase in its expression. Therefore, future work could look at the phosphorylation of major transcription factors known to regulate chemokine expression such as NF-κB and c-Jun N-terminal kinases (JNK) as previous studies have also shown that activation of these signalling cascades can lead to activation of hepatocellular inflammation [41–45].

Despite an increase in cytokine secretion in cells cultured in HFHS compared to LFLS, when these hepatocytes were co-cultured with HSCs there was no difference in HSC activation. HSC are generally activated by pro-fibrotic cytokines such as transforming growth factor-β, platelet-derived growth factor and vascular endothelial growth factor but are not typically activated by chemokines [172], which were the majority of cytokines that the hepatocytes were secreting. It is plausible that the chemokines secreted by the hepatocytes may have induced HSC chemotaxis which could have led to their activation had there been cellular contact. However, HSCs can also be activated by many other hepatic cell types [172] so it is also possible that hepatocellular chemokines mediate the recruitment and activation of other cells such as Kupffer cells and macrophages which in turn activate HSCs. This would

be in line with observations *in vivo* in humans which suggest that inflammatory activation precedes the induction of fibrosis in MASLD [40, 173].

5.4.4 The effect of FA composition on insulin resistance

Although previous *in vitro* studies have shown an increase in markers of IR in hepatocytes treated acutely with PA compared to OA [75, 77, 78], the effects of IR in hepatocytes treated chronically with FA mixtures enriched with SFAs or PUFAs is not known. I found that Huh7 cells treated with HFHS-POLA but not HFHS-OPLA, had higher basal levels of glucose production which were higher than both LFLS- and HFHS-OPLA-treated hepatocytes when stimulated with insulin. The increased glucose production in cells treated with POLA compared to OPLA was also associated with upregulation of PCK2 as identified through transcriptomic analysis. The PCK2 gene codes the mitochondrial form of phosphoenolpyruvate carboxykinase (PEPCK) which is one of the major regulatory enzymes in GNG [174] and although less is known about the mitochondrial form, increasing evidence suggests it also plays a substantial role in GNG regulation [175, 176]. It would therefore be of interest to measure the expression and phosphorylation of this protein in these samples to confirm its association.

5.4.5 The effect of hyperinsulinemia on autophagy and inflammatory activation

Although hyperinsulinemia has previously been associated with decreased autophagy and increased inflammatory activation both *in vivo* and *in vitro* [53, 55, 111], I found no effect on either with no difference in cytokine secretion, HSC activation, autophagic flux or gene expression of either associated pathway between Huh7 cells cultured in 0.1 nM insulin and 100 nM insulin. Despite this, there were clear indications from the transcriptomics that the cells did indeed respond to the insulin as the increase in media insulin concentration led to an increase in pathways associated with oxidative phosphorylation, glycolysis and carbon metabolism. Despite the prolonged and repeated exposure to insulin there was no difference in gene expression of the insulin receptor between cells cultured in high and low insulin concentrations but this does not necessarily rule out cellular desensitisation to insulin. It would be of interested to compare

insulin clearance on day 1 of the culture to that of day 7 as well as lower concentrations of insulin as the supraphysiological concentration used may have rapidly saturated the response.

5.4.6 Limitations

The work presented here is not without limitations and there were several more opportunities to make the model used more physiologically representative. For example, *in vivo* hepatocytes also receive dietary FAs through TG-rich lipoproteins (TRLs) as well as free FAs and the work in the next chapter explores the processing of these TRLs further which has recently been largely overlooked. It would also be of interest to repeat these experiments either in PHHs or in Huh7 cells for an even longer culture (10+ days) as this may give a more extreme phenotype which may closer resemble the pathogenesis of MASLD *in vitro*.

5.4.7 Conclusions

Taken together, I found that FA composition and hyperinsulinemia had no effect on total IHCTG accumulation but that culturing hepatocytes in media enriched in PUFAs may lead to a decrease in autophagic flux and was also associated with increased inflammatory activation through the secretion of chemokines. Future work could focus on establishing a causal relationship by using activators of autophagy such as spermidine to try to rescue the inflammatory activation observed when cells are treated with PUFAs. Additionally the elevated basal and insulin-stimulated glucose production in cells treated with media enriched in SFAs compared to PUFAs acts as a marker of IR which suggests that IHCTG composition may play a greater role in determining IR in hepatocytes rather than IHCTG content alone.

'Est in averno microscopium'

6

Investigating the role of autophagy in triglyceride-rich lipoprotein processing

Contents

6.1 Introduction 87
6.2 Methods 88
6.2.1 Overview of experimental design 88
6.2.2 Participants 90
6.2.3 Experimental diet 90
6.2.4 Post-prandial study day 90
6.2.5 Isolation and quantification of human-derived TRLs 90
6.2.6 Hepatocyte pretreatment 91
6.2.7 Incubation with TRLs 91
6.2.8 Lipid extraction and quantification 92
6.2.9 Imaging experiments 92
6.3 Results 93
6.3.1 TRLs are processed via the endolysosomal pathway 93
6.3.2 The effect of autophagic inhibition on TRL processing 93
6.3.3 The effect of intrahepatocellular triglyceride accumulation on TRL processing 95
6.3.4 The effect of TRLs on IHCTG accumulation 97
6.4 Discussion 97
6.4.1 The role of autophagy in TRL processing 98
6.4.2 The effect of IHCTG on TRL processing 99
6.4.3 The contribution of TRL to IHCTG accumulation 100
6.4.4 Limitations and future work 100
6.4.5 Conclusions 100

6.1 Introduction

Pathological lipid accumulation in the liver is characteristic of MASLD but the mechanisms underlying the development and/or progression remain unclear. Whilst research has been focused on the flux of non-esterified fatty acid (NEFA) to the liver, the contribution of triglyceride-rich lipoproteins (TRLs) has been largely overlooked.

In the blood, TGs are transported as TRL particles which consist of a TG-rich core surrounded by an apolipoprotein-containing phospholipid monolayer. These particles are produced in the intestine as chylomicrons after the consumption of a fat-containing meal or in the liver as very-low-density lipoprotein (VLDL) and are hydrolysed by LPL on extra-hepatic tissues (including adipose tissue and skeletal muscle) to TRL remnants. Although the majority of the lipids entering the liver are adipose tissue-derived FAs, hepatic uptake and processing of TRLs represents a potentially major source of lipid uptake [27, 177]. It has also been shown that obese individuals have decreased clearance of TRLs compared to lean individuals which may lead to higher levels of circulating TRLs with a greater TG content [28, 29]. Therefore, the contribution of TRLs to hepatic lipid uptake may be especially important in MASLD but hepatic TRL processing within this context is poorly understood.

Studies in the 1980s that labelled rodent TRLs with the radioiodine (^{125}I) and traced their fate through the liver observed that these particles are exclusively taken up by hepatocytes and metabolised via the endolysosomal pathway [5]. The role of this autophagy-mediated pathway was demonstrated by the addition of autophagic inhibitors, such as chloroquine, which prevented the fusion of the lysosome to the TRL-containing endosome and inhibited their metabolism [178]. Taken together, the findings of these studies showed that TRLs are taken up into endosomes which fuse with lysosomes to form endolysosomes where the TG in TRLs undergo lipolysis to liberate FAs. The endolysosomes then fuse with the cell surface membrane and release the liberated FA into the extracellular space to be recirculated back into the hepatocyte where they can enter the mitochondria and undergo oxidation or be esterified to TG for storage in LDs or secretion in VLDL (Figure 6.1) [5]. Despite elucidating this pathway of hepatic TRL metabolism, it was not until 20 years later that the link between autophagy and IHCTG accumulation was

made [51] and it is plausible that the aberrantly down-regulated autophagy observed in those with MASLD may affect hepatic TRL processing and contribute to further IHCTG accumulation. Therefore, by utilising human-derived TRLs labelled with ^{13}C palmitate (Figure 6.1), I aimed to investigate the role of autophagy in hepatocellular TRL processing and explore if TRL processing is impaired in the model of IHCTG accumulation described in Chapter 5.

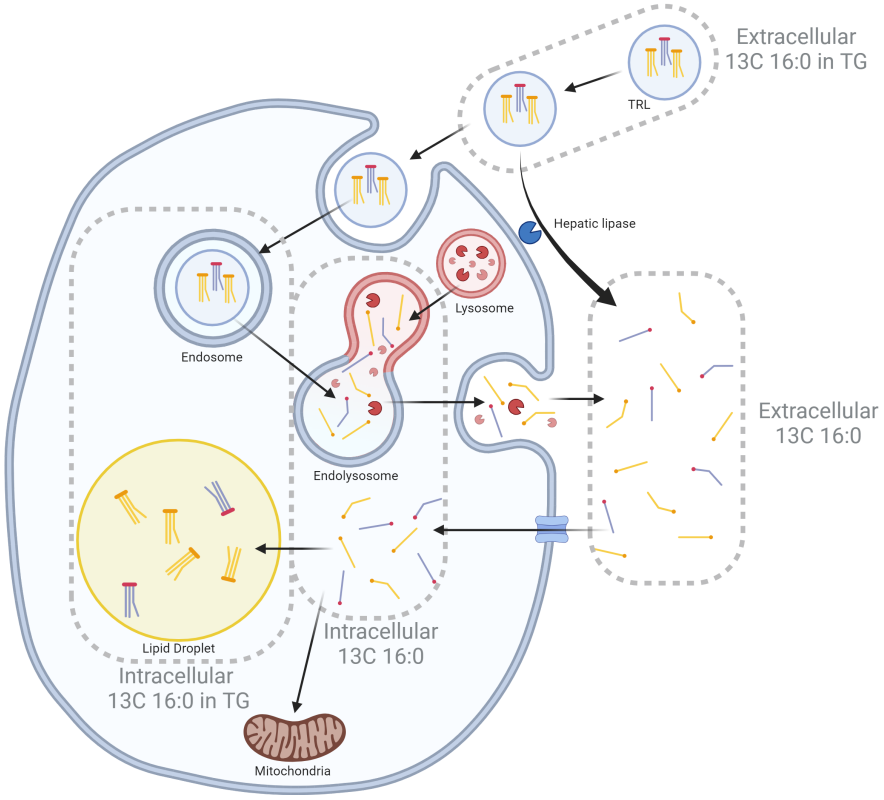


Figure 6.1: The proposed processing of TRL 13C 16:0 in TG by hepatocytes. TRL 13C 16:0 in TG is taken up by hepatocytes into the endosome and enters the intracellular 13C 16:0 in TG pool. On fusing with a lysosome, the 13C 16:0 in TG is lipolysed to 13C 16:0 which is then released into the extracellular space by the fusion of the endolysosome to the cell surface membrane. Extracellular 13C 16:0 can then be recirculated into the cell to be stored as TG in a lipid droplet or oxidised by mitochondria. Abbreviations: TG, Triglyceride; TRL, triglyceride-rich lipoprotein; 16:0, palmitate.

6.2 Methods

6.2.1 Overview of experimental design

To collect human-derived TRLs, participants free from known metabolic disease were recruited and consumed a high-carbohydrate, low-fat diet for three days. Following an overnight fast, participants attended a study day where they consumed a high-fat test meal containing the stable

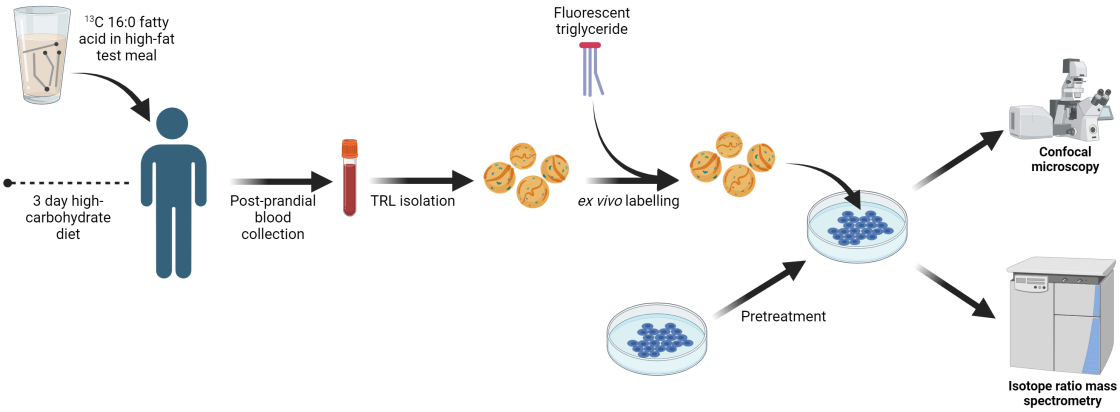


Figure 6.2: Overview of methods. Participants consumed a three-day high-carbohydrate diets before attending a post-prandial study day where they consumed a high-fat test meal containing ^{13}C fatty acid. Blood was collected during the post-prandial period and TRLs were isolated and added to the media of pretreated cells. Cells were harvested and lipids were extracted and quantified through isotope ratio mass spectrometry. In some experiments TRLs were *ex vivo* labelled with fluorescent triglyceride and their uptake and processing observed through confocal microscopy. Abbreviations: TRL, triglyceride-rich lipoprotein.

isotope tracer [U^{13}C] palmitate. Blood samples were taken over the course of the post-prandial period and TRLs particles isolated by density gradient ultra-centrifugation. Huh7 hepatocytes which had been cultured in LFLS, HFHS-OPLA or HFHS-POLA media for three days and pretreated with an autophagic inhibitor or vehicle control for 3 hours prior were cultured with the isolated TRLs for 2 hours before harvesting. TG and FAs were extracted from the cells and media supernatant samples and ^{13}C enrichment was quantified using gas chromatography-combustion-isotope ratio mass spectrometry (GC-C-IRMS). In some experiments the collected TRLs were *ex vivo* labelled with a fluorescently labelled TG and TRL uptake and processing was observed by confocal microscopy. A summary of the overall methods is shown in Figure 6.2.

6.2.2 Participants

Two men volunteered to take part in this study having been recruited from within the department. Both were free from any known metabolic disease, aged between 25-60 years, body mass index between 25-30 kg/m^2, were not taking medication known to affect lipid or glucose metabolism and did not smoke or consume alcohol above recommended limits. Volunteers gave written informed consent, and the study was approved by the University of Oxford Medical Sciences Interdivisional Research Ethics Committee (R75046/RE001).

6.2.3 Experimental diet

Prior to their study day, participants consumed a 3-day isocaloric high-carbohydrate diet consisting of 65 % total energy (TE) carbohydrate (with 35 % from free sugars), 15 % TE protein and 20 % TE fat to increase the production of TRLs by upregulating hepatic DNL and VLDL secretion [10, 179]. All food for the diet was provided and the daily caloric requirement was determined using the Mifflin-St Jeor equation and was designed to match individual energy requirements [180].

6.2.4 Post-prandial study day

After consuming the 3-day high carbohydrate diet, participants then attended the clinical research unit after an overnight fast and a cannula was inserted into an antecubital vein on one arm to allow for repeated blood sampling. To induce TRL production through chylomicron secretion, participants were fed a high-fat test meal containing 31.4 g carbohydrate, 83.6 g fat and 6.1 g protein and 400 mg of [U^{13}C] palmitate (16:0). Blood was collected at 120, 150, 180, 210 and 240 min from the consumption of the test meal and plasma was isolated by centrifugation and pooled.

6.2.5 Isolation and quantification of human-derived TRLs

TRL particles were then isolated from the pooled plasma using density gradient ultra-centrifugation (Svedberg flotation (Sf) $>$ 20) as previously described [124]. Briefly, sodium bromide was added to plasma to increase its density and is then pipetted into polyvinyl alcohol coated ultra-centrifuge centrifuge tubes (Beckman, 344060). Above this plasma layer a sequential density gradient of sodium chloride (1.063 - 1.006 kg/L) was made and tubes were ultra-centrifuged

in a Beckman SW40Ti swinging bucket rotor at 40,000 rpm at 14 °C. Gradients were initially run for 32 mins to collect particles with Sf > 400 (chylomicrons) before being centrifuged for a further 16.5 hours to collect particles with Sf 20 – 400 (chylomicron remnants and VLDL). These two fractions were pooled and the resulting pooled TRL TG concentration was measured on a semi-automatic analyser (ILab 600/650 clinical chemistry; Werfen, Warrington, U.K.).

6.2.6 Hepatocyte pretreatment

All work in this chapter utilised the same *in vitro* hepatocellular model characterised and described in Chapter 5. However, due to the complexity of these experiments and the results from the previous chapter, cells were only cultured in experimental media for three days and in 0.1 nM insulin. Briefly, Huh7 cells were cultured in base experimental media supplemented with 0.1 nM insulin and either 5.5 mM glucose and 200 μM OPLA (low-fat low-sugar media, LFLS), 11 mM glucose, 5.5 mM fructose and 800 μM OPLA (high-fat high-sugar OPLA media, HFHS-OPLA) or 11 mM glucose, 5.5 mM fructose and 800 μM POLA (high-fat high-sugar POLA media, HFHS-POLA) for three days with media changed every day.

To investigate the effects of autophagic inhibition, 25 nM BAF or vehicle control (DMSO) was added to the culture media for three hours prior to the cells being cultured with TRLs. The concentration and length of incubation with BAF is the same as optimised and used in the autophagic flux assay described in Chapter 2.

6.2.7 Incubation with TRLs

Experimental media was removed and cells were washed before being incubated in glucose-, phenol red- and glutamine-free DMEM supplemented with 2 % BSA, 25 nM of BAF or vehicle control (DMSO) and either TRLs (1000 μM of TG content) or vehicle control (saline). After two hours of incubation, the media supernatant was collected and cells were harvested.

The concentration of TRLs used was physiologically representative of what hepatocytes might be exposed *in vivo* [181, 182] and was optimised from a pilot study which suggested better TRL uptake and processing at 1000 μM of TG content compared to 500 μM . The 2 hour incubation time with TRLs was also derived from the pilot study which suggested limited

uptake after 30 mins incubation. This is in-line with previous literature which, although sparse, has suggested the majority of TRL uptake to occur between 1 - 6 hours of incubation [183, 184].

The concentration of BSA used was higher than conventionally used in other *in vitro* cell cultures but still under the physiological concentration found in human serum [185]. This concentration of BSA was used as it has been shown to limit the reuptake of secreted FAs into the cell [186] and was used in these experiments to trap any labelled FA liberated from TG lipolysis in the media to be collected rather than lost to oxidation once taken up into the cell.

6.2.8 Lipid extraction and quantification

TG and FAs were extracted from collected cell and media supernatant samples and converted into FAMEs as described in Chapter 2, section 2.6 before measurement by GC-C-IRMS. Sample FAMEs were identified by comparing their retention to a standard of 31 known FAMEs and quantified by comparing the peak area to that of the internal standard. The resulting concentrations were corrected to sample protein concentration as measured by protein assay (Chapter 2, section 2.4.1). The 16:0 tracer to tracee ratio was converted to molar percent enrichment (MPE) and the concentration of 13C 16:0 was calculated by subtracting the MPE of the saline treated samples from the MPE of the TRL treated samples and then multiplying by the total 16:0 concentration.

6.2.9 Imaging experiments

Human-derived TRLs were labelled *ex vivo* with fluorescent TGs (16:0-lissaminerhodamine / 18:1 / 18:1 TG; 810103C-1mg, Avanti Polar Lipids) based on a method by Paulus et al. [187]. Fluorescent TGs suspended in chloroform were dried down under nitrogen at 37 °C and then incubated in TRLs at a molar ratio of 1:20 (fluorescent TG:TRL TG content) on a shaker for 1 hour at 37 °C and 120 RPM.

50,000 Huh7 cells were seeded onto 24 mm diameter glass cover slips (VWR, 631-1583) in 6-well plates and left overnight in seeding media. The following day, cells were transfected with Rab5a-green fluorescent protein (GFP) using the CellLight™ Early Endosomes-GFP, BacMam 2.0 kit (ThermoFisher, C10586) at 50 particles per cell in 1 mL of low glucose DMEM with GlutaMAX™ and pyruvate supplemented with 0.2 % BSA and 1 % NEAA. The cells

were incubated overnight in this media before the tranfection was enhanced with the BacMam Enhancer Kit (ThermoFisher, B10107) used according to manufacturer's instructions. The transfected cells were kept in low glucose DMEM with GlutaMAX™ and pyruvate supplemented with 0.2 % BSA and 1 % NEAA overnight and were imaged the next day in glucose-, phenol red- and glutamine-free DMEM supplemented with 2 % BSA and fluorescently labelled TRLs (1000 μM of TG content) on an Olympus Flouview confocal microscope (Olympus Life Science, FV3000) at 60 x magnification for 30 mins with the help of Charlotte Frazer-Morris.

6.3 Results

6.3.1 TRLs are processed via the endolysosomal pathway

Although it is known that TRLs are internalised into hepatocytes through the LDL-receptor and processed through the endolysosomal pathway [5], I sought to confirm this in our hepatocytes and TRLs. Huh7 cells were transfected with Rab5a-GFP to fluorescently label the early endosomes and were incubated in human-derived TRLs that had been *ex vivo* labelled with fluorescent TGs for 30 mins. Compared to cells which had not been incubated with TRLs (Figures 6.3A-6.3B), TRL co-localisation to the early endosome was observed in those with TRL incubation (Figures 6.3C-6.3D).

6.3.2 The effect of autophagic inhibition on TRL processing

To determine the effects of autophagy on hepatocellular TRL processing, Huh7 cells were cultured for three days in LFLS media and then pretreated with 25 nM of the autophagic inhibitor BAF or vehicle control for three hours before incubation with TRLs containing 13C 16:0 in TG for two hours. Based on previous understanding of TRL processing in hepatocytes, the TG and FA fractions were extracted from both cell and media supernatant samples and concentration and enrichment was quantified by GC-C-IRMS (Figure 6.1). There was no difference in the disappearance of 13C 16:0 in TG from TRLs between hepatocytes treated with vehicle and with BAF, with approximately 20-25 % of the 13C 16:0 in TG from the TRLs being removed from the media over the 2 hour incubation period (Figure 6.4A). The lack of difference between conditions in intracellular 13C 16:0 in TG concentration (Figure 6.4B) suggests that BAF did not alter TRL uptake. When the FA fractions were analysed, it was found that, compared to

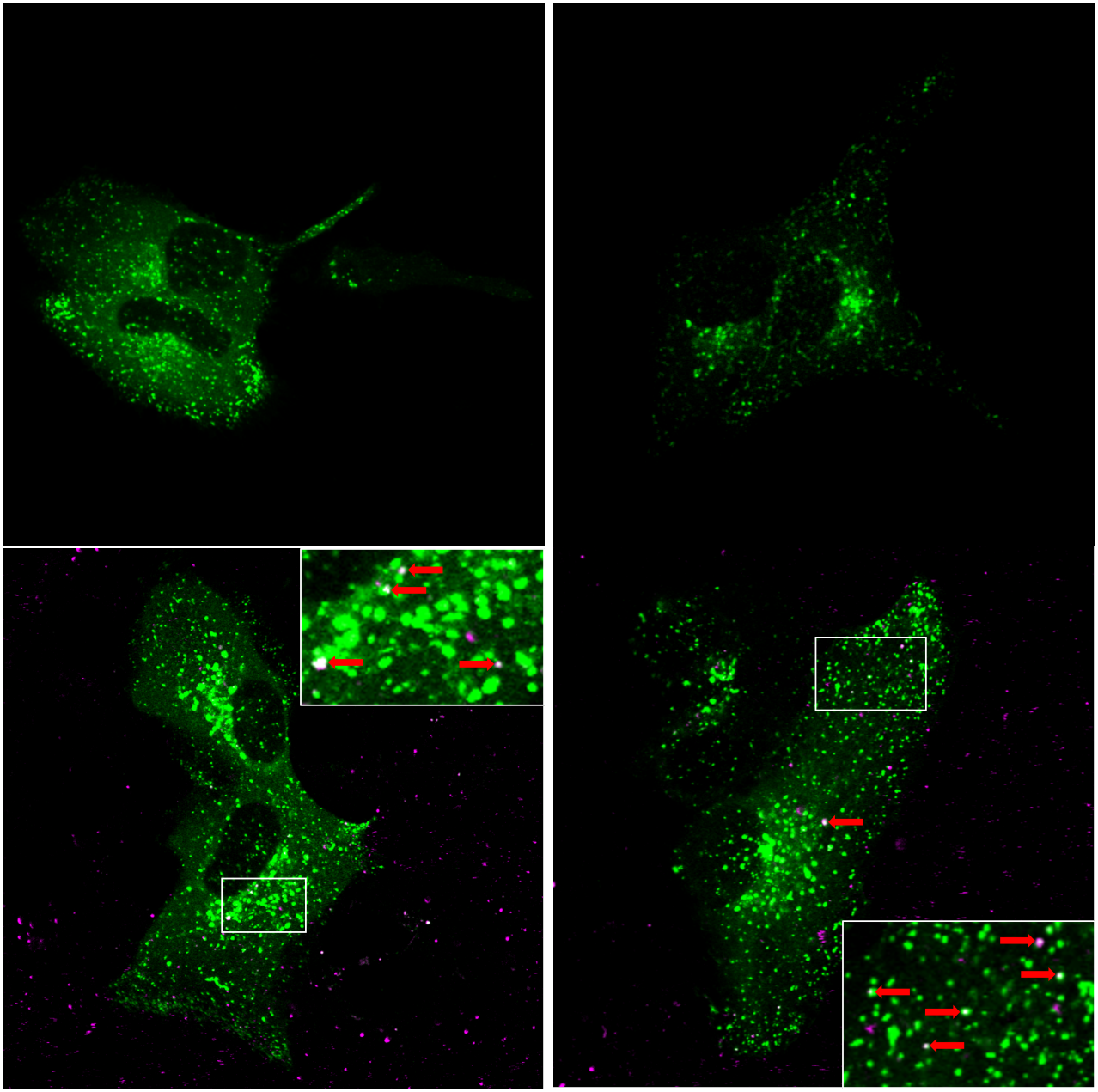


Figure 6.3: Localisation of TRLs to the early endosome. Representative images at 60x magnification of Huh7 cells transfected with Rab5a-GFP and incubated with flourescently labelled TRLs for Rab5a **A-B)** 0 mins or **C-D)** 30 mins. Early endosomes are shown in green, TRLs are shown in purple and co-localised TRLs with early endosome in white.

vehicle-treated hepatocytes, BAF-treated hepatocytes had a lower appearance of intracellular 13C 16:0 (Figure 6.4C) but no difference in extracellular 13C 16:0 (Figure 6.4D).

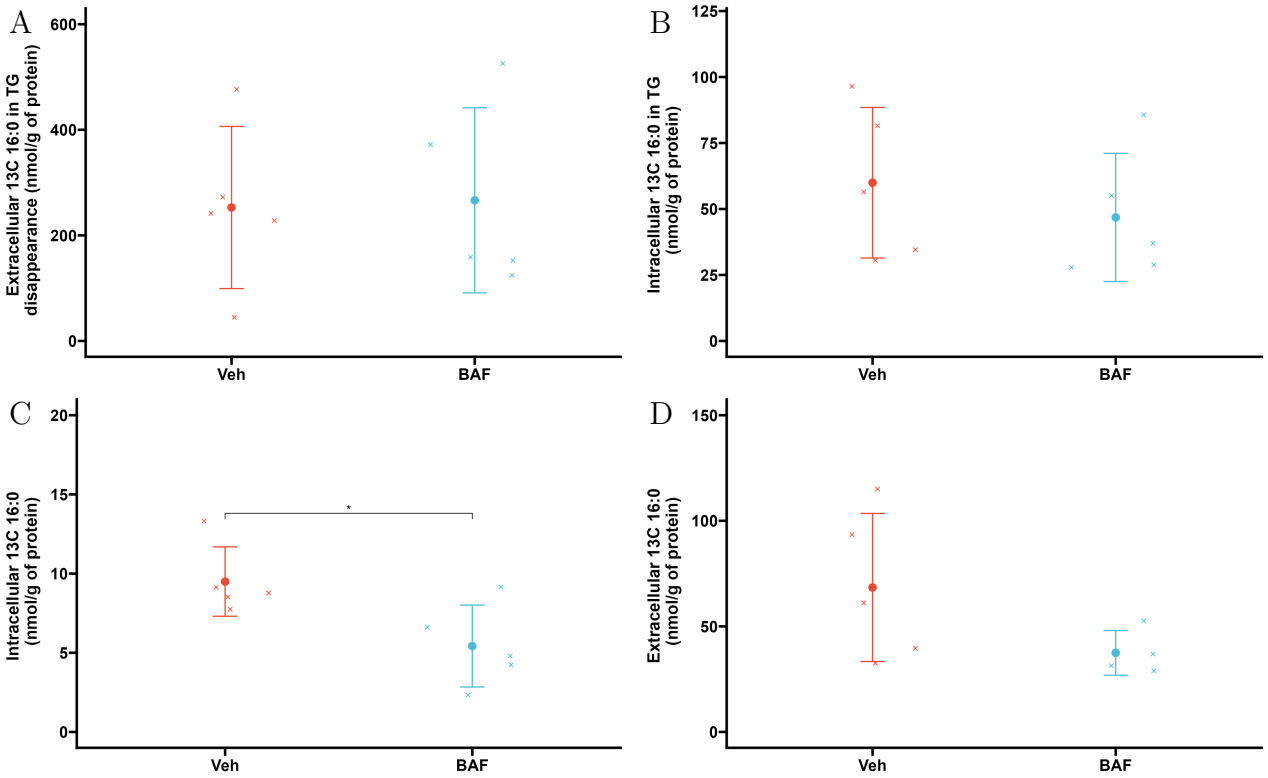


Figure 6.4: The effect of autophagy on TRL processing. Huh7 cells were cultured in low-fat low-sugar media (LFLS) for three days with daily media changes before a 3 hour preincubation with 25 nM BAF or DMSO vehicle. Cells were then cultured in TRLs (1000 μM of TG content) for a further 2 hours. Lipids were extracted from cells and media supernatant samples and analysed by GC-C-IRMS to quantify **A)** the disappearance of extracellular 13C 16:0 in TG, **B)** the intracellular 13C 16:0 in TG concentration and the **C)** intracellular and **D)** extracellular concentrations of 13C 16:0. Data presented as mean ± sd from five biological repeats (**n=5**) carried out in technical duplicate. Abbreviations: TRL, triglyceride-rich lipoprotein; TG, triglyceride; Veh, Vehicle; BAF, Bafilomycin A1; 16:0, palmitate.

6.3.3 The effect of intrahepatocellular triglyceride accumulation on TRL processing

To investigate if TRL processing is impaired in the model of IHCTG accumulation described in Chapter 5, Huh7 cells were cultured in either LFLS, HFHS-OPLA or HFHS-POLA media for three days prior to culture with TRLs. No difference was observed in extracellular 13C 16:0 in TG disappearance (Figure 6.5A) or the concentration of intracellular 13C 16:0 in TG (Figure 6.5B) across conditions suggesting equal uptake of TRLs into the cells. However, cells cultured in HFHS media had a lower concentration of intracellular 13C 16:0 than cells cultured in LFLS (Figure 6.5C), and there was no difference in extracellular 13C 16:0 concentration between all conditions (Figure 6.5D).

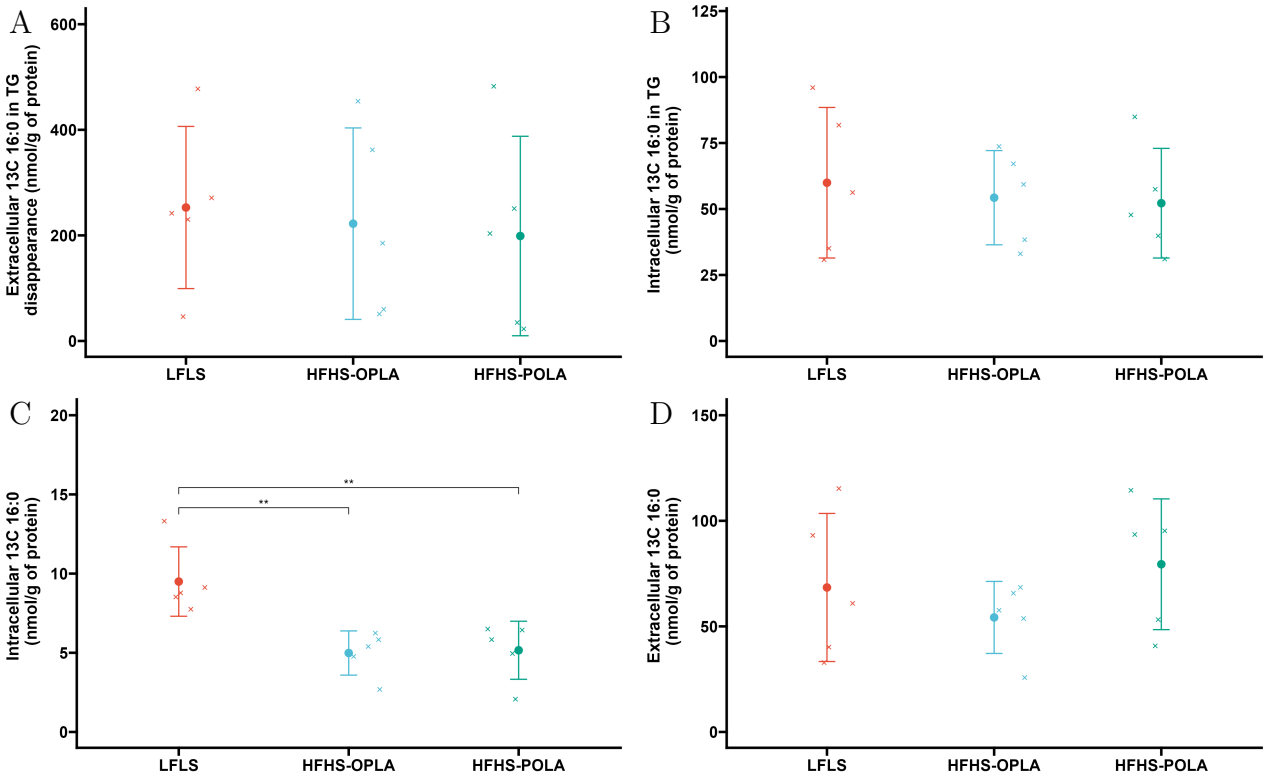


Figure 6.5: The effect of IHCTG accumulation on TRL processing. Huh7 cells were pretreated in low-fat low-sugar media (LFLS), high-fat high-sugar (HFHS-) OPLA or HFHS-POLA for three days with daily media changes before being cultured in TRLs (1000 μM of TG content) for a further 2 hours. Lipids were extracted from cell and media supernatant samples and analysed by GC-C-IRMS to quantify **A)** the disappearance of extracellular 13C 16:0 in TG, **B)** the intracellular 13C 16:0 in TG concentration and the **C)** intracellular and **D)** extracellular concentrations of 13C 16:0. $^{*}p<0.05$. Data presented as mean ± sd from five biological repeats (**n=5**) carried out in technical duplicate. Abbreviations: TRL, triglyceride-rich lipoprotein; TG, triglyceride; 16:0, palmitate.

To further investigate if this decrease in TRL TG lipolysis was due to a lower level of autophagy in the HFHS-treated cells, hepatocytes cultured in LFLS, HFHS-OPLA and HFHS-POLA were pretreated with 25 nM BAF or vehicle control before being cultured with TRLs. The concentration of 13C 16:0 measured in cells treated with BAF represents the contribution from non-autophagic lipolysis whereas the contribution of autophagic lipolysis was calculated from the difference between BAF- and vehicle-treated cells. Although there was no difference in the concentration of intracellular 13C 16:0 released from non-autophagic lipolysis (Figures 6.6A, there was a trend ($p = 0.065$) for a lower concentration of intracellular 13C 16:0 released from autophagic lipolysis in hepatocytes cultured in HFHS-OPLA compared to LFLS 6.6B.

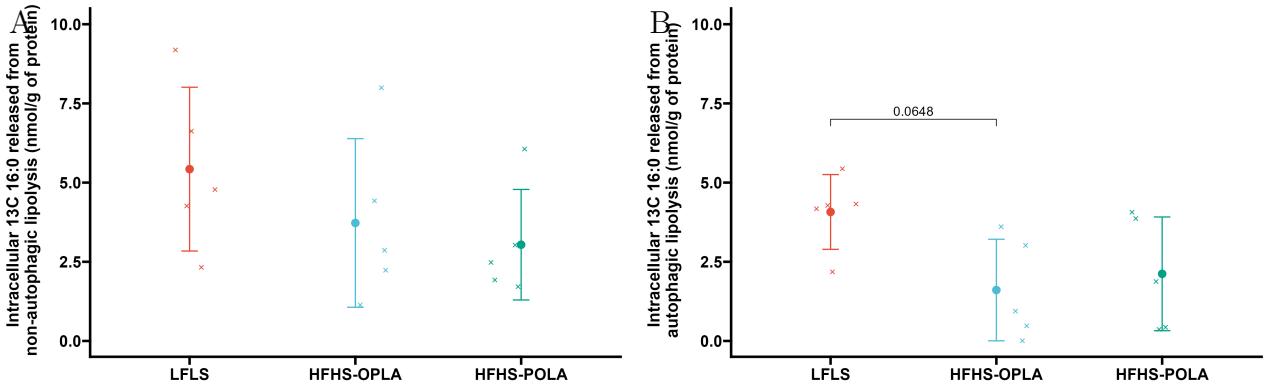


Figure 6.6: The contribution of autophagy to the lipolysis of TG from TRL. Huh7 cells were cultured in low-fat low-sugar media (LFLS), high-fat high-sugar (HFHS-) OPLA or HFHS-POLA for three days with daily media changes and then pretreated with 25 nM BAF or vehicle control (DMSO) before being cultured in TRLs (1000 μM of TG content) for a further 2 hours. Lipids were extracted from cell and media supernatant samples and analysed by GC-C-IRMS. The contribution of **A)** intracellular 13C 16:0 released from non-autophagic lipolysis was calculated from cells treated with BAF and the **B)** intracellular 13C 16:0 released from autophagic lipolysis was calculated as the difference between BAF- and vehicle-treated cells. Data presented as mean ± sd from five biological repeats (**n=5**) carried out in technical duplicate.

6.3.4 The effect of TRLs on IHCTG accumulation

It has been suggested that TG from TRLs may have a substantial contribution to IHCTG in MASLD [27, 177] but the evidence for this is currently lacking. To explore this, total IHCTG was measured in Huh7 cells which had been cultured in TRLs or vehicle control (saline) for two hours after three days pretreatment in LFLS, HFHS-OPLA or HFHS-POLA media. As shown in Chapter 5, hepatocytes cultured in HFHS had higher IHCTG accumulation than those cultured in LFLS however, there was no difference between cells treated with TRLs or saline (Figure 6.7).

6.4 Discussion

Although FA release from adipose tissue is a major source, TGs from TRLs may also contribute substantially to the hepatocellular lipid pool but have been largely overlooked due to the relative complexity of collecting and isolating them [27, 177]. Studies from the 1980s elucidated the pathway for hepatocellular TRL processing and demonstrated that autophagy plays a crucial role [178]. Since then, there has been evidence to suggest that autophagy may be aberrantly downregulated in MASLD however, the implications that this may have on TRL processing has yet to be fully explored. Therefore, the aim of this chapter was to confirm

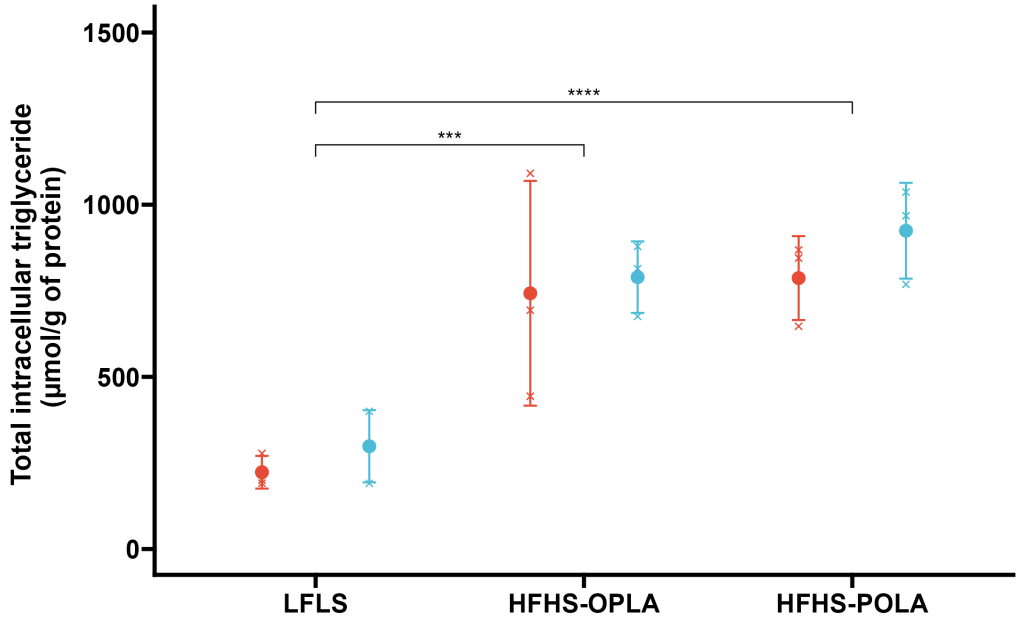


Figure 6.7: The effect of TRLs on IHCTG accumulation. Huh7 cells were cultured in low-fat low-sugar media (LFLS), high-fat high-sugar (HFHS-) OPLA or HFHS-POLA for three days with daily media changes before being cultured in 1000 μM of TG content of TRLs (blue) or saline vehicle control (red) for a further 2 hours. Lipids were extracted from cell samples and total triglyceride content quantified by GC-C-IRMS. $^{***}p<0.001$, $^{****}p<0.0001$. Data presented as mean ± sd from three biological repeats (**n=3**) carried out in technical duplicate.

the role of autophagy in TRL processing and investigate differences in TRL processing in my model of IHCTG accumulation described in Chapter 5.

6.4.1 The role of autophagy in TRL processing

In 1984, Hornick et al. demonstrated that radiolabelled low-density lipoprotein (LDL) particles accumulated in multivesicular bodies within rat hepatocytes treated with the autophagic inhibitor chloroquine [184]. It was concluded that chloroquine may prevent the fusion of endosomes with lysosomes and cause an accumulation of LDL particles in endosomes which then appear as multivesicular bodies [5]. Although the processes are thought to be similar, Hornick et al. utilised LDL and not TRLs and did not give any indication of the lipolysis of the TG stored within these particles. In this chapter, Huh7 cells were treated with the autophagic inhibitor BAF, which prevents lysosomal fusion and vesicle acidification [91], before incubation with TRLs containing 13C 16:0 in TG. There was no difference between BAF- and vehicle-treated cells in the disappearance of media 13C 16:0 in TG suggesting that autophagic inhibition does not affect

TRL uptake and/or the extracellular lipolysis of TRL TG by hepatic lipase. There was also no difference in the appearance of intracellular 13C 16:0 in TG or 13C 16:0 in the media. However, the concentration of intracellular 13C 16:0 was significantly lower in BAF-treated hepatocytes compared to vehicle-treated hepatocytes and this reduced appearance of the labelled FA within the cell suggests that BAF did inhibit the lipolysis of TG from the TRLs. In contrast to [184], there was not a corresponding increase in intracellular labelled TG as would be predicted and it is plausible that the effect size was below the level of detection of the GC-C-IRMS due to the substantially higher pool size of the IHCTG. This difference could also be due to a higher secretion of 13C 16:0 in TG as VLDL during BAF treatment and it would be of interest to measure VLDL secretion in future experiments to determine if this effect is substantial or not.

6.4.2 The effect of IHCTG on TRL processing

As shown in Chapter 5, cells cultured in HFHS-OPLA media tended to have lower autophagic flux compared to cells cultured in LFLS media but, it is unknown if this decrease in autophagy impacts hepatocellular TRL processing. To determine this, Huh7 cells were cultured in LFLS, HFHS-OPLA or HFHS-POLA media for three days prior to incubation with TRLs labelled with 13C 16:0 in TG for two hours. No difference was observed in the disappearance of 13C 16:0 in TG suggesting an equal uptake of TRLs and/or lipolysis of TRL TGs by hepatic lipase across the conditions. This indicates that IHCTG accumulation does not downregulate cell surface expression of TRL uptake machinery, such as the LDL-receptor. Although there was no significant difference in intracellular 13C 16:0 in TG or extracellular 13C 16:0 across the conditions, hepatocytes cultured in HFHS media compared to LFLS media had a lower concentration of intracellular 13C 16:0. This mirrors the results observed when LFLS-treated hepatocytes were incubated with BAF and therefore suggests a similar decrease in TRL TG lipolysis with HFHS-treatment. However, when confirming the contribution of autophagy to intracellular 13C 16:0 release, only hepatocytes treated with HFHS-OPLA but not HFHS-POLA tended to have lower 13C 16:0 release from autophagy-mediated lipolysis compared to LFLS-treated cells. This is in-line with the results of Chapter 5 which tended to show a decrease in autophagy in HFHS-OPLA but not HFHS-POLA compared to LFLS conditions.

6.4.3 The contribution of TRL to IHCTG accumulation

Those with metabolic diseases often have higher plasma VLDL-TG concentrations than those without [28, 29] and it has therefore been suggested that TRL TG may have a meaningful contribution to IHCTG accumulation through particle recycling. To explore this, IHCTG was measured in Huh7 cells cultured in LFLS, HFHS-OPLA or HFHS-POLA media were incubated with TRLs or vehicle control (saline) for two hours. Although HFHS-treated cells had higher IHCTG than LFLS-treated cells, there was no difference between cells incubated with TRL or saline. However, this was only after a 2 hour incubation with TRLs and it is plausible that longer or repeated exposures to TRLs, as would occur *in vivo*, may effect IHCTG.

6.4.4 Limitations and future work

TRL flux to the liver is a highly dynamic process that is largely dependent on an individual's metabolic state (fasting or postprandial) which could not be replicated *in vitro* by incubating hepatocytes in TRLs for two hours. Future work should aim to explore the effects of repeated hepatocyte incubation with TRLs in conjunction to FAs to better mirror what hepatocytes would be exposed to *in vivo*. Although only differences were seen in the intracellular FA pool, it is plausible that longer and repeated TRL exposures may lead to differences in the intracellular TG pool as well which could impact total IHCTG accumulation. As the composition of chylomicron TG is highly dependent on dietary fat composition, and it could also be of interest to explore the effects of TRL TG composition on TRL TG processing. Autophagy is a highly evolutionary conserved pathway with much mechanistic redundancy and whilst BAF is a frequently used chemical inhibitor, it is plausible that autophagic flux was not sufficiently inhibited. To confirm the role that autophagy has in TRL processing these experiments should be repeated with the use of other genetic or chemical inhibitors and/or activators.

6.4.5 Conclusions

Taken together, these findings suggest that autophagy plays a role in TRL processing and that the reduced autophagy observed in hepatocytes exposed to HFHS media enriched in PUFAs does decrease autophagy-mediated TRL processing. It is therefore plausible that TRL processing may be affected in those with MASLD due to their aberrant reduction in hepatic autophagy,

however more work is required to determine if this could then contribute to further IHTG accumulation. Furthermore, this work demonstrates that human-derived TRLs can be used in *in vitro* models of IHCTG accumulation and incorporation of TRLs into these models may aid in determining their role in MASLD development and progression.

'Nonnumquam ita est'

7 Discussion

Contents

7.1 The effect of liver fat content and composition on autophagy . . . 103
7.2 The effect of liver fat content and composition on insulin resistance 103
7.3 The effect of liver fat content and composition on inflammation . 104
7.4 Future directions 104

MASLD is the pathological accumulation of ectopic fat in the liver of those at risk of cardiometabolic disease which, although initially benign, can progress to MASH and more severe liver disease [17]. Although MASLD currently affects 1 in 3 individuals worldwide [18–20], there are limited treatment options available and the underlying pathogenesis is still poorly understood [22]. Autophagy has been shown to regulate TG accumulation in hepatocytes [51] and it has been suggested that those with MASLD may have an aberrant decrease in hepatic autophagy [50]. Dietary fat quantity and composition have been associated with IHCTG accumulation but their effects on hepatic autophagy and other markers of MASLD progression such as IR and inflammation are unclear. Therefore, the overarching aim of this thesis was to investigate the effect of liver fat content and composition on autophagy, insulin resistance and inflammation in humans both *in vivo* and in an *in vitro* model of IHCTG accumulation.

7.1 The effect of liver fat content and composition on autophagy

As hepatic autophagy cannot be measured *in vivo* in humans, an *in vitro* model was utilised whereby the IHCTG content and composition was manipulated by culturing hepatocytes in LFLS media or HFHS media of differing FA compositions. It was found that hepatocytes cultured in HFHS media enriched in unsaturated but not saturated FAs tended to have lower autophagic flux when compared to hepatocytes cultured in LFLS media. Following these observations, the effect that this decrease in autophagy may have on TRL processing was investigated in the same model and it was found that hepatocytes cultured in HFHS media had a lower TRL TG lipolysis than those cultured in LFLS media which could be attributed to lipolysis via autophagy. Taken together, these findings suggest that increasing IHCTG content may decrease hepatic autophagic flux, especially if IHCTG is predominantly unsaturated in composition, and this could decrease the processing of TRLs and potentially lead to further IHCTG accumulation. However, the biological significance of these findings is unclear and future work should further assess the contribution of this reduced autophagy to IHCTG accumulation within the context of MASLD. This may be achieved through the use of pharmacological modulators of autophagy in *in vivo* animal models with the view of developing a drug for human trials with MASLD patients.

7.2 The effect of liver fat content and composition on insulin resistance

Evidence from rodent studies had suggested that the fasting hyperglycemia and hypertriglyceridemia which are typically associated with metabolic disease may be driven by an upregulation of both GNG and DNL in the liver, known as selective hepatic IR. However, in a cohort of male and female UK adults I was unable to find this proposed metabolic signature to be associated with either hyperinsulinemia or high liver fat content. Instead, it was observed that DNL is driven by plasma insulin concentration rather than liver fat content and that GLY may play a larger role in contributing to fasting hyperglycemia than previously thought, especially in those with high liver fat content. However, it has been suggested that liver fat composition may play a larger role in hepatic IR than liver fat content itself [65, 66] and, as this cannot be easily

assessed *in vivo*, this was further investigated in an *in vitro* model of IHCTG accumulation. Increased saturation of IHCTG was associated with higher glucose production and signs of IR. It would be of interest to measure the contributions of GNG and GLY to glucose production in these hepatocytes to see if they mirror the *in vivo* findings.

7.3 The effect of liver fat content and composition on inflammation

Hyperinsulinemia and high liver fat content have both been associated with inflammation however, their frequent co-existence in individuals has made it challenging to disentangle the effects of each. In Chapter 3, two markers of systemic inflammation were measured in human fasting plasma samples and were found to be raised by both hyperinsulinemia and high liver fat content and it appeared that the effect of increasing liver fat content on inflammation may be greater in those with hyperinsulinemia. This was further explored in an *in vitro* model of IHCTG accumulation which demonstrated that hyperinsulinemia had no effect on hepatocellular inflammatory activation or hepatocellular injury. In contrast, accumulation of IHCTG was associated with hepatocellular injury and cytokine secretion which was more marked in hepatocytes treated with predominantly unsaturated FAs compared to saturated FAs. Although this cytokine secretion was not sufficient to activate stellate cells during a co-culture, and it would be of interested to repeat the co-culture with other immune cells that have been associated with the initiation of hepatic inflammation in MASLD such as macrophages or Kupffer cells [40]. Furthermore, as the majority of cytokines secreted by the activated hepatocytes were chemokines, it is probable that propagation of the inflammatory signal is transmitted through receptor signalling on the surface of the cells. Therefore, future co-culture studies should ensure that such direct contact is possible.

7.4 Future directions

Taken together, these results suggest that liver fat composition may be equally as important as liver fat content with unsaturated fat potentially decreasing hepatic autophagy and TRL processing and increasing inflammatory activation, whereas saturated fat may be more associated

with IR. Although liver fat composition is challenging to assess *in vivo*, understanding its effects should be prioritised for further research and could be done using novel imaging techniques or through dietary intervention studies measuring markers of IR and inflammation. It is plausible that the effect of unsaturated FAs on hepatocellular autophagy and inflammatory activation may be linked. Whilst this work did show such an association and autophagy is known to regulate inflammatory pathways, future studies should utilise further autophagic modulation to determine the causal relationship within this context and identify possible mechanisms.

Previous *in vivo* and *in vitro* studies have focused heavily on the role of insulin and GNG on hepatic glucose production in IR states; however, this work as well as that of others, has demonstrated that other metabolic processes and hormones (such as GLY and glucagon, respectively) may actually play a greater role in the pathogenesis of IR than previously thought and therefore should be considered in future studies. Similarly, the association between autophagy and IR is unclear but it is plausible that autophagy may have a role in IR [55]. The work for this thesis continued the development of a more physiological *in vitro* model of IHCTG accumulation which had been established by others in my lab group. The prolonged and repeated treatment of hepatocytes with a mixture of FAs and sugars has often provided less extreme differences between conditions than previous studies using a single treatment with a single FA. However, many of the results have been similar to others but have not come at the expense of decreased cellular viability and hopefully future studies will begin to adopt this more physiological model. Finally, in Chapter 6 I demonstrated how this model could be developed further through the addition of human-derived TRLs to the cell media. The regulation of TRL processing in states of health and metabolic disease is poorly understood and by showing their potential impact in MASLD and utilization in *in vitro* models, this work provides new insights and a model that can be used to undertake further work in the field.

In recent years, glucagon-like peptide-1 (GLP-1) receptor agonists have transformed the treatment of obesity and T2D. Although these agonists are not yet approved for the treatment of MASLD, their use in clinical research trials and in clinical practice has shown great therapeutic potential [188–190]. Though the liver does not express the GLP-1 receptor, GLP-1 receptor agonists are thought to decrease IHCTG accumulation through weight loss mediated through appetite suppression and the induction of satiety [191]. Aside from the effects on the central

nervous system, GLP-1 receptor agonists also act on metabolic organs such as the pancreas, skeletal muscle and adipose tissue to decrease plasma NEFA, TG and glucagon concentrations and increase plasma insulin concentrations and systemic insulin sensitivity [192]. Although questions still remain about the tolerability and long-term effects of these drugs, it is very likely that they may become a widely-used and effective treatment for MASLD. However, it is still plausible that a greater understanding of MASLD pathogenesis may make certain dietary and lifestyle interventions equally as effective, if not more so, over the long-term.

References

[1] Christina Mehrfeld et al. “The contribution of non-professional antigen-presenting cells to immunity and tolerance in the liver”. In: *Frontiers in Immunology* 9.MAR (Mar. 2018), p. 350648. DOI: 10.3389/FIMMU.2018.00635/BIBTEX.

[2] Andre Blouin, Robert P Bolender, and Ewald R Weibel. “DISTRIBUTION OF ORGANELLES AND MEMBRANES BETWEEN HEPATOCYTES AND NONHEPATOCYTES IN A Stereological Study”. In: *THE JOURr4AL OF CELL BIOLOGY* 9 (1977), pp. 441–455.

[3] Karin Ekberg et al. “Contributions by kidney and liver to glucose production in the postabsorptive state and after 60 h of fasting.” In: *Diabetes* 48.2 (Feb. 1999), pp. 292–298. DOI: 10.2337/DIABETES.48.2.292.

[4] Mary Courtney Moore et al. “Regulation of Hepatic Glucose Uptake and Storage In Vivo”. In: *Advances in Nutrition* 3.3 (May 2012), pp. 286–294. DOI: 10.3945/AN.112.002089.

[5] Richard J. Havel and Robert L. Hamilton. “Hepatocytic lipoprotein receptors and intracellular lipoprotein catabolism”. In: *Hepatology (Baltimore, Md.)* 8.6 (1988), pp. 1689–1704. DOI: 10.1002/HEP.1840080637.

[6] M C Petersen and G I Shulman. “Mechanisms of Insulin Action and Insulin Resistance”. In: *Physiol Rev* 98.4 (2018), pp. 2133–2223. DOI: 10.1152/physrev.00063.2017.

[7] Leanne Hodson and Fredrik Karpe. “Hyperinsulinaemia: does it tip the balance toward intrahepatic fat accumulation?” In: *Endocrine Connections* 8.10 (Oct. 2019), R157. DOI: 10.1530/EC-19-0350.

[8] Leanne Hodson and Keith N. Frayn. “Hepatic fatty acid partitioning”. In: *Current Opinion in Lipidology* 22.3 (June 2011), pp. 216–224. DOI: 10.1097/MOL.0b013e3283462e16.

[9] Leanne Hodson and Pippa J. Gunn. “The regulation of hepatic fatty acid synthesis and partitioning: the effect of nutritional state”. In: *Nature Reviews Endocrinology 2019 15:12* 15.12 (Sept. 2019), pp. 689–700. DOI: 10.1038/s41574-019-0256-9.

[10] Felix Westcott, David J. Dearlove, and Leanne Hodson. “Hepatic fatty acid and glucose handling in metabolic disease: Potential impact on cardiovascular disease risk”. In: *Atherosclerosis* 394 (July 2024). DOI: 10.1016/J.ATHEROSCLEROSIS.2023.117237.

[11] WHO (2016) factsheet. *Obesity and overweight*.

[12] Mariel M. Finucane et al. “National, regional, and global trends in body-mass index since 1980: systematic analysis of health examination surveys and epidemiological studies with 960 country-years and $9 \cdot 1$ million participants”. In: *Lancet (London, England)* 377.9765 (2011), pp. 557–567. DOI: 10.1016/S0140-6736(10)62037-5.

[13] Gerald M. Reaven. “Pathophysiology of insulin resistance in human disease”. In: *Physiological reviews* 75.3 (1995), pp. 473–486. DOI: 10.1152/PHYSREV.1995.75.3.473.

[14] Ralph A. DeFronzo et al. “Type 2 diabetes mellitus”. In: *Nature Reviews Disease Primers 2015 1:1* 1.1 (July 2015), pp. 1–22. DOI: 10.1038/nrdp.2015.19.

[15] Sadiya S. Khan et al. "Association of Body Mass Index With Lifetime Risk of Cardiovascular Disease and Compression of Morbidity". In: *JAMA cardiology* 3.4 (Apr. 2018), pp. 280–287. DOI: 10.1001/JAMACARDIO.2018.0022.

[16] Shehab M. Abd El-Kader and Eman M.Salah El-Den Ashmawy. "Non-alcoholic fatty liver disease: The diagnosis and management". In: *World Journal of Hepatology* 7.6 (Jan. 2015), pp. 846–858. DOI: 10.4254/wjh.v7.i6.846.

[17] Mary E. Rinella et al. "A multisociety Delphi consensus statement on new fatty liver disease nomenclature". In: *Hepatology* 78.6 (Dec. 2023), pp. 1966–1986. DOI: 10.1097/HEP.0000000000000520.

[18] Assist Prof et al. "The prevalence and incidence of NAFLD worldwide: a systematic review and meta-analysis". In: *Articles Lancet Gastroenterol Hepatol* 7 (2022), pp. 851–61. DOI: 10.1016/S2468-1253(22)00165-0.

[19] Zobair M. Younossi et al. "The global epidemiology of nonalcoholic fatty liver disease (NAFLD) and nonalcoholic steatohepatitis (NASH): a systematic review". In: *Hepatology (Baltimore, Md.)* 77.4 (Apr. 2023), pp. 1335–1347. DOI: 10.1097/HEP.0000000000000004.

[20] Brian P. Lee, Jennifer L. Dodge, and Norah A. Terrault. "National prevalence estimates for steatotic liver disease and subclassifications using consensus nomenclature". In: *Hepatology (Baltimore, Md.)* 79.3 (Mar. 2024), pp. 666–673. DOI: 10.1097/HEP.0000000000000604.

[21] Raluca Pais et al. "NAFLD and liver transplantation: Current burden and expected challenges". In: *Journal of hepatology* 65.6 (Dec. 2016), pp. 1245–1257. DOI: 10.1016/J.JHEP.2016.07.033.

[22] Mariana Verdelho Machado. "MASLD treatment—a shift in the paradigm is imminent". In: *Frontiers in Medicine* 10 (Dec. 2023), p. 1316284. DOI: 10.3389/FMED.2023.1316284/BIBTEX.

[23] Yuki Kawano and David E. Cohen. "Mechanisms of hepatic triglyceride accumulation in non-alcoholic fatty liver disease". In: *Journal of Gastroenterology* 48.4 (Apr. 2013), p. 434. DOI: 10.1007/S00535-013-0758-5.

[24] Zobair M. Younossi et al. "The global epidemiology of NAFLD and NASH in patients with type 2 diabetes: A systematic review and meta-analysis". In: *Journal of Hepatology* 71.4 (Oct. 2019), pp. 793–801. DOI: 10.1016/J.JHEP.2019.06.021.

[25] Quentin M. Anstee, Giovanni Targher, and Christopher P. Day. "Progression of NAFLD to diabetes mellitus, cardiovascular disease or cirrhosis". In: *Nature reviews. Gastroenterology & hepatology* 10.6 (June 2013), pp. 330–344. DOI: 10.1038/NRGASTRO.2013.41.

[26] Gisela Wilcox. "Insulin and Insulin Resistance". In: *Clinical Biochemist Reviews* 26.2 (2005), p. 19.

[27] Fredrik Karpe, Julian R. Dickmann, and Keith N. Frayn. "Fatty acids, obesity, and insulin resistance: Time for a reevaluation". In: *Diabetes* 60.10 (Oct. 2011), pp. 2441–2449. DOI: 10.2337/DB11-0425/-/DC1.

[28] C. Tollin et al. "Clearance of triglycerides from the circulation and its relationship to serum lipoproteins: influence of age and sex". In: *Scandinavian journal of clinical and laboratory investigation* 45.8 (1985), pp. 679–684. DOI: 10.3109/00365518509155279.

[29] Bettina Mittendorfer et al. "VLDL-triglyceride kinetics during hyperglycemia-hyperinsulinemia: effects of sex and obesity". In: *American journal of physiology. Endocrinology and metabolism* 284.4 (Apr. 2003). DOI: 10.1152/AJPENDO.00411.2002.

[30] J E Lambert et al. "Increased de novo lipogenesis is a distinct characteristic of individuals with nonalcoholic fatty liver disease". In: *Gastroenterology* 146.3 (2014), pp. 726–735. DOI: 10.1053/j.gastro.2013.11.049.

[31] G I Smith et al. "Insulin resistance drives hepatic de novo lipogenesis in nonalcoholic fatty liver disease". In: *J Clin Invest* 130.3 (2020), pp. 1453–1460. DOI: 10.1172/JCI134165.

[32] Ilaria Croci et al. "Whole-body substrate metabolism is associated with disease severity in patients with non-alcoholic fatty liver disease". In: *Gut* 62.11 (Nov. 2013), pp. 1625–1633. DOI: 10.1136/GUTJNL-2012-302789.

[33] Anna Kotronen et al. "Liver fat and lipid oxidation in humans". In: *Liver International* 29.9 (Oct. 2009), pp. 1439–1446. DOI: 10.1111/J.1478-3231.2009.02076.X.

[34] Nishanth E. Sunny et al. "Excessive Hepatic Mitochondrial TCA Cycle and Gluconeogenesis in Humans with Nonalcoholic Fatty Liver Disease". In: *Cell Metabolism* 14.6 (Dec. 2011), pp. 804–810. DOI: 10.1016/J.CMET.2011.11.004.

[35] Siôn A. Parry et al. "Oxidation of dietary linoleate occurs to a greater extent than dietary palmitate in vivo in humans". In: *Clinical nutrition (Edinburgh, Scotland)* 40.3 (Mar. 2021), pp. 1108–1114. DOI: 10.1016/J.CLNU.2020.07.013.

[36] Douglas L. Rothman et al. "Quantitation of hepatic glycogenolysis and gluconeogenesis in fasting humans with 13C NMR". In: *Science (New York, N.Y.)* 254.5031 (Oct. 1991), pp. 573–576. DOI: 10.1126/SCIENCE.1948033.

[37] R S Hundal et al. "Mechanism by which metformin reduces glucose production in type 2 diabetes". In: *Diabetes* 49.12 (2000), pp. 2063–2069. DOI: 10.2337/diabetes.49.12.2063.

[38] A Gastaldelli et al. "Relationship between hepatic/visceral fat and hepatic insulin resistance in nondiabetic and type 2 diabetic subjects". In: *Gastroenterology* 133.2 (2007), pp. 496–506. DOI: 10.1053/j.gastro.2007.04.068.

[39] B R Landau. "Methods for measuring glycogen cycling". In: *Am J Physiol Endocrinol Metab* 281.3 (2001), pp. 413–9. DOI: 10.1152/ajpendo.2001.281.3.E413.

[40] Susanne Schuster et al. "Triggering and resolution of inflammation in NASH". In: *Nature reviews. Gastroenterology & hepatology* 15.6 (June 2018), pp. 349–364. DOI: 10.1038/S41575-018-0009-6.

[41] Rajat Singh et al. "Differential Effects of JNK1 and JNK2 Inhibition on Murine Steatohepatitis and Insulin Resistance". In: *Hepatology (Baltimore, Md.)* 49.1 (2009), p. 87. DOI: 10.1002/HEP.22578.

[42] Harmeet Malhi et al. "Free fatty acids induce JNK-dependent hepatocyte lipoapoptosis". In: *Journal of Biological Chemistry* 281.17 (2006), pp. 12093–12101. DOI: 10.1074/jbc.M510660200.

[43] Ekihiro Seki, David A. Brenner, and Michael Karin. "A Liver Full of JNK: Signaling in Regulation of Cell Function and Disease Pathogenesis, and Clinical Approaches". In: *Gastroenterology* 143.2 (Aug. 2012), pp. 307–320. DOI: 10.1053/J.GASTRO.2012.06.004.

[44] Timea Csak et al. "Fatty acid and endotoxin activate inflammasomes in mouse hepatocytes that release danger signals to stimulate immune cells". In: *Hepatology (Baltimore, Md.)* 54.1 (July 2011), pp. 133–144. DOI: 10.1002/HEP.24341.

[45] Veerle Bieghs and Christian Trautwein. "The innate immune response during liver inflammation and metabolic disease". In: *Trends in Immunology* 34.9 (Sept. 2013), pp. 446–452. DOI: 10.1016/J.IT.2013.04.005.

[46] Jérémie Gautheron et al. "A positive feedback loop between RIP3 and JNK controls non-alcoholic steatohepatitis". In: *EMBO molecular medicine* 6.8 (Aug. 2014), pp. 1062–1074. DOI: 10.15252/EMMM.201403856.

[47] Alexander Wree et al. "NLRP3 inflammasome activation results in hepatocyte pyroptosis, liver inflammation, and fibrosis in mice". In: *Hepatology (Baltimore, Md.)* 59.3 (Mar. 2014), pp. 898–910. DOI: 10.1002/HEP.26592.

[48] Bedair Dewidar et al. "TGF-β in Hepatic Stellate Cell Activation and Liver Fibrogenesis—Updated 2019". In: *Cells* 8.11 (Nov. 2019). DOI: 10.3390/CELLS8111419.

[49] Wilhelmus J. Kwanten, Wim Martinet, and Sven M. Francque. "Autophagy in Non-Alcoholic Fatty Liver Disease (NAFLD)". In: *Autophagy in Current Trends in Cellular Physiology and Pathology* (Nov. 2016). DOI: 10.5772/64534.

[50] Mark J Czaja. "Function of Autophagy in Nonalcoholic Fatty Liver Disease". In: *Digestive Diseases and Sciences* 61.5 (2016), pp. 1304–1313. DOI: 10.1007/s10620-015-4025-x.

[51] Rajat Singh et al. "Autophagy regulates lipid metabolism". In: *Nature* 458.7242 (Apr. 2009), pp. 1131–1135. DOI: 10.1038/nature07976.

[52] Maryam Mehrpour et al. "Autophagy in health and disease. 1. Regulation and significance of autophagy: an overview". In: *American journal of physiology. Cell physiology* 298.4 (Apr. 2010). DOI: 10.1152/AJPCELL.00507.2009.

[53] Congcong He and Daniel J Klionsky. "Regulation Mechanisms and Signaling Pathways of Autophagy". In: (2009). DOI: 10.1146/annurev-genet-102808-114910.

[54] Yuchen Lei and Daniel J. Klionsky. "Transcriptional regulation of autophagy and its implications in human disease". In: *Cell Death & Differentiation 2023 30:6* 30.6 (Apr. 2023), pp. 1416–1429. DOI: 10.1038/s41418-023-01162-9.

[55] Junji Ezaki et al. "Liver autophagy contributes to the maintenance of blood glucose and amino acid levels". In: *Autophagy* 727.7 (2011), pp. 727–736. DOI: 10.4161/auto.7.7.15371.

[56] Asie Sadeghi et al. "Crosstalk between autophagy and insulin resistance: evidence from different tissues". In: *European journal of medical research* 28.1 (Dec. 2023). DOI: 10.1186/S40001-023-01424-9.

[57] Ryan J Schulze et al. "Direct lysosome-based autophagy of lipid droplets in hepatocytes". In: *Proceedings of the National Academy of Sciences of the United States of America* 117.51 (2020), pp. 32443–32452. DOI: 10.1073/pnas.2011442117.

[58] Carmine Settembre et al. "TFEB controls cellular lipid metabolism through a starvation-induced autoregulatory loop". In: *Nature cell biology* 15.6 (June 2013), p. 647. DOI: 10.1038/NCB2718.

[59] Xiwen Xiong et al. "The Autophagy-related Gene 14 (Atg14) Is Regulated by Forkhead Box O Transcription Factors and Circadian Rhythms and Plays a Critical Role in Hepatic Autophagy and Lipid Metabolism". In: *The Journal of Biological Chemistry* 287.46 (Nov. 2012), p. 39107. DOI: 10.1074/JBC.M112.412569.

[60] Klionsky DJ et al. "Guidelines for the use and interpretation of assays for monitoring autophagy (4th edition) 1". In: *Autophagy* 17.1 (2021), pp. 1–382. DOI: 10.1080/15548627.2020.1797280.

[61] Yuka Fukuo et al. "Abnormality of autophagic function and cathepsin expression in the liver from patients with non-alcoholic fatty liver disease". In: *Hepatology Research* 44.9 (2014), pp. 1026–1036. DOI: 10.1111/hepr.12282.

[62] Željko Reiner et al. "Lysosomal acid lipase deficiency – An under-recognized cause of dyslipidaemia and liver dysfunction". In: *Atherosclerosis* 235.1 (July 2014), pp. 21–30. DOI: 10.1016/J.ATHEROSCLEROSIS.2014.04.003.

[63] Donna L. Bernstein et al. "Cholesteryl ester storage disease: review of the findings in 135 reported patients with an underdiagnosed disease". In: *Journal of hepatology* 58.6 (June 2013), pp. 1230–1243. DOI: 10.1016/J.JHEP.2013.02.014.

[64] Monica Gomaraschi et al. "Lipid accumulation impairs lysosomal acid lipase activity in hepatocytes: Evidence in NAFLD patients and cell cultures". In: *Biochimica et Biophysica Acta - Molecular and Cell Biology of Lipids* 1864.12 (2019). DOI: 10.1016/j.bbalip.2019.158523.

[65] Panu K. Luukkonen et al. "Saturated Fat Is More Metabolically Harmful for the Human Liver Than Unsaturated Fat or Simple Sugars". In: *Diabetes care* 41.8 (Aug. 2018), pp. 1732–1739. DOI: 10.2337/DC18-0071.

[66] H. Sobrecases et al. "Effects of short-term overfeeding with fructose, fat and fructose plus fat on plasma and hepatic lipids in healthy men". In: *Diabetes & metabolism* 36.3 (June 2010), pp. 244–246. DOI: 10.1016/J.DIABET.2010.03.003.

[67] Fredrik Rosqvist et al. "Overfeeding polyunsaturated and saturated fat causes distinct effects on liver and visceral fat accumulation in humans". In: *Diabetes* 63.7 (2014), pp. 2356–2368. DOI: 10.2337/DB13-1622.

[68] Helena Bjermo et al. "Effects of n-6 PUFAs compared with SFAs on liver fat, lipoproteins, and inflammation in abdominal obesity: a randomized controlled trial". In: *The American journal of clinical nutrition* 95.5 (May 2012), pp. 1003–1012. DOI: 10.3945/AJCN.111.030114.

[69] Johane P. Allard et al. "Nutritional assessment and hepatic fatty acid composition in non-alcoholic fatty liver disease (NAFLD): a cross-sectional study". In: *Journal of hepatology* 48.2 (Feb. 2008), pp. 300–307. DOI: 10.1016/J.JHEP.2007.09.009.

[70] Silvia Marinho Ferolla et al. "Dietary patterns in Brazilian patients with non-alcoholic fatty liver disease: a cross-sectional study". In: *Clinics* 68.1 (2013), p. 11. DOI: 10.6061/CLINICS/2013(01)OA03.

[71] Charlotte J. Green et al. "From whole body to cellular models of hepatic triglyceride metabolism: man has got to know his limitations". In: *American Journal of Physiology - Endocrinology and Metabolism* 308.1 (Jan. 2015), E1. DOI: 10.1152/AJPENDO.00192.2014.

[72] Isy F. de Sousa et al. "Dose-and time-dependent effects of oleate on mitochondrial fusion/fission proteins and cell viability in hepg2 cells: Comparison with palmitate effects". In: *International Journal of Molecular Sciences* 22.18 (Sept. 2021), p. 9812. DOI: 10.3390/IJMS22189812/S1.

[73] Andrea Eynaudi et al. "Differential Effects of Oleic and Palmitic Acids on Lipid Droplet-Mitochondria Interaction in the Hepatic Cell Line HepG2". In: *Frontiers in Nutrition* 8 (Nov. 2021), p. 775382. DOI: 10.3389/FNUT.2021.775382/BIBTEX.

[74] María José Gómez-Lechón et al. "A human hepatocellular in vitro model to investigate steatosis". In: *Chemico-Biological Interactions* 165.2 (2007), pp. 106–116. DOI: 10.1016/j.cbi.2006.11.004.

[75] Matteo Ricchi et al. "Differential effect of oleic and palmitic acid on lipid accumulation and apoptosis in cultured hepatocytes". In: *Journal of Gastroenterology and Hepatology (Australia)* 24.5 (2009), pp. 830–840. DOI: 10.1111/J.1440-1746.2008.05733.X.

[76] Laura L. Listenberger et al. "Triglyceride accumulation protects against fatty acid-induced lipotoxicity". In: *Proceedings of the National Academy of Sciences of the United States of America* 100.6 (Mar. 2003), pp. 3077–3082. DOI: 10.1073/PNAS.0630588100.

[77] Sindiyan Alshaikh Mubarak et al. "Reduction in Insulin Mediated ERK Phosphorylation by Palmitate in Liver Cells Is Independent of Fatty Acid Induced ER Stress". In: *Nutrients* 14.17 (Sept. 2022). DOI: 10.3390/NU14173641.

[78] Jin young Lee, Hyang Ki Cho, and Young Hye Kwon. "Palmitate induces insulin resistance without significant intracellular triglyceride accumulation in HepG2 cells". In: *Metabolism* 59.7 (July 2010), pp. 927–934. DOI: 10.1016/J.METABOL.2009.10.012.

[79] Seiji Nakamura et al. "Palmitate induces insulin resistance in H4IIEC3 hepatocytes through reactive oxygen species produced by mitochondria". In: *The Journal of biological chemistry* 284.22 (May 2009), pp. 14809–14818. DOI: 10.1074/JBC.M901488200.

[80] A. Moravcová et al. "The effect of oleic and palmitic acid on induction of steatosis and cytotoxicity on rat hepatocytes in primary culture". In: *Physiological research* 64.Suppl 5 (2015), S627–S636. DOI: 10.33549/PHYSIOLRES.933224.

[81] Shawn C. Burgess et al. "Cytosolic Phosphoenolpyruvate Carboxykinase Does Not Solely Control the Rate of Hepatic Gluconeogenesis in the Intact Mouse Liver". In: *Cell Metabolism* 5.4 (Apr. 2007), pp. 313–320. DOI: 10.1016/J.CMET.2007.03.004.

[82] Varman T. Samuel et al. "Fasting hyperglycemia is not associated with increased expression of PEPCK or G6Pc in patients with type 2 diabetes". In: *Proceedings of the National Academy of Sciences of the United States of America* 106.29 (July 2009), pp. 12121–12126. DOI: 10.1073/PNAS.0812547106/SUPPL{_}FILE/0812547106SI.PDF.

[83] Pippa J Gunn et al. "Modifying nutritional substrates induces macrovesicular lipid droplet accumulation and metabolic alterations in a cellular model of hepatic steatosis". In: *Physiological Reports* 8 (2020), p. 14482. DOI: 10.14814/phy2.14482.

[84] Shilpa R Nagarajan et al. "Determining the temporal, dose, and composition effects of nutritional substrates in an in vitro model of intrahepatocellular triglyceride accumulation". In: *Physiological Reports* 10 (2022), p. 15463. DOI: 10.14814/phy2.15463.

[85] Leanne Hodson, C. Murray Skeaff, and Barbara A. Fielding. "Fatty acid composition of adipose tissue and blood in humans and its use as a biomarker of dietary intake". In: *Progress in lipid research* 47.5 (Sept. 2008), pp. 348–380. DOI: 10.1016/J.PLIPRES.2008.03.003.

[86] Mark D. Robinson and Alicia Oshlack. "A scaling normalization method for differential expression analysis of RNA-seq data". In: *Genome Biology* 11.3 (Mar. 2010), pp. 1–9. DOI: 10.1186/GB-2010-11-3-R25/FIGURES/3.

[87] Mark D. Robinson, Davis J. McCarthy, and Gordon K. Smyth. "edgeR: A Bioconductor package for differential expression analysis of digital gene expression data". In: *Bioinformatics* 26.1 (Jan. 2009), pp. 139–140. DOI: 10.1093/bioinformatics/btp616.

[88] Matthew E. Ritchie et al. "limma powers differential expression analyses for RNA-sequencing and microarray studies". In: *Nucleic Acids Research* 43.7 (Apr. 2015), e47. DOI: 10.1093/NAR/GKV007.

[89] Minoru Kanehisa and Susumu Goto. "KEGG: Kyoto Encyclopedia of Genes and Genomes". In: *Nucleic Acids Research* 28.1 (Jan. 2000), p. 27. DOI: 10.1093/NAR/28.1.27.

[90] Arthur Liberzon et al. "The Molecular Signatures Database (MSigDB) hallmark gene set collection". In: *Cell systems* 1.6 (Dec. 2015), p. 417. DOI: 10.1016/J.CELS.2015.12.004.

[91] Caroline Mauvezin and Thomas P. Neufeld. "Bafilomycin A1 disrupts autophagic flux by inhibiting both V-ATPase-dependent acidification and Ca-P60A/SERCA-dependent autophagosome-lysosome fusion". In: *Autophagy* 11.8 (Jan. 2015), p. 1437. DOI: 10.1080/15548627.2015.1066957.

[92] Yumei Yan et al. "Bafilomycin A1 induces caspase-independent cell death in hepatocellular carcinoma cells via targeting of autophagy and MAPK pathways". In: *Scientific Reports* 6 (Nov. 2016). DOI: 10.1038/SREP37052.

[93] Hongfeng Yuan, Brandon Tan, and Shou-Jiang Gao. "Tenovin-6 impairs autophagy by inhibiting autophagic flux". In: *Cell Death and Disease* 8 (2017). DOI: 10.1038/cddis.2017.25.

[94] A. González-Rodríguez et al. "Impaired autophagic flux is associated with increased endoplasmic reticulum stress during the development of NAFLD". In: *Cell Death and Disease* 5.4 (2014). DOI: 10.1038/cddis.2014.162.

[95] J. FOLCH, M. LEES, and G. H. SLOANE STANLEY. "A SIMPLE METHOD FOR THE ISOLATION AND PURIFICATION OF TOTAL LIPIDES FROM ANIMAL TISSUES". In: *Journal of Biological Chemistry* 226.1 (May 1957), pp. 497–509. DOI: 10.1016/S0021-9258(18)64849-5.

[96] G. C. Burdge et al. "A method for separation of phosphatidylcholine, triacylglycerol, non-esterified fatty acids and cholesterol esters from plasma by solid-phase extraction*". In: *British Journal of Nutrition* 84.5 (2000), pp. 781–787. DOI: 10.1017/S0007114500002154.

[97] Valeska Ormazabal et al. "Association between insulin resistance and the development of cardiovascular disease". In: *Cardiovascular Diabetology 2018 17:1* 17.1 (Aug. 2018), pp. 1–14. DOI: 10.1186/S12933-018-0762-4.

[98] M D Michael et al. "Loss of insulin signaling in hepatocytes leads to severe insulin resistance and progressive hepatic dysfunction". In: *Mol Cell* 6.1 (2000), pp. 87–97.

[99] S B Biddinger and C R Kahn. "From mice to men: insights into the insulin resistance syndromes". In: *Annu Rev Physiol* 68 (2006), pp. 123–158. DOI: 10.1146/annurev.physiol.68.040104.124723.

[100] M S Brown and J L Goldstein. "Selective versus total insulin resistance: a pathogenic paradox". In: *Cell Metab* 7.2 (2008), pp. 95–96. DOI: 10.1016/j.cmet.2007.12.009.

[101] X Wu, K Chen, and K J Williams. "The role of pathway-selective insulin resistance and responsiveness in diabetic dyslipoproteinemia". In: *Curr Opin Lipidol* 23.4 (2012), pp. 334–344. DOI: 10.1097/MOL.0b013e3283544424.

[102] N Kubota et al. "Differential hepatic distribution of insulin receptor substrates causes selective insulin resistance in diabetes and obesity". In: *Nat Commun* 7 (2016), p. 12977. DOI: 10.1038/ncomms12977.

[103] S F Previs et al. "Contrasting effects of IRS-1 versus IRS-2 gene disruption on carbohydrate and lipid metabolism in vivo". In: *J Biol Chem* 275.50 (2000), pp. 38990–38994. DOI: 10.1074/jbc.M006490200.

[104] J R Cook et al. "Pathogenesis of selective insulin resistance in isolated hepatocytes". In: *J Biol Chem* 290.22 (2015), pp. 13972–13980. DOI: 10.1074/jbc.M115.638197.

[105] S Li, M S Brown, and J L Goldstein. "Bifurcation of insulin signaling pathway in rat liver: mTORC1 required for stimulation of lipogenesis, but not inhibition of gluconeogenesis". In: *Proc Natl Acad Sci U S A* 107.8 (2010), pp. 3441–3446. DOI: 10.1073/pnas.0914798107.

[106] Robert Steele. "INFLUENCES OF GLUCOSE LOADING AND OF INJECTED INSULIN ON HEPATIC GLUCOSE OUTPUT*". In: *Annals of the New York Academy of Sciences* 82.2 (Sept. 1959), pp. 420–430. DOI: 10.1111/J.1749-6632.1959.TB44923.X.

[107] S T Chung et al. "Measurements of Gluconeogenesis and Glycogenolysis: A Methodological Review". In: *Diabetes* 64.12 (2015), pp. 3996–4010. DOI: 10.2337/db15-0640.

[108] S K Chacko et al. "Measurement of gluconeogenesis using glucose fragments and mass spectrometry after ingestion of deuterium oxide". In: *J Appl Physiol (1985)* 104.4 (2008), pp. 944–951. DOI: 10.1152/japplphysiol.00752.2007.

[109] R K Semple et al. "Postreceptor insulin resistance contributes to human dyslipidemia and hepatic steatosis". In: *J Clin Invest* 119.2 (2009), pp. 315–322. DOI: 10.1172/JCI37432.

[110] Zachary P. Fricker et al. "Liver Fat is Associated With Markers of Inflammation and Oxidative Stress in Analysis of Data From the Framingham Heart Study". In: *Clinical gastroenterology and hepatology : the official clinical practice journal of the American Gastroenterological Association* 17.6 (May 2019), p. 1157. DOI: 10.1016/J.CGH.2018.11.037.

[111] A. Enrique Caballero. "Endothelial dysfunction, inflammation, and insulin resistance: a focus on subjects at risk for type 2 diabetes". In: *Current diabetes reports* 4.4 (2004), pp. 237–246. DOI: 10.1007/S11892-004-0074-9.

[112] F Karpe et al. "Cohort Profile: The Oxford Biobank". In: *Int J Epidemiol* 47.1 (2018), pp. 21–21. DOI: 10.1093/ije/dyx132.

[113] L Hodson et al. "The contribution of splanchnic fat to VLDL triglyceride is greater in insulin-resistant than insulin-sensitive men and women: studies in the postprandial state". In: *Diabetes* 56.10 (2007), pp. 2433–2441. DOI: 10.2337/db07-0654.

[114] C Pramfalk et al. "Fasting Plasma Insulin Concentrations Are Associated With Changes in Hepatic Fatty Acid Synthesis and Partitioning Prior to Changes in Liver Fat Content in Healthy Adults". In: *Diabetes* 65.7 (2016), pp. 1858–1867. DOI: 10.2337/db16-0236.

[115] S Lallukka et al. "Predictors of Liver Fat and Stiffness in Non-Alcoholic Fatty Liver Disease (NAFLD) - an 11-Year Prospective Study". In: *Sci Rep* 7.1 (2017), p. 14561. DOI: 10.1038/s41598-017-14706-0.

[116] E M Petaja and H Yki-Jarvinen. "Definitions of Normal Liver Fat and the Association of Insulin Sensitivity with Acquired and Genetic NAFLD-A Systematic Review". In: *Int J Mol Sci* 17.5 (2016). DOI: 10.3390/ijms17050633.

[117] L S Szczepaniak et al. "Magnetic resonance spectroscopy to measure hepatic triglyceride content: prevalence of hepatic steatosis in the general population". In: *Am J Physiol Endocrinol Metab* 288.2 (2005), pp. 462–8. DOI: 10.1152/ajpendo.00064.2004.

[118] C J Green et al. "Hepatic de novo lipogenesis is suppressed and fat oxidation is increased by omega-3 fatty acids at the expense of glucose metabolism". In: *BMJ Open Diabetes Res Care* 8.1 (2020). DOI: 10.1136/bmjdrc-2019-000871.

[119] C J Green et al. "Metformin maintains intrahepatic triglyceride content through increased hepatic de novo lipogenesis". In: *Eur J Endocrinol* 186.3 (2022), pp. 367–377. DOI: 10.1530/EJE-21-0850.

[120] T Marjot et al. "Sodium-glucose cotransporter 2 inhibition does not reduce hepatic steatosis in overweight, insulin-resistant patients without type 2 diabetes". In: *JGH Open* 4.3 (2020), pp. 433–440. DOI: 10.1002/jgh3.12274.

[121] W S Low et al. "Sex Differences in Hepatic De Novo Lipogenesis with Acute Fructose Feeding". In: *Nutrients* 10.9 (2018). DOI: 10.3390/nu10091263.

[122] L Hodson et al. "Menopausal Status and Abdominal Obesity Are Significant Determinants of Hepatic Lipid Metabolism in Women". In: *J Am Heart Assoc* 4.10 (2015), e002258. DOI: 10.1161/JAHA.115.002258.

[123] S A Parry et al. "Intrahepatic Fat and Postprandial Glycemia Increase After Consumption of a Diet Enriched in Saturated Fat Compared With Free Sugars". In: *Diabetes Care* 43.5 (2020), pp. 1134–1141. DOI: 10.2337/dc19-2331.

[124] K E Pinnick, P J Gunn, and L Hodson. "Measuring Human Lipid Metabolism Using Deuterium Labeling: In Vivo and In Vitro Protocols". In: *Methods Mol Biol* 1862 (2019), pp. 83–96. DOI: 10.1007/978-1-4939-8769-6{_}6.

[125] F Shojaee-Moradie et al. "Quantitative measurement of 3-O-methyl-D-glucose by gas chromatography-mass spectrometry as a measure of glucose transport in vivo". In: *J Mass Spectrom* 31.9 (1996), pp. 961–966. DOI: 10.1002/(SICI)1096-9888(199609)31:9<961::AID-JMS359>3.0.CO;2-H.

[126] J C Levy, D R Matthews, and M P Hermans. "Correct homeostasis model assessment (HOMA) evaluation uses the computer program". In: *Diabetes Care* 21.12 (1998), pp. 2191–2192. DOI: 10.2337/diacare.21.12.2191.

[127] Nicolai J. Wewer Albrechtsen et al. "Evidence of a liver-alpha cell axis in humans: hepatic insulin resistance attenuates relationship between fasting plasma glucagon and glucagonotropic amino acids". In: *Diabetologia* 61.3 (Mar. 2018), pp. 671–680. DOI: 10.1007/S00125-017-4535-5.

[128] Anna Wieckowska et al. "Increased hepatic and circulating interleukin-6 levels in human nonalcoholic steatohepatitis". In: *The American journal of gastroenterology* 103.6 (June 2008), pp. 1372–1379. DOI: 10.1111/J.1572-0241.2007.01774.X.

[129] Maria D. Giraldez et al. "New insights into IL-6 family cytokines in metabolism, hepatology and gastroenterology". In: *Nature reviews. Gastroenterology & hepatology* 18.11 (Nov. 2021), pp. 787–803. DOI: 10.1038/S41575-021-00473-X.

[130] James D. Otvos et al. "GlycA: A Composite Nuclear Magnetic Resonance Biomarker of Systemic Inflammation". In: *Clinical Chemistry* 61.5 (May 2015), pp. 714–723. DOI: 10.1373/CLINCHEM.2014.232918.

[131] Scott T. Chiesa et al. "Glycoprotein Acetyls: A Novel Inflammatory Biomarker of Early Cardiovascular Risk in the Young". In: *Journal of the American Heart Association* 11.4 (Feb. 2022), p. 24380. DOI: 10.1161/JAHA.121.024380/SUPPL{_}FILE/JAH37176-SUP-0001-SUPINFO.PDF.

[132] G Marchesini et al. "Nonalcoholic fatty liver disease: a feature of the metabolic syndrome". In: *Diabetes* 50.8 (2001), pp. 1844–1850. DOI: 10.2337/diabetes.50.8.1844.

[133] S Jiang et al. "Diabetic-induced alterations in hepatic glucose and lipid metabolism: The role of type 1 and type 2 diabetes mellitus (Review)". In: *Mol Med Rep* 22.2 (2020), pp. 603–611. DOI: 10.3892/mmr.2020.11175.

[134] R Basu et al. "Obesity and type 2 diabetes impair insulin-induced suppression of glycogenolysis as well as gluconeogenesis". In: *Diabetes* 54.7 (2005), pp. 1942–1948. DOI: 10.2337/diabetes.54.7.1942.

[135] R Basu et al. “Plasma C5 glucose-to-2H2O ratio does not provide an accurate assessment of gluconeogenesis during hyperinsulinemic-euglycemic clamps in either nondiabetic or diabetic humans”. In: *Diabetes* 57.7 (2008), pp. 1800–1804. DOI: 10.2337/db08-0195.

[136] Ralph A DeFronzo and Devjit Tripathy. “Skeletal Muscle Insulin Resistance Is the Primary Defect in Type 2 Diabetes”. In: *Diabetes Care* 32.suppl_2 (Nov. 2009), S157–S163. DOI: 10.2337/dc09-S302.

[137] G I Shulman et al. “Quantitation of muscle glycogen synthesis in normal subjects and subjects with non-insulin-dependent diabetes by 13C nuclear magnetic resonance spectroscopy”. In: *N Engl J Med* 322.4 (1990), pp. 223–228. DOI: 10.1056/NEJM199001253220403.

[138] D S Allende et al. “Glycogenosis is common in nonalcoholic fatty liver disease and is independently associated with ballooning, but lower steatosis and lower fibrosis”. In: *Liver Int* 41.5 (2021), pp. 996–1011. DOI: 10.1111/liv.14773.

[139] Malte P. Suppli et al. “Glucagon Resistance at the Level of Amino Acid Turnover in Obese Subjects With Hepatic Steatosis”. In: *Diabetes* 69.6 (June 2020), pp. 1090–1099. DOI: 10.2337/DB19-0715.

[140] Alan D. Cherrington. “Banting Lecture 1997. Control of glucose uptake and release by the liver in vivo”. In: *Diabetes* 48.5 (1999), pp. 1198–1214. DOI: 10.2337/DIABETES.48.5.1198.

[141] K L Donnelly et al. “Sources of fatty acids stored in liver and secreted via lipoproteins in patients with nonalcoholic fatty liver disease”. In: *J Clin Invest* 115.5 (2005), pp. 1343–1351. DOI: 10.1172/JCI23621.

[142] M Hatting et al. “Insulin regulation of gluconeogenesis”. In: *Ann N Y Acad Sci* 1411.1 (2018), pp. 21–35. DOI: 10.1111/nyas.13435.

[143] R A Rizza. “Pathogenesis of fasting and postprandial hyperglycemia in type 2 diabetes: implications for therapy”. In: *Diabetes* 59.11 (2010), pp. 2697–2707. DOI: 10.2337/db10-1032.

[144] R Basu, W F Schwenk, and R A Rizza. “Both fasting glucose production and disappearance are abnormal in people with "mild" and "severe" type 2 diabetes”. In: *Am J Physiol Endocrinol Metab* 287.1 (2004), pp. 55–62. DOI: 10.1152/ajpendo.00549.2003.

[145] G Boden, X Chen, and T P Stein. “Gluconeogenesis in moderately and severely hyperglycemic patients with type 2 diabetes mellitus”. In: *Am J Physiol Endocrinol Metab* 280.1 (2001), pp. 23–30. DOI: 10.1152/ajpendo.2001.280.1.E23.

[146] Xinhua Chen, Nayyar Iqbal, and Guenther Boden. “The effects of free fatty acids on gluconeogenesis and glycogenolysis in normal subjects”. In: *The Journal of clinical investigation* 103.3 (1999), pp. 365–372. DOI: 10.1172/JCI5479.

[147] Joseph Katz and John A. Tayek. “Gluconeogenesis and the Cori cycle in 12-, 20-, and 40-h-fasted humans”. In: *The American journal of physiology* 275.3 (1998). DOI: 10.1152/AJPENDO.1998.275.3.E537.

[148] Muhammad Amir and Mark J Czaja. “Autophagy in nonalcoholic steatohepatitis”. In: *Expert Rev Gastroenterol Hepatol* 5.2 (2011), pp. 159–166. DOI: 10.1586/egh.11.4.

[149] Leanne Hodson, Fredrik Rosqvist, and Siôn A. Parry. “The influence of dietary fatty acids on liver fat content and metabolism”. In: *The Proceedings of the Nutrition Society* 79.1 (2020), pp. 30–41. DOI: 10.1017/S0029665119000569.

[150] Hannele Yki-Järvinen et al. *Dietary carbohydrates and fats in nonalcoholic fatty liver disease.* 2021. DOI: 10.1038/s41575-021-00472-y.

[151] Matteo Bordi et al. "A gene toolbox for monitoring autophagy transcription". In: *Cell Death and Disease* 12.11 (2021). DOI: 10.1038/s41419-021-04121-9.

[152] Shuang Mei et al. "Differential roles of unsaturated and saturated fatty acids on autophagy and apoptosis in hepatocytes". In: *Journal of Pharmacology and Experimental Therapeutics* 339.2 (2011), pp. 487–498. DOI: 10.1124/jpet.111.184341.

[153] Ricky H Bhogal et al. "Isolation of Primary Human Hepatocytes from Normal and Diseased Liver Tissue: A One Hundred Liver Experience". In: (2011). DOI: 10.1371/journal.pone.0018222.

[154] Zoë J. Huggett et al. "A Comparison of Primary Human Hepatocytes and Hepatoma Cell Lines to Model the Effects of Fatty Acids, Fructose and Glucose on Liver Cell Lipid Accumulation". In: *Nutrients* 15.1 (Jan. 2022). DOI: 10.3390/NU15010040.

[155] Francisca S. Teixeira et al. "Differential Lipid Accumulation on HepG2 Cells Triggered by Palmitic and Linoleic Fatty Acids Exposure". In: *Molecules* 28.5 (Mar. 2023). DOI: 10.3390/MOLECULES28052367.

[156] Pradjna N. Paramitha et al. "Raman Study on Lipid Droplets in Hepatic Cells Co-Cultured with Fatty Acids". In: *International journal of molecular sciences* 22.14 (July 2021). DOI: 10.3390/IJMS22147378.

[157] Fredrik Rosqvist et al. "Overeating Saturated Fat Promotes Fatty Liver and Ceramides Compared With Polyunsaturated Fat: A Randomized Trial". In: *The Journal of clinical endocrinology and metabolism* 104.12 (Dec. 2019), pp. 6207–6219. DOI: 10.1210/JC.2019-00160.

[158] Wim Martinet et al. "In situ detection of starvation-induced autophagy". In: *The journal of histochemistry and cytochemistry : official journal of the Histochemistry Society* 54.1 (Jan. 2006), pp. 85–96. DOI: 10.1369/JHC.5A6743.2005.

[159] Bodduluri Haribabu et al. "Article 1802 (2020) Chemokines in Non-alcoholic Fatty Liver Disease: A Systematic Review and Network Meta". In: *Analysis. Front. Immunol* 11 (2020), p. 1802. DOI: 10.3389/fimmu.2020.01802.

[160] Binxia Chang et al. "Short- or long-term high fat diet feeding plus acute ethanol binge synergistically induce acute liver injury in mice: an important role for CXCL1". In: *Hepatology (Baltimore, Md.)* 62.4 (Oct. 2015), p. 1070. DOI: 10.1002/HEP.27921.

[161] Weiran Dai et al. "Key Genes Associated with Non-Alcoholic Fatty Liver Disease and Acute Myocardial Infarction". In: (). DOI: 10.12659/MSM.922492.

[162] Amin Ullah et al. "A narrative review: CXC chemokines influence immune surveillance in obesity and obesity-related diseases: Type 2 diabetes and nonalcoholic fatty liver disease". In: *Reviews in Endocrine and Metabolic Disorders* 24 (2023), pp. 611–631. DOI: 10.1007/s11154-023-09800-w.

[163] Songtao Li et al. "Sirtuin 3 acts as a negative regulator of autophagy dictating hepatocyte susceptibility to lipotoxicity". In: *Hepatology* 66.3 (2017), pp. 936–952. DOI: 10.1002/hep.29229.

[164] Qian-Qian Tu et al. "Palmitic acid induces autophagy in hepatocytes via JNK2 activation". In: *Acta Pharmacologica Sinica* 35 (2014), pp. 504–512. DOI: 10.1038/aps.2013.170.

[165] Hui Yu Liu et al. "Hepatic autophagy is suppressed in the presence of insulin resistance and hyperinsulinemia. Inhibition of FoxO1-dependent expression of key autophagy genes by insulin". In: *Journal of Biological Chemistry* 284.45 (Nov. 2009), pp. 31484–31492. DOI: 10.1074/jbc.M109.033936.

[166] Martin Lundberg et al. "Homogeneous antibody-based proximity extension assays provide sensitive and specific detection of low-abundant proteins in human blood". In: *Nucleic Acids Research* 39.15 (Aug. 2011), e102. DOI: 10.1093/NAR/GKR424.

[167] Masaaki Komatsu et al. "Impairment of starvation-induced and constitutive autophagy in Atg7-deficient mice". In: *The Journal of Cell Biology* 169.3 (2005), pp. 425–434. DOI: 10.1083/jcb.200412022.

[168] Ann Britt Marcher et al. "Transcriptional regulation of Hepatic Stellate Cell activation in NASH". In: *Scientific Reports 2019 9:1* 9.1 (Feb. 2019), pp. 1–13. DOI: 10.1038/s41598-019-39112-6.

[169] Ariel E. Feldstein et al. "Cytokeratin-18 fragment levels as noninvasive biomarkers for nonalcoholic steatohepatitis: A multicenter validation study". In: *Hepatology* 50.4 (2009), pp. 1072–1078. DOI: 10.1002/hep.23050.

[170] A. Chabowski et al. "Fatty acid transporters involved in the palmitate and oleate induced insulin resistance in primary rat hepatocytes". In: *Acta physiologica (Oxford, England)* 207.2 (Feb. 2013), pp. 346–357. DOI: 10.1111/APHA.12022.

[171] J H Moffitt B A Fielding R Evershed R Berstan J M Currie A Clark. "Adverse physicochemical properties of tripalmitin in beta cells lead to morphological changes and lipotoxicity in vitro". In: *Diabetologia* 48 (2005), pp. 1819–1829. DOI: 10.1007/s00125-005-1861-9.

[172] Takuma Tsuchida and Scott L Friedman. "Mechanisms of hepatic stellate cell activation". In: *Nature Publishing Group* 14 (2017). DOI: 10.1038/nrgastro.2017.38.

[173] Christina C. Lindenmeyer and Arthur J. McCullough. "The Natural History of Nonalcoholic Fatty Liver Disease - An Evolving View". In: *Clinics in liver disease* 22.1 (Feb. 2018), p. 11. DOI: 10.1016/J.CLD.2017.08.003.

[174] Xueping Zhang et al. "Unraveling the Regulation of Hepatic Gluconeogenesis". In: *Frontiers in Endocrinology* 9.JAN (2018). DOI: 10.3389/FENDO.2018.00802.

[175] Andrés Méndez-Lucas et al. "PEPCK-M expression in mouse liver potentiates, not replaces, PEPCK-C mediated gluconeogenesis". In: *Journal of hepatology* 59.1 (July 2013), pp. 105–113. DOI: 10.1016/J.JHEP.2013.02.020.

[176] Romana Stark et al. "A role for mitochondrial phosphoenolpyruvate carboxykinase (PEPCK-M) in the regulation of hepatic gluconeogenesis". In: *The Journal of biological chemistry* 289.11 (Mar. 2014), pp. 7257–7263. DOI: 10.1074/JBC.C113.544759.

[177] Willemien van Zwol et al. "VLDL Biogenesis and Secretion: It Takes a Village". In: *Circulation research* 134.2 (Jan. 2024), pp. 226–244. DOI: 10.1161/CIRCRESAHA.123.323284.

[178] A. L. Jones et al. "Uptake and processing of remnants of chylomicrons and very low density lipoproteins by rat liver." In: *Journal of Lipid Research* 25.11 (Nov. 1984), pp. 1151–1158. DOI: 10.1016/S0022-2275(20)34458-8.

[179] Jean Marc Schwarz et al. "Short-term alterations in carbohydrate energy intake in humans. Striking effects on hepatic glucose production, de novo lipogenesis, lipolysis, and whole-body fuel selection". In: *The Journal of clinical investigation* 96.6 (1995), pp. 2735–2743. DOI: 10.1172/JCI118342.

[180] Mark D. Mifflin et al. “A new predictive equation for resting energy expenditure in healthy individuals”. In: *The American journal of clinical nutrition* 51.2 (1990), pp. 241–247. DOI: 10.1093/AJCN/51.2.241.

[181] J. S. Cohn et al. “Plasma apolipoprotein changes in the triglyceride-rich lipoprotein fraction of human subjects fed a fat-rich meal”. In: *Journal of Lipid Research* 29.7 (July 1988), pp. 925–936. DOI: 10.1016/S0022-2275(20)38485-6.

[182] “Triglyceride-rich lipoproteins and their role in cardiovascular disease”. In: *British Journal of Cardiology* (2023). DOI: 10.5837/BJC.2023.S06.

[183] Javier S. Perona et al. “Uptake of triacylglycerol-rich lipoproteins of differing triacylglycerol molecular species and unsaponifiable content by liver cells”. In: *British Journal of Nutrition* 95.5 (May 2006), pp. 889–897. DOI: 10.1079/BJN20061730.

[184] C. A. Hornick, A. L. Jones, and G. Renaud. “Effect of chloroquine on low-density lipoprotein catabolic pathway in rat hepatocytes”. In: *The American journal of physiology* 246.2 Pt 1 (1984). DOI: 10.1152/AJPGI.1984.246.2.G187.

[185] Arik Sheinenzon et al. “Serum albumin levels and inflammation”. In: *International Journal of Biological Macromolecules* 184 (2021). DOI: 10.1016/j.ijbiomac.2021.06.140.

[186] Wenqi Cui et al. “Lipophagy-derived fatty acids undergo extracellular efflux via lysosomal exocytosis”. In: *Autophagy* 17.3 (Mar. 2021), pp. 690–705. DOI: 10.1080/15548627.2020.1728097.

[187] Andreas Paulus et al. “[18F]BODIPY-triglyceride-containing chylomicron-like particles as an imaging agent for brown adipose tissue in vivo”. In: *Scientific Reports* 9.1 (Dec. 2019). DOI: 10.1038/S41598-019-39561-Z.

[188] Matthew James Armstrong et al. “Liraglutide safety and efficacy in patients with non-alcoholic steatohepatitis (LEAN): a multicentre, double-blind, randomised, placebo-controlled phase 2 study”. In: *Lancet (London, England)* 387.10019 (Feb. 2016), pp. 679–690. DOI: 10.1016/S0140-6736(15)00803-X.

[189] Philip N. Newsome et al. “A Placebo-Controlled Trial of Subcutaneous Semaglutide in Nonalcoholic Steatohepatitis”. In: *The New England journal of medicine* 384.12 (Mar. 2021), pp. 1113–1124. DOI: 10.1056/NEJMOA2028395.

[190] Mohammad S. Kuchay et al. “Effect of dulaglutide on liver fat in patients with type 2 diabetes and NAFLD: randomised controlled trial (D-LIFT trial)”. In: *Diabetologia* 63.11 (Nov. 2020), pp. 2434–2445. DOI: 10.1007/S00125-020-05265-7/TABLES/3.

[191] Julian M. Yabut and Daniel J. Drucker. “Glucagon-like Peptide-1 Receptor-based Therapeutics for Metabolic Liver Disease”. In: *Endocrine Reviews* 44.1 (Jan. 2023), pp. 14–32. DOI: 10.1210/ENDREV/BNAC018.

[192] Layla A. Abushamat et al. “The Emerging Role of Glucagon-Like Peptide-1 Receptor Agonists for the Treatment of Metabolic Dysfunction-Associated Steatohepatitis”. In: *Clinical Gastroenterology and Hepatology* 22.8 (Aug. 2024), pp. 1565–1574. DOI: 10.1016/J.CGH.2024.01.032.

Thanks to MJL for the translation of chapter quotes into Latin: "Liver, laugh, love", "No thoughts just vibes", "Do not feed caramel to expensive machines", "Cells do require oxygen to live", "Who needs statistical significance anyway?", "There's a microscope in hell", "Sometimes it just do be like that"